New Strategies for Cooperative and Multi-Band Spectrum Sensing

A

Thesis Submitted

in Partial Fulfilment of the Requirements

for the Award of the Degree of

Doctor of Philosophy

By

Kukil Khanikar

Department of Electronics and Electrical Engineering

Indian Institute of Technology Guwahati

Guwahati - 781 039, Assam, India

February, 2018

Dedicated

to

My Parents

Certificate

This is to certify that the thesis titled "**New Strategies for Cooperative and Multi-Band Spectrum Sensing**", submitted by **Kukil Khanikar** (11610208), a research scholar in the *Department of Electronics and Electrical Engineering, Indian Institute of Technology Guwahati*, for the award of the degree of **Doctor of Philosophy**, is a record of an original research work carried out by him under our supervision and guidance. The thesis has fulfilled all requirements as per the regulations of the institute and in our opinion has reached the standard needed for submission. The results embodied in this thesis have not been submitted to any other University or Institute for the award of any degree or diploma.

Date:

Place: Guwahati.

Prof. Rohit Sinha
Dept. of Electronics and Electrical Engg
Indian Institute of Technology Guwahati
Guwahati - 781 039, Assam, India.

Date:

Place: Guwahati.

Prof. Ratnajit Bhattacharjee
Dept. of Electronics and Electrical Engg
Indian Institute of Technology Guwahati
Guwahati - 781 039, Assam, India.

Acknowledgements

At the very outset, I would like to offer my heartfelt gratitude to my supervisors, Prof. Rohit Sinha and Prof. Ratnajit Bhattacharjee for their excellent guidance and constant support. Their valuable advice aided me in gaining insights into intricate topics in the research area. I sincerely thank them for the pain they undertook in scrutinizing every manuscript I presented to them and offering critical comments.

I am deeply thankful to other members of my doctoral committee, Prof. S. R. M. Prasanna (Chariman), Prof. S. Nandi, Dr. K. Karthik and Dr. T. Jacob for taking out their valuable time for attending the seminars I presented and providing valuable comments. My gratitude also extends to Dr. P. R. Sahu who had been a former member of my doctoral committee.

I offer my deepest gratitude to all other faculty members of the Department of Electronics and Electrical Engineering, Indian Institute of Technology Guwahati, without whose cooperation, this journey would not have been possible. I would like to make special mention of Prof. P. K. Bora, Prof. A. Gogoi, Prof. S. K. Bose, Prof. K. R. Singh, Dr. A. Rajesh, Dr. S. Chouhan, Dr. R. K. Sonkar and Dr. N. Nallam under whom I served as a teaching assistant during my period of assistantship. My special thanks to the technical and non-technical staffs of the department and the institute, Dr. L. N. Sharma, Mr. Sanjib Das, Mr. P. J. Goswami, Ms. Riju Rabha, Ms. Josephine. S, Dr. M. P. Das, Mr. M. Baruah, Mr. Uday, Mr. Dasarath Das and all others.

My heartiest thanks extends to all my senior and fellow research scholars of the Indian Institute of Technology Guwahati fraternity with whom I have shared a wonderful campus environment. I would like to specially thank my labmates and friends Mrinmoy, Dibyajyoti, Anand, Jitendra, Niladri, Himangshu Jyoti Das, Krishna Mohan, Darpan, Manoranjan, Khaing Thin Zar for the constant and all-round support they have provided me. My special thanks extend to my friends Biswajit Dev Sarma, Pranabjytoi Haloi, Sushanta Kundu, Sikandar Kumar, Santosh Kumar Yadav, Rohan Kumar Das, Brajesh Rawat, Ashif Iqbal, Ashim Kumar, Parikshit Saikia, Mr. Arijit Bhattacharjee and others who made my stay in the campus enjoyable. My deepest

gratitude to senior research scholars, Dr. Sam Darshi, Dr. B. Kumbhani, Dr. R. Jana, Dr. Haris B.C., Dr. S. Shahnawazuddin, Dr. Deepak. K. T., Dr. Shivanshu and all others for their help, cooperation and support.

I would like to thank Indian Institute of Technology Guwahati for providing a serene environment. I would also like to acknowledge the financial support provided by the Ministry of Human Resource Development, Government of India.

Finally, I would like to offer my deepest gratitude to my family, my parents, my sister, Kunhi and my brother-in-law, Barun for supporting me throughout this journey and bearing all the pain that may have ensued due to my prolonged distraction.

Kukil Khanikar

Abstract

Cognitive radio technology offers the possibility of opportunistically utilizing the unused radio spectrum, referred to as the spectrum holes. Spectrum sensing is a key tool enabling cognitive radios to locate spectrum holes. Although considerable research effort has been put into developing efficient spectrum sensing techniques, certain gaps in the state-of-the-art still exist. This thesis work has sought to address a few less-explored issues concerning spectrum sensing in cognitive radio networks.

The primary focus in this work is on improving the performance of cooperative spectrum sensing (CSS) implemented in the absence of dedicated reporting channels. Two contributions are made in this regard. Firstly, a scenario is considered in which a conventional hard decision fusion CSS network is assumed to be operating without dedicated reporting channels. In this case, the reported decisions suffer different rates of outage depending on the presence or absence of the primary user (PU) signal. This differential outage information is utilized in further optimizing the well-known n-out-of-K voting rule. On measuring the performance in terms of the total error rate, the incorporation of the said information resulted in the improvement of performance compared to the case when this information is not used. Secondly, a novel decentralized CSS network architecture that operates in the absence of dedicated reporting channels, is proposed. The proposed architecture supports soft decision fusion and is capable of preventing collision among the secondary users in the network. The thesis also derives closed form analytical expressions for probability of detection and probability of false alarm for the proposed CSS model.

The thesis also explores the sensing of fast-switching primary users over a wideband of interest (WBOI). In this regard, a sparse coding approach is introduced to track frequency hopping spread spectrum (FHSS) PUs present in the WBOI. Studies carried out through simulation establish the superiority of the proposed technique compared to the state-of-the-art, *fast Fourier transform averaging ratio* (FAR) based sensing algorithm both in terms of sensing time and detection performance.

Contents

List of Figures

List of Tables

List of Acronyms

ADC	Analog to Digital Converter
ASK	Amplitude Shift Keying
AWGN	Additive White Gaussian Noise
BP	Basis Pursuit
BSR	Best-Selection Reporting
CDF	Cumulative Distribution Function
CFAR	Constant False Alarm Rate
CR	Cognitive Radio
CRC	Cyclic Redundancy Check
CSMA/CA	Carrier Sense Multiple Access/Collision Avoidance
CSS	Cooperative Spectrum Sensing
CSU	Cooperating Secondary User
DVR	Default Voting Rule
FAR	Fast Fourier Transform Averaging Ratio
FC	Fusion Centre
FFT	Fast Fourier Transform
FHSS	Frequency Hopping Spread Spectrum
FSK	Frequency Shift Keying
GFSK	Gaussian Frequency Shift Keying
LED	Learned Exemplar Dictionary
LSSN	Leading Secondary Sensor Node
MP	Matching Pursuit

NSS	Narrowband Spectrum Sensing
OMP	Orthogonal Matching Pursuit
PDF	Probability Distribution Function
PSD	Power Spectral Density
PSK	Phase Shift Keying
PU	Primary User
PVR	Proposed Voting Rule
RF	Radio Frequency
Rx	Receiver
SDR	Software Defined Radio
SINR	Signal to Interference plus Noise Ratio
SNR	Signal to Noise Ratio
SPTF	Spectrum Policy Task Force
SRC	Sparse Representation Classification
SU	Secondary User
TE	Total Error
TER	Total Error Rate
Tx	Transmitter
WBOI	Wide Band of Interest
WSS	Wideband Spectrum Sensing

List of Symbols

P	Primary user transmitter node
R	Primary user receiver node
F	Fusion center
C_i	ith CSU node
S	Secondary user transmitter that has won the contention
B	Leading secondary sensor node
$\mathcal{H}_i$	ith hypothesis
$\Gamma(\cdot)$	Gamma function
$\Gamma(\cdot,\cdot)$	Upper incomplete Gamma function
$Pr\{\cdot\}$	Probability of an event
$\mathbb{E}_W[\cdot]$	Expectation operator over random variable or random vector W
$\mathcal{U}(a,b)$	Uniform distribution with lower and upper limits a and b, respectively
$Ceil(\cdot)$	Ceiling operator
$NormCol(\mathbf{.})$	Operator for normalizing columns of a matrix
$Diag(\mathbf{.})$	Operator for convertin vector to diagonal matrix
N	Number of CSUs
N_c	Number of non-overlapping frequency channels in the WBOI
N_p	Maximum number of operating FHSS PUs
$s_i(n)$	Signal from the ith FHSS PU
$x(n)$	Wideband signal processed at the SU detector which is an aggregate of multiple signals from unknown number of FHSS PUs
$w(n)$	White Gaussian noise

$\bar{\gamma}_{XY}$	Average SNR of signal from arbitrary node X at arbitrary node Y
$\bar{\gamma}_{\mathsf{P}i}$	equivalent notation for $\bar{\gamma}_{\mathsf{PC}_i}$
$\bar{\gamma}_{XY,\text{nom}}$	Nominal SNR of the signal from an arbitrary node X at an arbitrary node Y
$\delta_{\bar{\gamma}_{XY}}$	Uncertainty parameter associated with nominal SNR $\bar{\gamma}_{XY,\text{nom}}$
γ_{XY}	Instantaneous SNR of the signal from an arbitrary node X at an arbitrary node Y
$\gamma_{\mathsf{P}i}$	equivalent notation for γ_{PC_i}
N_s	Samples available for sensing
N_F	Number of FFT points used in the FAR scheme
T_F	Number of frames used in the FAR scheme for averaging
λ_i	Detector threshold at C_i
λ_{S}	Detector threshold at S
λ_C	Threshold set at S for joint detection
λ_{BSR}	Threshold set for the detector for the BSR scheme
$\lambda_{\mathsf{S},o}$	Value of λ_{S} returned by Algorithm 1
$\lambda_{C,o}$	Value of λ_C returned by Algorithm 1
σ_n^2	Noise variance
Ξ_{S}	Event that sensor node at node S is able to detect the PU
Ξ_{S}^c	Event that sensor node at node S is unable to detect the PU
E_{S}	Energy statistics at S
E_{B}	Energy statistics at B
d	Number of bits used for quantization
D	Number of quantization levels
$E'_{\mathsf{B,q}}$	Random variable denoting quantized version of E'_{B}
$e'_{\mathsf{B},q,n}$	value corresponding to the nth quantization level set by node B
E'_C	Combined test statistics at S, $= E'_{\mathsf{B},q} + E'_{\mathsf{S}}$
$\boldsymbol{D}_i$	Sub-dictionary corresponding to the ith FHSS channel

$\boldsymbol{D}$	Concatenated dictionary,= $[\boldsymbol{D}_1, \boldsymbol{D}_2, \ldots, \boldsymbol{D}_{N_c}]$
f_s	Sampling rate of wideband received FHSS signal
f_{ADC}	Sampling rate of ADCs
F_c	Sub-sampling factor = f_s/f_{adc}
$\boldsymbol{\Phi}_l$	Sub-sampling matrix corresponding to the lth pair of ADC sub-branch
$\boldsymbol{x}$	Vector form of received wideband signal sampled at f_s
$\tilde{\boldsymbol{x}}$	$\frac{\boldsymbol{x}}{\|\|x\|\|_2}$
$\tilde{\boldsymbol{D}}_l$	$= NormCol\,(\boldsymbol{\Phi}_l \boldsymbol{D})$
$\boldsymbol{x}_l$	$= \boldsymbol{\Phi}_l \tilde{\boldsymbol{x}}$
$\boldsymbol{y}_l$	Sparse vector obtained by coding $\boldsymbol{x}_l$ over $\tilde{\boldsymbol{D}}_l$
t_h	Detector threshold set for deciding the presence of a FHSS PU at a given channel
K_c	Number of atoms per channel
S	Sparsity constraint
m_s	Number of samples obtained at the output of an I-Q ADC pair
T_s	Symbol period of FHSS PUs
T_{sns}	Sensing interval used by the sparse coding based detection technique
$f_{E'_{\mathsf{B}}}(x)$	PDF of E'_{B}
$f_{E'_{\mathsf{B}}\|\mathcal{H}_i}(x)$	PDF of E'_{B} under hypothesis $\mathcal{H}_i$, $i = 0, 1$
$F_{E'_{\mathsf{B}}\|\mathcal{H}_i}(x)$	CDF of E'_{B} under hypothesis $\mathcal{H}_i$, $i = 0, 1$
$F_{C\|\mathcal{H}_i}(x)$	CDF of E'_C under $\mathcal{H}_i$, $i = 0, 1$
$P_{f,X}$ or $P_{f,X}(\cdot)$	Probability of false alarm at an arbitrary sensor node X, i.e., $X \in \{\mathsf{P}, \mathsf{R}, \mathsf{F}, \mathsf{C}_i, \mathsf{S}, \mathsf{B}\}$
P_{f_i} or $P_{f_i}(\cdot)$	equivalent notation for P_{f,C_i}
$P_{d,X}$ or $P_{d,X}(\cdot)$	Probability of detection at an arbitrary sensor node X
P_{d_i} or $P_{d_i}(\cdot)$	equivalent notation for P_{d,C_i}
P_F or $P_F(\cdot)$ or $P_F(\cdot,\cdot)$	The overall probability of false alarm of a particular scheme (at the FC or at S for instance)

P_D or $P_D(\cdot)$ or $P_D(\cdot,\cdot)$	The overall probability of detection of a particular scheme
P_M or $P_M(\cdot)$ or $P_M(\cdot,\cdot)$	The overall probability of miss detection of a particular scheme
P_{Fa}	Probability of false alarm considering uncertainty of outage rate of reporting packets
P_{Da}	Probability of detection considering uncertainty of outage rate of reporting packets
$P_{F,\mathrm{BSR}}$	Probability of false alarm for the BSR scheme considering uncertainty of outage rate of reporting packets
$P_{D,\mathrm{BSR}}$	Probability of detection for the BSR scheme considering uncertainty of outage rate of reporting packets
$P_{CF}(\lambda_C, \lambda_{\mathsf{S}})$	$= Pr\{E'_C > \lambda_{\mathrm{C}} \vert \mathcal{H}_0, \Xi_{\mathsf{S}}^c, \mathcal{G}\}$
$\tilde{P}_{CF}(\lambda_C)$	$= P_{CF}(\lambda_C, \infty)$
$P_{Ei_{XY}}$	Outage probability of signal from arbitrary node X to arbitrary node Y under hypothesis $\mathcal{H}_i$
$\bar{P}_{Ei_{XY}}$	Average outage probability of signal from arbitrary node X to arbitrary node Y under hypothesis $\mathcal{H}_i$ considering uncertainty of SNR of the signal from node X
$\mathcal{G}$	The event denoting the the successful relaying of the quantized statistics from the LSSN is to S
$\beta_{\mathcal{H}_i}$	$= Pr\{\mathcal{G} \vert \mathcal{H}_i, \Xi_{\mathsf{S}}^c\}\ i = 0, 1$
$\bar{\beta}_{\mathcal{H}_i}$	Expectation of $\beta_{\mathcal{H}_i}$
γ_{out}	Outage SNR of the reporting signal for the system considered in Chapter 2
$\gamma_{\mathsf{P}\mathrm{out}}$	Outage SNR of the PU Tx signal
r_{P}	Information rate of the PU Tx node P
r_{S}	Information rate of an SU Tx node S
$P_{P\mathrm{out}}$	Tolerable PU outage probability at a PU Rx
P_{P}	PU transmit power

P_S	SU transmit power
P_{s_t}	Upper limit of SU transmit power
$P_{s_t,\mathrm{BSR}}$	Upper limit of SU transmit power for the BSR scheme
Θ	$= P_{\mathrm{P}}\sigma^2_{\mathrm{PR}}/\sigma^2_{X_i\mathrm{R}}$
h_{XY}	Instantaneous gain of the channel from arbitrary node X to arbitrary node Y
$h_{\mathrm{P}i}$	equivalent notation for h_{PC_i}
σ^2_{XY}	Average gain of the channel from arbitrary node X to arbitrary node Y
$\sigma^2_{\mathrm{P}i}$	equivalent notation for $\sigma^2_{\mathrm{PC}_i}$
K	Number of valid votes (with CRC intact) received at the FC
n_K	Minimum number of votes considered by the FC to declare the presence of the PU when K valid votes are received
$n_{K_{\mathrm{opt}}}$	Optimum voting rule when K number of votes are received, which results in minimum TE for a give value of detection threshold
$F(\cdot,\cdot)$	Total error = $P_F + P_M$
T_R	Data rate of reporting scheme
L_R	Length of the reported packet
E_R	Maximum number of errors that can be corrected by the error correcting scheme
C_{out}	Outage capacity of the reporting channel
B	Bandwidth of the reporting channel
ζ	T_R/B
η	E_R/B
s_i	ith sub-slot of the sensing time slot considered for Chapter 3
C_w	Current upper limit of the contention window
$C_{w_{\max}}$	Set threshold for the maximum upper limit of the contention window
$C_{w_{\min}}$	Set threshold for the minimum upper limit of the contention window

1

Introduction

Contents

Radio frequency (RF) spectrum is a limited natural resource. The traditional policy of RF spectrum allotment grants exclusive rights or license to a specific set of users to operate in a particular band of spectrum. However, the demands on the licensed wireless services are on the rise due to increasing consumer needs. Technologies supporting massive machine-to-machine communication, such as *internet of things* [1] are on the horizon. Ever increasing demand of higher data rate services is posing a severe constraint on the available RF spectrum. The scheme of fixed spectrum allocation and the widespread use of wireless technologies is likely to contribute to an apparant scarcity of the RF spectrum in the very near future. With an eye towards addressing this issue, the spectrum policy task force presented the idea of secondary spectrum access of the licensed spectrum in its report of 2002 [2]. The proposal stemmed from the observation that a bulk of the RF spectrum licensed to incumbent users remain underutilized. Cognitive radio (CR) [3, 4] technology offers the possibility of increasing the utilization of the licensed radio spectra. The term *cognitive radio* was first coined by Joseph Mitola III in [3]. He used the term to describe a smart, environment-aware radio system that is capable of keeping track of its operational states (e.g., transmit power, modulation scheme, media access schemes etc.). Such a system can intelligently adapt those states to operate optimally in a given situation. For having secondary access to the licensed spectra, lower priority secondary devices must adhere to stringent regulations so that the operations of the incumbent users, commonly referred to as the primary users (PUs), are not significantly affected. These lower priority devices, also referred to as the secondary users (SUs), must be agile CRs that should be aware of the local radio environment. Spectrum sensing forms an essential activity in the implementation of a CR. Spectrum sensing refers to the active search for spectrum holes [5] that are representative of spectral voids capable of supporting opportunistic SU transmissions. The licensed RF spectrum can be accessed by secondary devices using multiple ways. The following section discusses the modes of secondary access of the licensed spectrum.

1.1 Modes of Secondary Spectrum Access

There are primarily three modes of secondary spectrum access [6]. The SUs can utilize one or a combination of these schemes listed below to access the licensed spectrum.

- Underlay spectrum access
- Overlay spectrum access
- Interweave spectrum access

The *underlay* and the *overlay* [6] spectrum access paradigms allow the SUs to transmit concurrently with the PUs in the licensed bands. The SUs using these schemes adopt transmit power control and interference cancellation as means to limit the interference on the PUs. Overlay systems assume the complete knowledge of the PU transmission and hence use interference cancellation schemes such as dirty paper coding [7] to minimize interference caused to the PU. Underlay systems have no prior knowledge of the PU transmission and instead use power control to limit interference on PUs. In general, the underlay and overlay systems are required to have the knowledge of the channels between the transmitting SU nodes and the PU receivers (Rxs) in order to minimize the interference caused to the incumbent users.

In the *interweave* spectrum access paradigm, the SUs follow the principle of interference avoidance. In order to avoid causing interference to the PUs, prior to transmission, the SUs ensure that the licensed band is not occupied by any PU. To achieve this, the SUs must be aware of the radio environment around themselves. Spectrum sensing is the sensory perception that enables CRs to possess this awareness. Under the interweave spectrum access paradigm, the SUs do not need to have the knowledge regarding the instantaneous channel conditions between them and every PU Rx. This knowledge is a necessary for underlay and overlay schemes and is usually difficult to obtain in real-time systems. In this dissertation, only systems operating under the interweave spectrum access paradigm are considered.

1.2 Spectrum Sensing

Spectrum sensing enables CRs to maintain an awareness regarding the utilization of the licensed radio spectrum. Spectrum sensing is primarily used by SUs operating under the interweave paradigm. Lately, it is also adopted by underlay systems operating in hybrid modes as interweaving systems [8]. Several spectrum sensing algorithms have been discussed in the literature. These can be categorically classified as energy detectors, feature detectors and matched filter based detectors. Each class of detectors has associated pros and cons. Some of the detectors may be more suitable than others in a given situation. For instance, the energy detector is simple to implement and require no prior knowledge about the signal structure. However, it performs badly in low signal to noise ratio (SNR) and under noise uncertainty conditions. Matched filter based detectors can perform better than energy detectors in low SNR condition but require perfect knowledge of the waveform of the signal to be detected. Detailed reviews on various spectrum sensing algorithms can be found in [9, 10]. The next section discusses how spectrum sensors can be operated under different scenarios.

1.3 Operating Modes of Spectrum Sensors

Based on the number of CRs involved and the cooperation sought amongst themselves during spectrum sensing, the operation of spectrum sensors can be classified into two categories, namely,

- Standalone sensing
- Cooperative sensing.

Depending on how many licensed spectral frequency bands are scanned during spectrum sensing, spectrum sensors can be divided into two broad categories, namely,

- Single-band spectrum sensors
- Multi-band spectrum sensors.

The choice of selecting the operating mode of spectrum sensing is influenced by the type of the PU operator(s)/signal(s) and considerations regarding the implementation complexity. More details are discussed in the following sub-sections.

1.3.1 Standalone Spectrum Sensing

Standalone spectrum sensing involves a single CR independently assessing the radio environment using a spectrum sensor. The concerned CR transmits its data only if it is unable to detect a PU transmission during spectrum sensing. Standalone spectrum sensing is simple to implement as it does not involve any communication between devices during the sensing operation. This mode of operation of spectrum sensing is suitable when the spatial density of SU sensors in a geographical location is sparse and the PU signal reception is relatively good. Depending upon the availability of knowledge regarding the PU signalling scheme, an appropriate spectrum sensing algorithm can be adopted to realize the spectrum sensor.

1.3.2 Cooperative Spectrum Sensing

The signal fluctuation inherent to a radio channel degrades the performance of standalone spectrum sensing. Cooperative spectrum sensing (CSS) helps in coping with the ill-effects of fading, shadowing and the hidden node problem. In CSS, multiple SUs, located across different spatial locations are involved in the spectrum sensing process. CSS utilizes the benefit of spatial diversity. Although CSS provides immense benefits, they come at the cost of increased complexity associated with certain implementation issues. For example, different units associated with a CSS network need to maintain communication among themselves. To support such communications, additional control channels are required to be allocated in the already spectrum-scarce scenario. Real-time sensing data are exchanged among cooperating units using special control channels called *reporting channels* and these are discussed later in Section 1.4. Based on the network architecture, CSS schemes can be classified under two categories, namely,

- Centralized CSS
- Decentralized CSS

1.3.2.1 Centralized CSS

In centralized CSS, a central entity, often referred to as the fusion centre (FC), is responsible for taking the final decision regarding the state of spectrum occupancy. The FC is aided by other CRs referred to, in this dissertation, as cooperating secondary users (CSUs) to arrive at a decision. Centralized CSS is suitable when conditions are favourable for setting up a network for supporting reliable two-way communication between CSUs and a designated FC. Centralized CSS can be implemented using relatively simpler sensors as the more complex post-processing steps required during spectrum sensing may be carried out at the FC. The drawback of centralized CSS lies in its dependence on a sole FC for the decision making process. This makes it vulnerable in case the FC becomes inaccessible.

1.3.2.2 Decentralized CSS

Decentralized CSS forms an alternative to centralized CSS. Unlike centralized CSS, there is no designated decision-making entity (or FC) in decentralized CSS. In decentralized CSS, under certain cases, the authority of final decision-making may change with time. While in other cases, the sensing may be distributed wherein, each participating node (or SU) arrives at the final decision on its own after receiving inputs from other SUs. The primary advantage of decentralized CSS is in its ability to operate in the absence of a well established infrastructure.

1.3.3 Single-band Spectrum Sensing

The single-band spectrum sensing scheme involves one or more SU(s) for sensing one particular licensed band. Spectrum sensing may be narrowband or wideband depending on the nature of the band of interest. Technically, single-band spectrum sensing is a binary hypothesis problem [11] involving a null hypothesis and an alternate hypothesis represented as $\mathcal{H}_0$ and $\mathcal{H}_1$, respectively. The null and alternate hypotheses correspond to the absence and presence of the PU transmission, respectively. The performance of a single-band spectrum sensing scheme can be stated in terms of the probabilities of false alarm and miss detection associated with the detection problem.

1.3.4 Multi-band Spectrum Sensing

Multi-band spectrum sensing is the simultaneous sensing of multiple licensed bands. It can be implemented by deploying single-band sensing techniques across the individual bands using dedicated front-ends for each band. Multi-band sensing can also be implemented at each secondary sensor using a single wideband radio front-end and signal processing algorithms such as fast Fourier transform (FFT) or wavelet transform. Such wideband signal acquisition requires very high sampling rate. Apart from using complex sinusoids and wavelets for signal representation as in FFT and wavelet transforms, respectively, algorithms involving *sparse representation* [12–14] can also be adopted for wideband multi-band spectrum sensing.

The study of multi-band spectrum sensing involves a null and an alternate hypotheses corresponding to each of the multiple bands sensed. Let the null and the alternate hypotheses corresponding to the ith band be denoted by $\mathcal{H}_{0i}$ and $\mathcal{H}_{1i}$, respectively. When multi-band sensing technique such as FFT is implemented, there is a non-zero probability of PU signal active in one band being associated with another due to frequency leakage. This gives rise to false associations in addition to miss detection and false alarms as in single-band sensing.

1.4 Reporting Channels

A CSS network requires control channels in order to be operative. In particular, such a network requires reporting channels along with spectrum sensors to be functional. *Reporting channels* are the control channels that carry the information related to spectrum sensing in the network. The quality of the reporting channel has a direct impact on the performance of the CSS network. Such channels can either be dedicated or non-dedicated. For implementing systems with dedicated reporting channels, separate spectral resources are required to be held reserved. However, in the spectrum scarce environment it may not be always possible to have access to vacant bands of spectrum for this purpose. Further, it is difficult to manage such limited resources among multiple CSS networks. Thus, under many circumstances, it is preferable to have a CSS network without dedicated reporting channels.

1.5 Literature Review

The prospect of employing CR technology for solving the spectrum scarcity problem has motivated researchers to look into different aspects of the problem. Spectrum sensing, being a key enabler of this technology has garnered considerable attention in the recent times. In the interweave spectrum access domain, notable research is directed towards development of new spectrum sensing techniques.

1.5.1 Single-band Standalone Spectrum Sensing

As already pointed out, several spectrum sensing algorithms have been reported in the literature. These algorithms can be directly implemented at a lone CR for single-band standalone spectrum sensing. Some significant developments related to important spectrum sensing algorithms are presented here. In [15], Urkowitz analysed the performance of the energy detector for unknown deterministic signals embedded in bandlimited flat Gaussian noise. In [16], Digham *et.al.* analysed the performance of the same detector over Rayleigh and Nakagami fading channels. The performances of the energy detector with diversity reception over κ-μ shadowed fading and κ-μ extreme shadowed fading channels are analysed in [17]. In [18], Chen presented the improved energy detector, a variant of the original energy detector, where the squaring operation of the signal amplitude in the conventional energy detector is replaced with an arbitrary positive power operation. Analysis of energy detectors under various conditions using different system setups are presented in [19–23]

While energy detectors are relatively simple to implement, they suffer from problems associated with noise uncertainty [24] and perform badly in very low SNR conditions. If the signal to be detected is known to possess specific features, feature detectors, which are lesser prone to the noise uncertainty problem [25] can be adopted. Modulated signals are known to inherit cyclostationary features. Gardner discussed the theoretical aspects of signal detection using cyclostationary features for analog modulation schemes in [26]. The discussion was extended to digital modulation schemes in [27]. Cyclostationary feature based detectors for CR applications are discussed in [28–31]. In general, cyclostationary detectors are complex to implement due to

the large number of samples required to perform detection. Practical implemetations of cyclo-stationary based detectors are presented in [32–34]. Another popular class of feature detectors discussed in the literature are the eigen-value based signal detectors. In [35], two detectors: the first, based on the ratio of the maximum to the minimum eigen-values and the second, based on the ratio of the average to the minimum eigen-values of the covariance matrix, are presented. Eigen value based detector in the presence of noise correlation is discussed in [36]. Performance analysis of various eigen-value based detectors are presented in [37].

1.5.2 Single-band Cooperative Spectrum Sensing

Standalone spectrum sensors suffer from the shadowing and fading effects of the wireless channels. As such, a lone spectrum sensor often has difficulty detecting the PU Tx due to the *hidden node problem*, wherein, the PU to be detected remains hidden from the operating sensor. In order to mitigate these issues, CSS scheme was introduced in [38]. The performance improvement achieved by a simple two-user CSS network is analysed in [39]. This analysis was extended to multi-user CSS networks in [40].

The final decsion in a CSS scheme is obtained using either decision or data fusion. In hard decision fusion, the final decision is derived from the binary decisions transmitted by the CSUs. These binary decisons are represented by single bits. In general decision fusion is implemeted using the OR, AND and n-out-of-K voting rules. Hard decision fusion based systems have been explored in [38, 41–44]. In [42, 43] the optimal 'n' in the n-out-of-K voting rule are derived under the minimum total error constraint. In [44] an optimal weighted decision fusion rule is derived assuming different PU SNRs at each CSU sensor. A softened decision fusion using two bits is explored in [45]. Performance of soft decision fusion using arbitrary number of bits is presented in [46]. Data fusion schemes [47–49], that utilize amplify and forward principle to retransmit the test statistics collected by CSUs located across differently to a central FC are known to perform optimally, albeit using more resources for reporting than decision fusion.

Although the literature on CSS, in general, is rich, there are fewer works which consider implementation issues related to reporting channels which are vital for any CSS network. The

reporting channels which are used to exchange sensing information among CSUs or between CSUs and the FC may not be perfect. Several works [42–45, 50–52] either do not consider the effect of the reporting channels or consider them to be error-free. At the same time, some works do exist that include the impact of imperfect reporting channels in the analysis [46, 53–59]. Most of these works assume that the reporting channels are dedicated, i.e., they are separate from the data channels. However, having access to a dedicated frequency band for reporting purposes may not be easy in the spectrum-scarce scenario. Moreover, managing separate dedicated reporting channels increases the overall system complexity. As of now, few works exist that consider the implementation of reporting channels in absence of dedicated resources. In [60–62], schemes are proposed wherein, CSS is implemented without dedicated reporting channels.

1.5.3 Multi-band Spectrum Sensing

The prospect of success in locating spectral vacancies for communication opportunities is significantly enhanced when a search over multiple bands is undertaken instead of a single band. Multi-band spectrum sensing typically requires wideband sensing techniques for implementation. Wideband spectrum sensing (WSS) can be implemented as an extension to the single-band narrowband spectrum sensing (NSS) problem. In this case, the wideband spectrum of interest can be divided into either orthogonal or non-orthogonal overlapping narrow bands where conventional narrowband spectrum sensing can be applied independently using separate radio front-ends. In [63], such an approach is adopted using a bank of polyphase filters where each filter is tuned to a particular band. Alternatively, spectrum sensing can be implemented for the entire wideband using a single radio front-end. In [64] and [65], such WSS is implemented using FFT and wavelet transform, respectively. In [64], an optimal multi-band joint wideband spectrum sensing is presented which jointly maximizes the secondary throughput across all the bands.

Wideband spectrum sensing requires the input radio signal to be sampled at a very high rate to fulfil the conventional Nyquist sampling rate criteria. Analog to digital converters supporting

very high sampling rate are either unavailable or very expensive to be implemented in power-limited devices. This has motivated the adoption of compressive sampling techniques [66] at the radio front-end. These techniques rely on the sparsity of the signal to be detected. Tian and Ginnakis applied wavelet based edge detection techniques on samples obtained by compressive sensing to identify contiguous mass of busy and free spectrum in [67]. Several compressive sampling based techniques are also reported in [68–71].

The domain of WSS is widely explored in general. However, most of the research targets special signals such as OFDM signals as in digital TV broadcasts which vary slowly. Spread spectrum signals represent another important class of wideband signals. These signals are particularly important in military and other secure wireless communications. Frequency hopping spread spectrum (FHSS) is an important spread spectrum technology, usually popular in military communications due to its resilience to frequency selective fading and robustness to eavesdropping. In civilian operations, FHSS is used in popular standards such as bluetooth [72]. Due to fast frequency switching, spectrum sensing in presence of FHSS PU remains a challenging task and conventional spectrum sensing techniques are not always applicable. There are very limited works which deal with the spectrum sensing of FHSS PUs. In [73], an algorithm called FFT averaging ratio (FAR) is developed for wideband sensing. In [74], FAR is adopted in order to detect a single FHSS PU.

1.6 Motivation

The review of the existing literature on spectrum sensing has brought to light certain shortcomings in the state-of-the-art. Reporting channels are vital for any CSS networks. However, reserving dedicated spectrum resources for reporting would only intensify the spectrum scarcity problem. This is specially true for the amplify and forward CSS systems, where the bandwidth requirement for the reporting channels is atleast as much as that of the licensed channel. Practical issues related to the operation of CSS in the absence of dedicated reporting channels have not been extensively treated in the literature. There appears to be ample scope for improvement in this area, which includes the design of novel CSS architecture capable of operating without

dedicated reporting channels.

Secondly, although the literature on spectrum sensing, in general, is rich, sensing of certain class of PU signals such as FHSS signals have not been treated adequately. FHSS signals are difficult to track in the real-time using conventional single-band, multi-band and cooperative sensing techniques due to their fast varying nature. Presence of multiple FHSS PUs makes the problem still harder. Faster and improved tracking techniques are required to deal with such signals.

This research has sought to address these two shortcomings by introducing novel optimization approach, system implementation and detection techniques for improving the performance of spectrum sensing in relation to the state-of-the-art.

1.7 Thesis Contribution

The following are the main contributions of this thesis work:

(i) Derived an optimal voting rule for a conventional hard decision based centralized CSS network operating without dedicated reporting channels. The novelty was in using the added information of difference in the outage probabilities of the reported decisions due to varying PU interference during its presence and absence while deriving the optimal number 'n' in the n-out-of-K voting rule. More specifically,

- Derived the analytical expression for the optimal number 'n' in the n-out-of-K voting rule under the minimum total error constraint, where, total error is defined as the sum of the probability of miss detection and the probability of false alarm.
- Derived the transmit power constraint to be followed by all CSUs during reporting in order to limit the interference on the PU.

(ii) Developed a novel decentralized CSS scheme capable of operating in the absence of dedicated reporting channels and analysed its performance. In particular,

- Presented a CSS model that uses minimal number of sensors for power conservation.

- Developed an infrastructure capable of supporting transmission of quantized version of the test statistics generated at a remote sensor for possible soft decision fusion.
- Included features in cognitive radio network design to avoid traffic congestion among contending SU Txs.
- Derived transmit power constraint for SU Txs to minimize the interference at PU.
- Proposed a joint test using local and quantized test statistics from a remote sensor.
- Derived closed form analytical expressions for the probability of detection and the probability of false alarm under ideal and realistic operating conditions.

(iii) Presented sparse representation based spectrum sensing techniques for fast real-time detection of FHSS PUs. The thesis

- Introduced and implemented the idea of application of data-dependent *exemplar dictionary* for tracking FHSS PU Tx in the multi-band spectrum sensing scenario.
- Developed a framework for detection of multiple FHSS PUs present in the wideband of interest using data-dependent exemplar dictionary.

1.8 Thesis Organization

The remaining of this dissertation is organized as follows.

Chapter 2 presents a novel strategy of implementing CSS in a conventional centralized decision fusion CSS network, operating without dedicated reporting channels. The knowledge regarding the difference in outage of the reported decisions from the CSUs to the FC, due to presence and absence of the PU, is utilized to optimize and improve the performance of the n-out-of-K voting rule. The optimal value of 'n' for the n-out-of-K voting rule is derived subject to minimum total error, where, the total error is defined as the sum of probability of miss detection and probability of false alarm. Also derived in this chapter is the transmit power constraint that each CSU must follow to limit interference to any PU.

Chapter 3 presents a novel decentralized CSS architecture capable of operating in absence of dedicated reporting channels. The proposed architecture supports a mobile sensor and is

accompanied by SU relays, to assist a potential SU Tx in spectrum sensing. The CSS network leverages on the superior sensing performance of the mobile sensor which can place itself in an area of good PU signal reception with ease, using radio environment maps [75]. The mobile sensor also has capability to transmit quantized test statistics which can be used for soft decision fusion. The network model also adopts well-tested random access and exponential backoff principles to resolve and minimize conflicts among multiple contending SU Txs. The chapter also derives closed form expressions for probability of detection and probability of false alarm associated with the CSS scheme.

Chapter 4 presents sparse representation based spectrum sensing techniques for the real-time detection of multiple unknown number of FHSS PUs. It introduces the novel idea of using data-dependent exemplar dictionary for faster spectrum sensing of FHSS signals. Simulations were conducted which established the superiority of the data-dependent exemplar dictionary over conventional Fourier dictionary both in terms of sensing time and detection performance.

Finally, Chapter 5 summarizes the contributions made in the thesis. This chapter also discusses some of the issues which can be addressed as future extension of the works reported in this thesis.

2

Utilizing PU Interference in Centralized Cooperative Spectrum Sensing

Contents

In a conventional centralized decision fusion CSS scheme [38, 41–44], decisions from multiple CSUs are fused in an FC using OR/AND or n-out-of-K voting rule. In this chapter, a novel strategy for enhancing the performance of a conventional centralized decision fusion CSS scheme operating in the absence of dedicated reporting channels is presented. The hard decisions of the CSUs are reported to the FC through the licensed channel. In such a CSS network, the reported decisions suffer higher rates of outage when the PU Tx is active than when it is inactive. This difference in outage rates is attributed to the higher interference of signals from CSUs due to the additional interference from the active PU Tx. The knowledge of this difference in outage probability is utilized to derive the optimal n-out-of-K voting rule. It is found that the application of this knowledge improves the performance of CSS compared to the case when that is not applied.

Section 2.1 describes the system model. Section 2.2 describes the scheme in detail. Equation (2.10) states the optimal value of 'n' for the n-out-of-K voting rule. Equation (2.11) represents the total error for the CSS schemes considering difference in outage rates when the detection thresholds at each CSU is set at infinity. Equation (2.12) represents the same for the case without considering difference of outage rates. The transmit power limit for each CSU for limiting interference caused to any PU is also derived. Numerical examples are presented in Section 2.3. Finally, the summary is presented in Section 2.4.

2.1 System Model Description

A decision fusion cooperative spectrum sensing scenario consisting of a PU transmitter P, a PU receiver R, N CSUs (C_i, $i = 1, 2 \ldots, N$) and an FC F is considered as shown in Figure 2.1. The cognitive radio system follows the interweave model [6] for avoiding interference with the PU. The distances of the CSUs and the FC from the PU are assumed to be large in comparison to the distances between any two CSUs or those between any CSU and the FC. This scenario typically prevails in most urban localities where the indoor secondary networks are sufficiently far from a PU transmitter such as a TV or a radio station. All wireless channels are assumed to undergo Rayleigh flat fading although the proposed scheme can be extended to other channel

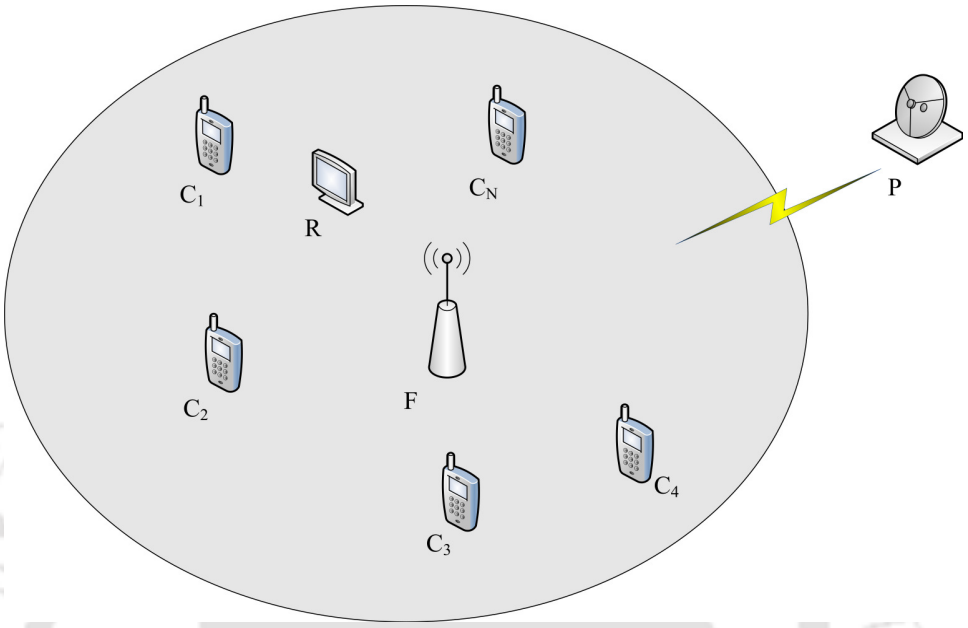

Figure 2.1: *Centralized cooperative sensing network consisting of N cooperating secondary users ($C_i, i = 1, 2 \ldots N$), one fusion center (F), one PU transmitter (P) and one PU receiver (R).*

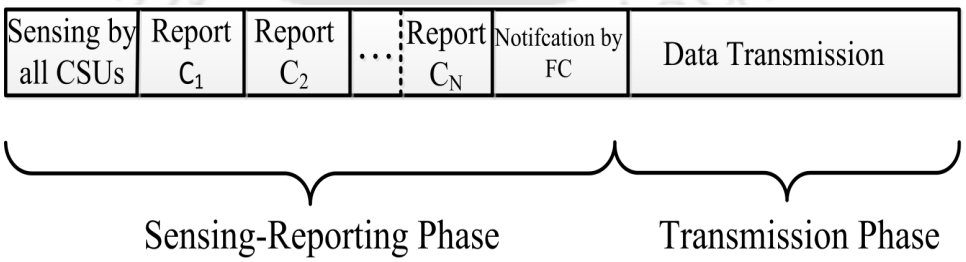

Figure 2.2: *Time-slot structure of the secondary network in the proposed CSS scheme.*

models. The time-frame of the secondary network is divided into a sensing-reporting (SR) phase and a transmission (TR) phase [42, 76] as shown in Figure 2.2. Each spatially distributed CSU senses the spectrum in a periodic sensing slot at the beginning of the SR phase and takes a decision regarding the presence or absence of the PU. This decision is forwarded to the FC in a fixed time slot allotted to each CSU within the remaining duration of the SR phase. For spectrum sensing, the CSUs can employ any suitable scheme such as energy detection [16], cyclostationarity [77] criterion, eigenvalue decomposition [35] and compressive sensing [67]. Energy detectors are simple to implement in practice since they do not require prior knowledge about the signal structure. In this work, we assume that each CSU employs an energy detector for spectrum sensing. The average probability of detection at the ith CSU can be represented as $P_{d_i}(\lambda_i, N_s, \bar{\gamma}_{\mathsf{P}_i})$, which is a function of the detection threshold λ_i [16, 42], the time-bandwidth product N_s of the detector and the average received PU *signal to noise ratio* (SNR) $\bar{\gamma}_{\mathsf{P}_i}$. Similarly, the false alarm can be represented as $P_{f_i}(\lambda_i, N_s)$. The explicit expressions for $P_{f_i}(\lambda_i, N_s)$ and $P_{d_i}(\lambda_i, N_s, \bar{\gamma}_{P_i})$ under Rayleigh fading are derived in [16] and are given as

$$P_{f_i} = \frac{\Gamma(N_s/2, \lambda_i/2\sigma_n^2)}{\Gamma(N_s/2)} \tag{2.1}$$

$$P_{d_i} = \exp\left(-\frac{\lambda_i}{2\sigma_n^2}\right) \sum_{l=0}^{\frac{N_s}{2}-2} \frac{\left(\frac{\lambda_i}{2\sigma_n^2}\right)^l}{l!} + \left(\frac{2\sigma_n^2 + a\bar{\gamma}_i}{a\bar{\gamma}_i}\right)^{\frac{N_s}{2}-1} \times \left[\exp\left(-\frac{\lambda_i}{2\sigma_n^2 + a\bar{\gamma}_i}\right) - \exp\left(-\frac{\lambda_i}{2\sigma_n^2}\right) \sum_{l=0}^{\frac{N_s}{2}-2} \frac{\left(\frac{\lambda_i a\bar{\gamma}_i}{2\sigma_n^2(2\sigma_n^2 + a\bar{\gamma}_i)}\right)^l}{l!}\right], \tag{2.2}$$

where, $a = 2$, and σ_n^2 is the noise variance.

It is assumed that the reporting channel, the CSU data channel and the PU licensed channel are coincident, i.e., sharing the same frequency band. In practice, the reporting channels are perturbed by noise and fading effects. This leads to outages in reporting. In order to detect these outages, it is assumed that the reported decisions are encoded with error control codes such as cyclic redundancy check (CRC) codes. It is to be noted that typically CRC is used to detect errors during transmission and initiate retransmission if found. However, in our proposal, CRC is used for the purpose of error detection only. Retransmission of decisions by the CSUs

is avoided so that the additional slots required for the same can be utilized during the TR phase. Instead of retransmitting the decisions, the proposed scheme takes cue from the number of outages itself to enhance sensing. At the FC, the outage probability of the ith reporting channel in presence of the PU is denoted as P_{E1_i} while the same in absence of the PU is denoted as P_{E0_i}. It is argued that in general $P_{E1_i} \geq P_{E0_i}$, since a higher level of interference from the PU transmitter would lead to a higher outage. The decision by the FC is transmitted to the secondary transmitter at the end of the SR phase. Finally, the secondary transmitter sends its message in the TR phase.

2.2 Decision Fusion under Outage Difference

Assume, at the FC, only K out of N reported decisions are decodable (i.e., with CRC intact) while the rest undergo outage. The outage probabilities at the FC are given as

$$P_{E0_i} = Pr\{\gamma_{i\mathsf{F}} < \gamma_{\text{out}}\} = 1 - \exp\left(-\frac{\gamma_{\text{out}}}{\bar{\gamma}_{i\mathsf{F}}}\right), \tag{2.3}$$

$$P_{E1_i} = Pr\left\{\frac{\gamma_{i\mathsf{F}}}{1+\gamma_{\mathsf{PF}}} < \gamma_{\text{out}}\right\} = 1 - \frac{\exp\left(-\frac{\gamma_{\text{out}}}{\bar{\gamma}_{i\mathsf{F}}}\right)\bar{\gamma}_{i\mathsf{F}}}{\gamma_{\text{out}}\bar{\gamma}_{\mathsf{PF}} + \bar{\gamma}_{i\mathsf{F}}} \tag{2.4}$$

where $\gamma_{i\mathsf{F}}$ is the instantaneous SNR of the reporting signal from the ith CSU at the FC, γ_{PF} is the instantaneous SNR of the PU signal at the FC and γ_{out} is the outage *signal to interference plus noise ratio* (SINR), i.e., below which a reported decision is lost. The determination of γ_{out} is discussed in Section 2.3. The channels between the ith CSU and the FC, and the PU and the FC are assumed to be under Rayleigh fading with average SNRs $\bar{\gamma}_{i\mathsf{F}}$ and $\bar{\gamma}_{\mathsf{PF}}$, respectively. The value of $\bar{\gamma}_{\mathsf{PF}}$ can be obtained using radio environment mapping technique as described in [78–80]. The value of $\bar{\gamma}_{i\mathsf{F}}$ can be updated periodically using periodic training sequences between CSUs and the FC.

Under the assumption that the secondary network elements (the CSUs and the FC) occupy a limited spatial area, which aptly fits the network model considered in this chapter, the average signal to noise ratios at these devices can be assumed to be same i.e., $\bar{\gamma}_{\mathsf{P}i} = \bar{\gamma}_{\mathsf{PF}}$. The CSU sensors are operated at thresholds, $\lambda_i = \lambda$ (say) to satisfy a false alarm constraint of ϵ. The n-out-of-K voting rule [42] is the optimal fusion rule under such circumstances. The AND, OR, and the

MAJORITY fusion rules are special cases of this voting rule where the 'n' is adjusted to be K, 1 and $\lceil (K/2) \rceil$, respectively. In [42], the optimal 'n' for the voting rule has been derived under perfect reporting channel conditions. In this letter, we derive the optimal 'n' taking into account the number of outages $(N - K)$ which has a statistical dependence on the presence or absence of the PU. For brevity, $P_{f_i}(\lambda, N_s)$ and $P_{d_i}(\lambda, N_s, \bar{\gamma}_{P_i})$ are, henceforth, denoted as P_{f_i} and P_{d_i}, respectively. The false alarm $P_F(N, \lambda)$ and the probability of missed detection $P_M(N, \lambda)$ at the FC are given as

$$P_F(N,\lambda) = \sum_{K=0}^{N} \sum_{l=n_K}^{K} \left[\binom{K}{l} P_{f_i}^{l} (1 - P_{f_i})^{K-l} \times \binom{N}{K} P_{E0_i}^{N-K} (1 - P_{E0_i})^{K} \right] \equiv P_F, \tag{2.5}$$

$$P_M(N,\lambda) = 1 - \sum_{K=0}^{N} \sum_{l=n_K}^{K} \left[\binom{K}{l} P_{d_i}^{l} (1 - P_{d_i})^{K-l} \times \binom{N}{K} P_{E1_i}^{N-K} (1 - P_{E1_i})^{K} \right] \equiv P_M \tag{2.6}$$

where n_K denotes the minimum number of votes required in favour of PU's presence. An objective function referred to as total error (TE) is defined as follows [42]

$$\text{TE} = F(N,\lambda) = P_F + P_M = 1 + \sum_{K=0}^{N} S(n_K, \lambda), \tag{2.7}$$

where

$$S(n_K,\lambda) = \sum_{l=n_K}^{K} \binom{K}{l} \Big[P_{f_i}^{l} (1 - P_{f_i})^{K-l} \times P_{E0_i}^{N-K} (1 - P_{E0_i})^{K} - P_{d_i}^{l} (1 - P_{d_i})^{K-l} \times P_{E1_i}^{N-K} (1 - P_{E1_i})^{K} \Big] \binom{N}{K}. \tag{2.8}$$

Note that, the objective function TE is proportional to the total error rate (TER) defined in [43], when P_0, the prior probability assigned to the PU inactive state is taken as 0.5. Adopting TE as the objective function is appropriate when P_0 is not known. Ignorance of P_0 is very likely considering that the SUs do not have any information about the operating schedule of the PU.

2.2.1 Derivation of Optimal Voting Rule given N and λ

Minimizing $F(N, \lambda)$ boils down to the problem of minimization of the summand $S(n_K, \lambda)$ in (2.7) with respect to n_K for $K = 1, 2 \ldots, N$. It is to be noted that choosing $n_K = n$ (i.e.,

independent of K) could have been another approach but that would be suboptimal. In the following derivation, we denote n_K by m for brevity. As outlined in [42], the partial derivative of $S(m, \lambda)$ with respect to m can be expressed as

$$\begin{aligned}\frac{\partial S(m,\lambda)}{\partial m} &\approx S(m+1,\lambda) - S(m,\lambda) \\ &= \binom{N}{K}\binom{K}{m}\Big[P_{d_i}^{m}(1-P_{d_i})^{K-m}P_{E1_i}^{N-K}(1-P_{E1_i})^{K} \\ &\qquad \times P_{f_i}^{m}(1-P_{f_i})^{K-m}P_{E0_i}^{N-K}(1-P_{E0_i})^{K}\Big]. \end{aligned} \tag{2.9}$$

Setting (2.9) to zero and noting that the derived value should be a whole number between 0 and K, the optimal value of n_K, denoted as, $n_{K_{\text{opt}}}(\lambda)$, is given as

$$n_{K_{\text{opt}}}(\lambda) = \max\left\{0, \min\left\{K, \left\lceil \frac{K\,[1+\beta(\lambda)]}{1+\alpha(\lambda)} + \frac{[N-K]\,\theta(\lambda)}{1+\alpha(\lambda)} \right\rceil\right\}\right\} \tag{2.10}$$

where $\theta(\lambda) = \log_Y\{P_{E1_i}/P_{E0_i}\}$, $\alpha(\lambda) = \log_Y\{P_{f_i}/P_{d_i}\}$ and $\beta(\lambda) = \log_Y\{(1-P_{E1_i})/(1-P_{E0_i})\}$ with $Y = \frac{1-P_{d_i}}{1-P_{f_i}}$. For $P_{E0_i} = P_{E1_i}$, the required optimum number of favouring votes (i.e., $n_{K_{\text{opt}}}$) in (2.10) becomes invariant to N. Note that, this rule also becomes similar to the one derived for the dedicated reporting channel in [42, Eqn. 8]. The decision rule in (2.10) is referred to as the *proposed* voting rule (PVR). The decision rule given in [42, Eqn. 8] is referred to as the *default* voting rule (DVR) and is used here in a slightly different context to provide a fair contrast to the PVR. Unlike in [42], where K denotes the total number of CSUs, here, it represents the number of valid votes received at the FC. To demonstrate how the inclusion of the effect of the difference in outage affects the performance of the n-out-of-K voting rule, let us consider a specific case where $N = 8$, $N_s = 6$ and the PU-SNR at a secondary user is 0 dB. The TE plots of the PVR and DVR for varying detection threshold are shown in Figure 2.3. It can be observed that the PVR consistently yields lower TE values than the DVR in the case when $P_{E0_i} < P_{E1_i}$. Thus, with the exploitation of differences in the outage probabilities, a boost in the detection performance of the FC detection is observed. For $P_{E0_i} < P_{E1_i}$, as $\lambda \to \infty$, the TE hits saturation values. Let AsyTE_p and AsyTE_e denote the asymptotic TE values for the PVR and DVR, respectively. The

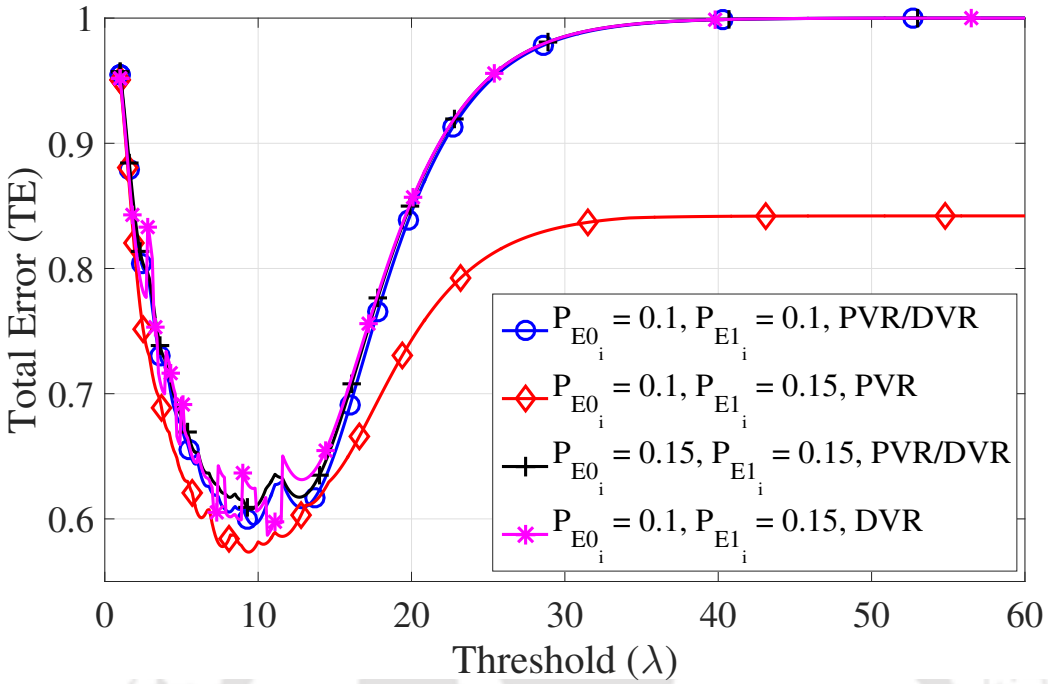

Figure 2.3: *Effect of different outage probabilities on Total Error. It can be noted that the proposed voting rule (PVR) provides boost in the PU detection when outage probabilities differ across PU active and inactive cycles, whereas it converges to the DVR when no such difference exists.*

asymptotic TEs are given as

$$\begin{aligned}\text{AsyTE}_p &\equiv \lim_{\lambda\to\infty} F(N,\lambda)|_{\text{proposed}} \\ &= 1 + \sum_{K=0}^{K_l} \binom{N}{K} \left[P_{E0_i}^{N-K}(1-P_{E0_i})^K - P_{E1_i}^{N-K}(1-P_{E1_i})^K \right] \end{aligned} \tag{2.11}$$

$$\text{AsyTE}_e \equiv \lim_{\lambda\to\infty} F(N,\lambda)|_{\text{default}} = 1 + P_{E0_i}^N - P_{E1_i}^N, \tag{2.12}$$

where $K_l = \left\lfloor \frac{-N\log(P_{E1_i}/P_{E0_i})}{\log[\{(1-P_{E1_i})P_{E0_i}\}/\{(1-P_{E0_i})P_{E1_i}\}]} \right\rfloor$. The proofs of (2.11) and (2.12) are outlined in Appendix A. The asymptotic TE is a measure of how much information can be derived from the difference in outages alone. It can be easily verified that when $P_{E1_i} = P_{E0_i}$, the Asymptotic TEs for both PVR and DVR converge to unity.

2.2.2 Interference Limiting at the PU receiver

Let Z represent the interference power received at a PU receiver due to the reporting by CSUs. It can be expressed as

$$Z = \frac{1}{N} \sum_{i=1}^{N} P_s |h_{i\mathsf{R}}|^2 \tag{2.13}$$

where P_s represents the power of the reporting signal transmitted by each of the CSUs and $h_{i\mathsf{R}}$ is the gain of the channel between the ith CSU and the PU receiver. The factor $1/N$ accounts for the fact that each CSU occupies Nth fraction of the PU channel during reporting due to the time-slotted structure. The instantaneous signal to interference ratio (SIR) at the primary receiver is given as

$$\gamma_{\mathsf{PR}} = \frac{P_P |h_{\mathsf{PR}}|^2}{(1/N) \sum_{i=1}^{N} P_s |h_{i\mathsf{R}}|^2} \tag{2.14}$$

where h_{PR} is the gain of the channel between primary transmitter and receiver. Let $P_{\mathsf{Pout}} = Pr\{\gamma_{\mathsf{PR}} < \gamma_{P\mathsf{out}}\}$ represent the tolerable outage probability at the PU receiver due to interference by CSUs. We use the fact that $|h_{\mathsf{PR}}|^2$ is exponentially distributed random variable (RV) with mean σ^2_{PR}. And $|h_{i\mathsf{R}}|^2$s are independent and exponentially distributed RVs with mean $\sigma^2_{i\mathsf{R}}$. Following [81], the maximum reporting power that is permissible without affecting the quality of service of the primary network can be expressed as

$$P_{s_t} = \frac{P_{\mathsf{P}} \sigma^2_{\mathsf{PR}} N[1 - (1 - P_{\mathsf{Pout}})^{(1/N)}]}{\sigma^2_{i\mathsf{R}} (1 - P_{\mathsf{Pout}})^{(1/N)} \gamma_{\mathsf{Pout}}} \tag{2.15}$$

where $\gamma_{\mathsf{Pout}} = 2^{r_{\mathsf{P}}} - 1$ is the outage SNR threshold at the PU receiver with r_{P} being the PU data rate.

2.3 Numerical Examples

Let T_R be the rate of transmission of the reporting scheme in symbols per second, L_R be the length of the packet including the CRC and optional forward error correction codes. Let E_R be the maximum number of errors that can be corrected by any error correction code if included. It is assumed that the error control scheme would be able to detect any residual errors and discard corrupted and unintelligible reported packets before applying the optimal n-out-of-K rule on K

valid reports. If C_{out} represents the outage capacity of the reporting channel between any CSU and the FC, then

$$C_{\text{out}} = T_R\left(1 - \frac{E_R}{L_R}\right) \tag{2.16}$$

and the corresponding outage SINR γ_{out} can be expressed as

$$\gamma_{\text{out}} = M^{C_{\text{out}}/B} - 1 = M^{\zeta(1-\eta)} - 1 \tag{2.17}$$

where M is the number of symbols which is dependent on the type of modulation adopted in the reporting scheme, B is the bandwidth of the reporting channel, $\zeta = \frac{T_R}{B}$ and $\eta = \frac{E_R}{L}$.

The performances have been evaluated for $M = 2$, $\zeta = 0.005$ and noise variance σ_n^2 at each node set as unity. The average channel gain between two nodes X and Y is denoted as σ_{XY}^2 where, $X, Y \in \{\mathsf{P}, \mathsf{R}, \mathsf{C}_i, \mathsf{F}\}$. For notational simplicity, C_i is replaced by i in the rest of this chapter, thus, $\sigma_{\mathsf{C}_i\mathsf{R}}^2 \equiv \sigma_{i\mathsf{R}}^2$. Figure 2.4 shows the variation of the optimal number of votes with λ for the PVR and the DVR. From Figure 2.3, we note that the TE obtains a global minimum value for given P_{E0_i} and P_{E1_i}. For different values of received PU-SNR ($\bar{\gamma}_{\mathsf{PF}}$) and N, the operating threshold λ corresponding to the minimum TE is determined by linear grid search using (2.3), (2.4), (2.7), (2.17) and setting $\bar{\gamma}_{iF} = P_{s_t}\left(\frac{\sigma_{i\mathsf{F}}^2}{\sigma_n^2}\right)$. In Figure 2.5, the minimum TEs associated with the DVR and the PVR are plotted against $\bar{\gamma}_{\mathsf{PF}}$. As expected, the PVR, in general outperforms the DVR. However, the curves corresponding to both the rules, tend to coincide at extremely low as well as high PU-SNRs. At very low PU-SNRs, the difference in outages becomes negligible and can be noted from Table 2.1. Hence, both the rules converge. At extremely high PU-SNRs, the loss of all the reported decisions becomes inevitable when the PU is active. Thus, both the rules decide in favour of the presence of the PU in the event of such total outage. In those cases, the performance of the DVR depends on the number of false alarms and on total outages occurring during the absence of the PU. On the other hand, the proposed rule is invariant to false alarms in those cases. Since, at high PU-SNRs, there is very low false alarm rate at each of the CSUs, the DVR performs as good as the PVR. Figure 2.6 shows Asymptotic TE versus PU-SNR for different values of N.

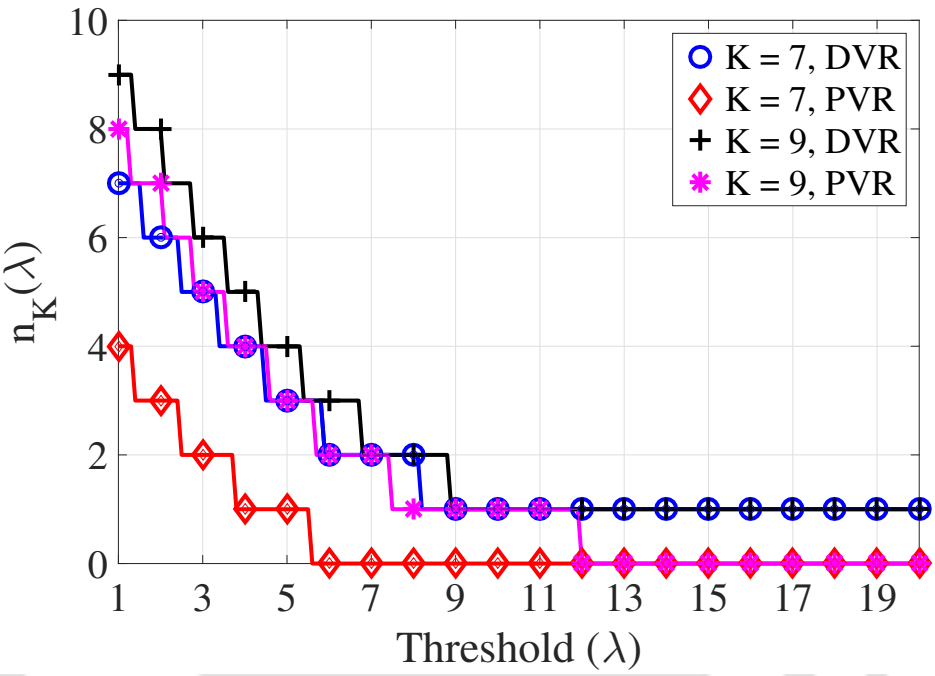

Figure 2.4: *Variation of optimal number of votes with respect to λ for $N = 10$, $N_s = 4$, $\eta = 0.3$, $\zeta = 0.005$, $P_{Pout} = 0.08$, $\bar{\gamma}_{PF} = -1$ dB, $\sigma^2_{iR} = \sigma^2_{iF} = 1$, $\sigma^2_{PF} = \sigma^2_{PR} = \sigma^2_{Pi} = 0.5$ and $r_P = 1$ bit/s/Hz for different number of valid votes (K) received at the FC.*

Table 2.1: Effect of very high and low PU-SNRs on outage probabilities.

η	P_{Pout}	$\bar{\gamma}_{PR}$ (in dB)	P_{E0_i}	P_{E1_i}
0.3	0.08	-10	0.376	0.405
		10	0.024	0.214
0.8	0.05	-10	0.611	0.644
		10	0.009	0.095

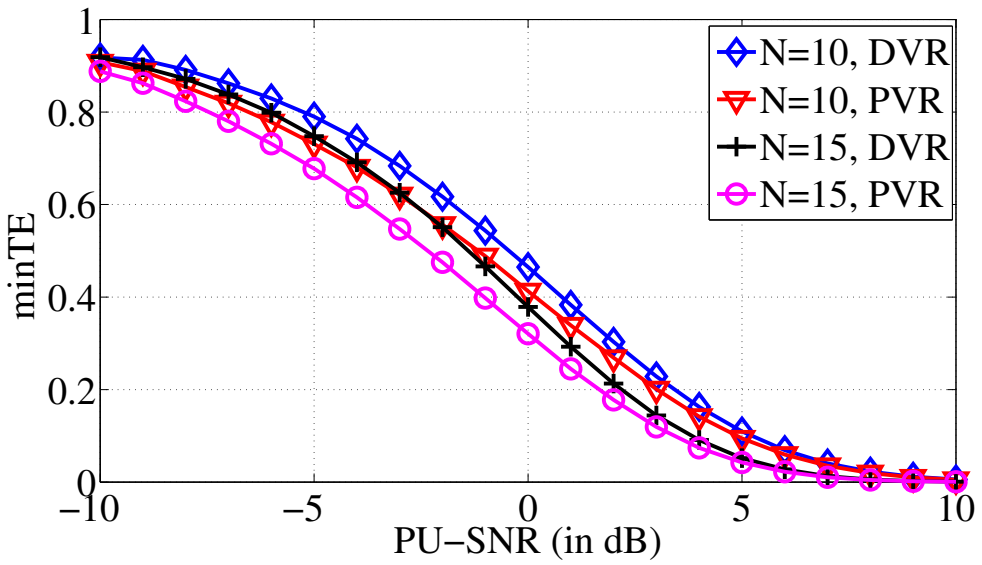

Figure 2.5: *Variation of minTE with PU-SNR ($\bar{\gamma}_{\mathrm{PF}}$) for $N_s = 4$, $\eta = 0.3$, $P_{\mathrm{P}_{out}} = 0.08$, $\zeta = 0.005$, $\sigma^2_{i\mathrm{R}} = \sigma^2_{i\mathrm{F}} = 1$, $\sigma^2_{\mathrm{PF}} = \sigma^2_{\mathrm{PR}} = \sigma^2_{\mathrm{P}i} = 0.5$ and $r_{\mathrm{P}} = 1$ bit/s/Hz.*

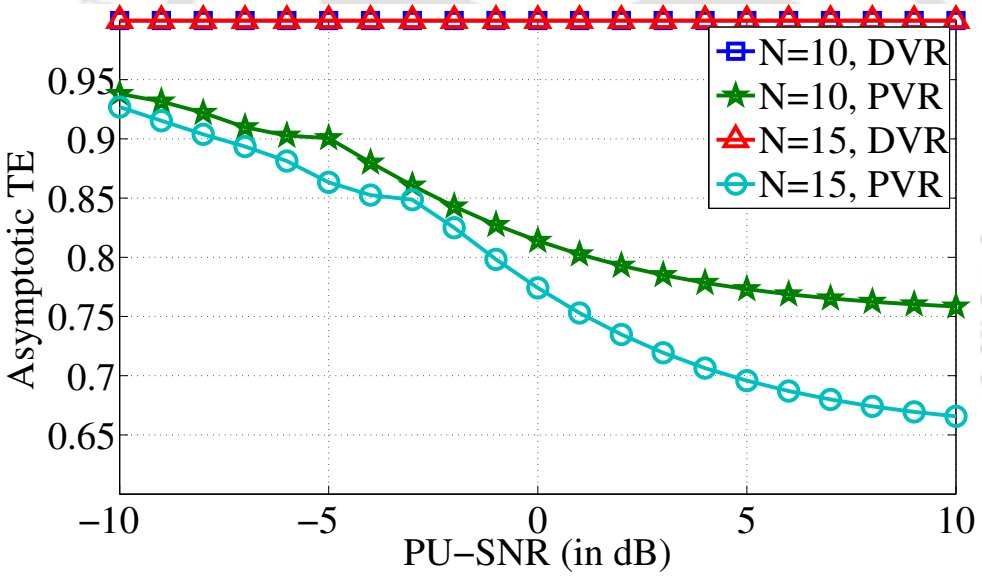

Figure 2.6: *Variation of AsyTE with PU-SNR ($\bar{\gamma}_{\mathrm{PF}}$) for $N_s = 4$, $\eta = 0.3$, $P_{\mathrm{P}_{out}} = 0.08$, $\zeta = 0.005$, $\sigma^2_{i\mathrm{R}} = \sigma^2_{i\mathrm{F}} = 1$, $\sigma^2_{\mathrm{PF}} = \sigma^2_{\mathrm{PR}} = \sigma^2_{\mathrm{P}i} = 0.5$ and $r_{\mathrm{P}} = 1$ bit/s/Hz.*

2.4 Summary

This chapter introduced a novel approach for optimizing the performance of a conventional centralized decision fusion CSS network operating in the absence of dedicated reporting channels. The optimal number 'n' in the n-out-of-K voting rule has been derived as a function of the

detector threshold at each CSU and the total number of votes N. Here, K represents the number of votes out of N that have been successfully decoded at the FC in a particular sensing slot. For optimization purpose, the objective function is taken as the total error which is defined as the sum of probability of miss detection and the probability of false alarm. With the reduction with the total error jointly reduces both kinds of errors get minimized. As a result, the overall utilization of the spectral band is maximized.

The conventional centralized model presented in this chapter has certain limitations. Firstly, the procedure of electing one SU transmitter among multiple contending SU transmitters is neither defined nor integrated in such a CSS scheme. The election has to be done separately using techniques such as polling or interrupts. This would cost additional resources in the form of time-slot or spectrum. Secondly, additional resources would also be required to transmit the decision transmitted by the FC to the transmitting SU. The transmission containing the decision has to be highly redundant so that outage is avoided. In the next chapter, a decentralized model of CSS is proposed which removes the need of having a centralized FC and integrates the process of electing an SU Tx with the CSS scheme.

3

Decentralized Cooperative Spectrum Sensing and Access in Absence of Dedicated Reporting Channels

Contents

In Chapter 2, a strategy for improving the performance of a conventional centralized decision fusion CSS scheme was presented. Although, the centralized schemes have a simple architecture and apparently easier to implement, there are certain drawbacks. Firstly, there is no mechanism integrated in such a CSS scheme to resolve conflict among multiple contending SU transmitters. In the centralized architecture discussed in Chapter 2, the SU transmitter is assumed to be determined *apriori* by other independent mechanisms e.g., polling, interrupts etc. Secondly, the system requires additional resources to broadcast the decision taken by the FC about the presence/absence of the PU to the CSUs. In the absence of a dedicated reporting channel, this resource can be in the form an additional time slot. The scheme proposed in this chapter can sort out the conflicts among contending SU transmitters. Further, its performance has been analysed including the effect of uncertainty in the received SNR of the signal from another SU node. This uncertainty arises due to the imperfection in the feedback mechanisms that are meant to update the information at an SU node about the signal strengths from other SU sources in the network.

The fact that CSS based on soft decision fusion can potentially provide dection gain over hard decision fusion has already been reported in [46]. Unlike hard decision fusion, the systems employing soft decision fusion segregate the range of the test statistics into more than two levels. This allows for more close replication of the performance of an optimal data fusion system. However, when the reporting channels are very poor, the use of higher level quantization levels does not help. Instead, the increased information rate leads to higher outages of the reported test statistics. This, in turn, degrades the overall detection performance of CSS [54]. There are existing works which treat the problem of soft decision fusion in presence of dedicated reporting channels [55–57]. However, while reporting through the licensed channel, special care has to taken in order to prevent interference caused to the incumbent PUs. To the best of the authors' knowledge, the utilization of the possible benefit of soft decision fusion in a CSS network, operating without dedicated reporting channels is not yet reported. Previous works [60–62] consider hard decision fusion in which sensing information is transmitted using a single bit. The CSS scheme proposed in this chapter facilitates the transmission of quantized test statistics

in a scenario without dedicated reporting channels for possible soft decision fusion. Moreover, the proposed CSS system possesses some additional features which are not supported in the related models presented in [60, 61] and the centralized scheme discussed in Chapter 2. Those are summarized as follows:

(i) *On-demand Service*: All the SUs in the network get equal opportunity to access a detected spectral hole when it is needed for data transmission. In the proposed scheme, there is no need for any centralized entity or additional time for setting up a SU Tx. Channel access is integrated with the CSS scheme.

(ii) *Energy Conservation*: It has the minimal number of sensing elements to reduce the energy consumption during spectrum sensing.

(iii) *Collision Avoidance*: It employs the principle of random access scheme to avoid collision among the contending SU transmitters in the network.

Although *on-demand service* is claimed to be supported in the model presented in [61], it is not specified how a particular SU transmitter would be selected amongst the set of contending SUs. The inclusion of the above features has been made possible by the selection of the network structure, details of which will be discussed in Section 3.1. Power control is adopted to limit interference at any PU receiver. Closed form expressions for the overall false alarm and probability of detection are derived for the proposed model. Finally, using numerical experiments and Monte-Carlo simulations, conclusions are drawn regarding situations where the use of quantized test statistics can benefit the proposed CSS scheme.

The rest of this chapter is organized as follows. Section 3.1 describes the system model. In Section 3.2, a limit on the transmission power to be used by secondary users while reporting is derived. The outages of various secondary links when the primary user is present and absent are derived in Section 3.3. The details pertaining to the proposed CSS scheme is discussed in Section 3.4. Section 3.5 presents the performance analysis of the proposed system. In Section 3.6 an existing selective-reporting based CSS scheme has been discussed and the same is used to provide a contrast to the proposed CSS scheme. Section 3.7 presents some numerical

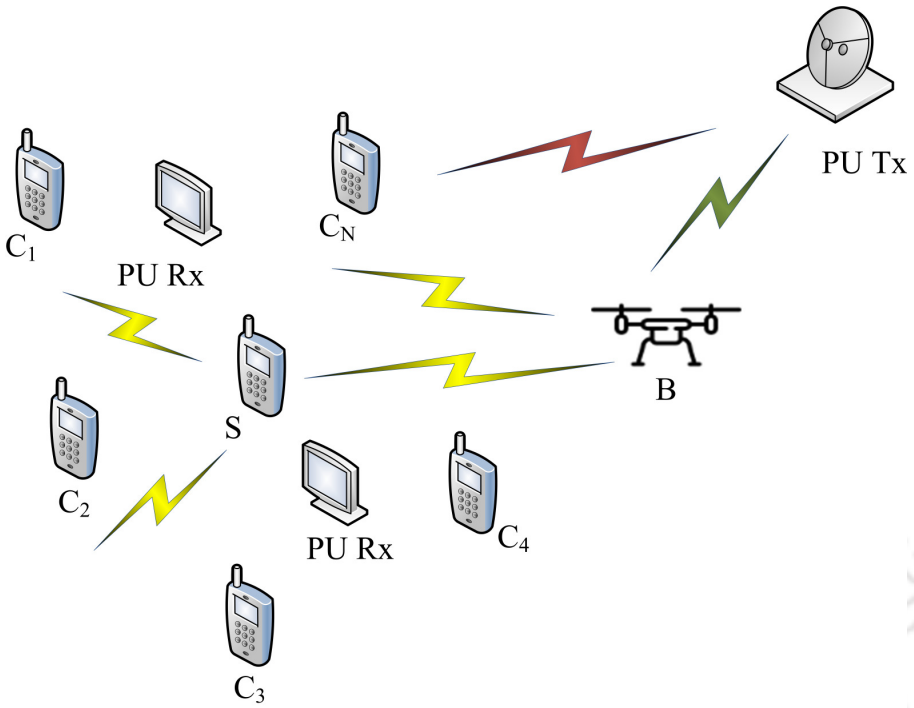

Figure 3.1: A radio environment comprising of PUs and a set of $N + 2$ SUs $(\mathsf{B}, \mathsf{S}, \mathsf{C}_1, \mathsf{C}_2, \ldots, \mathsf{C}_N)$.

examples, results, and validation through simulation. Finally, Section 3.8 concludes the chapter with a brief summary.

3.1 System Model Description

The PU network consists of one PU transmitter (PU Tx) and multiple spatially distributed PU receivers as shown in Figure 3.1. The CSS network consists of $N + 2$ SUs which include one leading secondary sensor node (LSSN) B. It is assumed that B has a good reception of the PU signal. How this is achieved is discussed later in this section. The node B senses and evaluates a test statistics and quantizes it using an appropriate quantizer. In this work, for simplicity and mathematical tractability, we assume that all secondary sensors employ a energy detector for local spectrum sensing. Note that the energy detectors can be easily replaced by other kinds of spectrum detectors in the network model considered here. All the wireless links are assumed to undergo Rayleigh flat fading although this system model can also be extended to other channel models. When a particular SU needs to transmit data to any other node in the network, it assumes the role of a SU transmitter and spectrum sensor. We refer to this particular

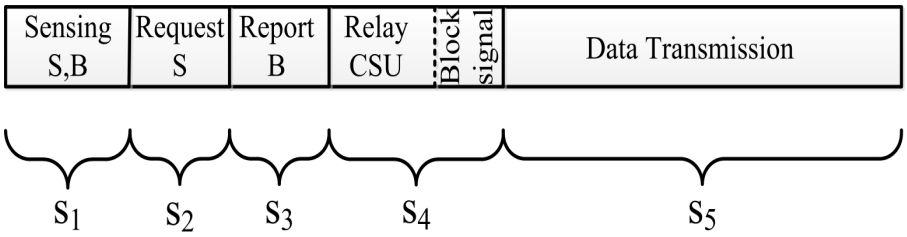

Figure 3.2: Time-slot structure of the secondary network in the proposed CSS scheme.

SU node as S. The N remaining SUs, excluding B are referred to as the cooperating secondary users (CSUs) with respect to S and denoted by C_i, $i = 1, 2, \ldots, N$. The SU node S requests for assistance from the other CSUs only when it does not detect the PU Tx on its own. A time slotted network structure is assumed as shown in Figure 3.2. The secondary network time slot is divided into five sub-slots, denoted as s_1, s_2, s_3, s_4 and s_5. In sub-slot s_1, both B and S nodes perform independent spectrum sensing. The sub-slot s_2 is reserved for transmission by S, to inform other CSUs of its intention to transmit, if it is able to detect the PU on its own. This sub-slot is also used by S to request for cooperation from other CSUs in the network in the event it does not detect the PU Tx. Additionally, prior to sending out the request, S transmits a pilot sequence within this sub-slot. This pilot is used by all CSUs lying within reach to estimate the instantaneous state of the channels between them and S. Any message by S in the sub-slot s_2, is regarded by the listening C_is as an indication of the intention by S to transmit. Note that, multiple SUs may wish to transmit in a given time slot (i.e., more than one SU may wish to take the role of S) and hence, several simultaneous transmissions may arise in s_2. To resolve this, the random access principle, adopted for IEEE 802.11 based WiFi networks, is followed. Each SU that wishes to transmit, waits for a random period of time from the sub-slot start time before actually transmitting in s_2. If any SU Tx detects any other SU transmitting before it, it holds its transmission. There might still be some contending SU Txs that had missed the previous transmission(s) by other contending SU Tx(s) in s_2. Those SUs will transmit anyway. The CSUs which register multiple transmissions (either overlapping or non-overlapping) in s_2 will keep a note of those events.

In sub-slot s_3, B broadcasts the observed test statistics in the quantized form through the

licensed channel using power control to avoid unintended interference at any PU receiver (PU Rx). The details of power control will be discussed in Section 3.2. In sub-slot s_4, the quantized statistics broadcast by B is relayed to S by the most suited CSU. This choice corresponds to a CSU which has the highest instantaneous channel-gain with S and which had correctly decoded both the request by S in s_2 and the transmission from B in s_3. The best reporting channel is selected as in [61] for the best-selection reporting scheme. In order to restrict interference to any PU Rx in the area, power control is adopted while relaying. A segment of sub-slot s_4 is reserved for transmission by any CSU which had earlier recorded more than one transmission in sub-slot s_2. One among these CSUs will transmit in this time slot using random access principle and send a blocking signal preventing all contending SU transmitters to abandon their transmission attempt. This *prevents the occurrence of potential collision* among the SUs contending to begin their transmissions.

In order to control the SU traffic, in this work, a technique similar to the *carrier sense multiple access, collision avoidance* (CSMA/CA) random access principle with variable contention window, is adopted. This technique is widely used in current WiFi networks to avoid contention among equally prioritized network users. In the case of a blocking event, the contending SU transmitters defer their transmission to a future time slot. The waiting time interval after the sub-slot start instant and before sending a request in s_2 is equal to a random number generated based on the current maximum length of the contention window C_w. The random number is drawn uniformly from $[0, C_w]$ and C_w is exponentially incremented after every blocking event upto a certain upper limit $C_{w_{\max}}$. Conversely, if no blocking occurs the contention window is decremented until a lower limit $C_{w_{\min}}$ is reached.

All transmissions are assumed to be secured by forward error control codes such as cyclic redundancy check (CRC) which enable all network entities to discard erroneous packets prior to processing. There is *no requirement of separate control channels or additional setup time* for setting up a SU transmitter. One among the contending SU transmitters can be unambiguously selected following the communication protocol in s_2 as already described. Furthermore, in any slot, sensing is carried out by *only two sensor nodes* (B and S). Hence, there is energy saving

compared to traditional CSS where multiple secondary sensors are involved in simultaneous spectrum sensing.. This saving is in line with the emerging trend of promoting *green communications*. The benefit of cooperative sensing is harnessed by using a good spectrum sensor in the form of B rather than using multiple sensors. This strategy is adopted not only to save energy but also to preserve reporting channel resources compared to the technique used in [60]. Finally, in sub-slot s_5, S transmits the data packet.

The overall performance of the proposed CSS system is dependent on the ability of B to correctly detect an active PU Tx. For setting up the LSSN, two approaches that can be adopted:

(i) selecting one among the existing bank of SU sensors that has good reception of the PU's signal,

(ii) using a sensor, integrated to a mobile platform, such as a drone and placing it in a location where the average PU signal reception is found to be sufficiently good.

If a mobile platform based sensor is present, it can refer to *radio environment map (REM)* [79, 80, 82, 83] for identifying a location where the PU-SNR is sufficiently good and place itself there. In the absence of a mobile platform, one among the available SUs, which has the best PU-SNR as indicated by REM may be chosen as the LSSN. Note that, in general, a mobile LSSN has greater operational flexibility and may easily locate in an area of good PU signal reception. However, if the spatial density of SUs is high (as can be expected with the popularization of *internet of things* [1]), the SU based LSSN model can be equally good. Figure 3.1 represents the system model with a mobile LSSN.

3.2 Interference Limiting at Primary Users

In order to limit the interference on any PU during the reporting phase of the proposed scheme, a transmit power control scheme is adopted at each SU transmitter. All SUs in the network can transmit using a maximum power limit of P_{s_t} during the reporting phase. In this sub-section, we derive the transmit power limit to be imposed on a SU transmitter.

Let Z represent the interference power received at a PU receiver due to any transmission by a SU during reporting. It can be expressed as

$$Z = \frac{1}{3}\sum_{i=1}^{3} P_s |h_{X_i\mathsf{R}}|^2 \tag{3.1}$$

where P_s represents the power of the reporting signal transmitted by a SU and $|h_{X_i\mathsf{R}}|^2$ is the gain of the channel between a SU node (say X_i) and the PU receiver R. The factor $1/3$ arises due to the fact that each SU transmission occupies a third of the PU channel during reporting in the time-slotted structure. This factor takes into account the three mandatory secondary transmissions that are made in s_2, s_3 and s_4 while reporting. The instantaneous signal to interference ratio γ_{PR} at the primary receiver is given as

$$\gamma_{\mathsf{PR}} = \frac{P_{\mathsf{P}}|h_{\mathsf{PR}}|^2}{(1/3)\sum_{i=1}^{3} P_s |h_{X_i\mathsf{R}}|^2} \tag{3.2}$$

where P_{P} is the power of the primary transmitter and $|h_{\mathsf{PR}}|^2$ is the gain of the channel between primary transmitter and receiver. Let $P_{\text{Pout}} = Pr\{\gamma_{\mathsf{PR}} < \gamma_{\text{Pout}}\}$ represent the tolerable outage probability at the PU receiver due to interference by SUs. We use the fact that $|h_{\mathsf{PR}}|^2$ is exponentially distributed random variable (RV) with mean σ^2_{PR}. And each $|h_{X_i\mathsf{R}}|^2$ is independent and exponentially distributed RV with mean $\sigma^2_{X_i\mathsf{R}}$. Following [81], the maximum reporting power that is permissible without affecting the quality of service of the primary network can be expressed as

$$P_{s_t} = \frac{3\Theta[1-(1-P_{\text{Pout}})^{(1/3)}]}{(1-P_{\text{Pout}})^{(1/3)}\gamma_{\text{Pout}}} \tag{3.3}$$

where $\gamma_{\text{Pout}} = 2^{r_{\mathsf{P}}}-1$ is the outage SNR threshold at the PU receiver with r_{P} being the PU data rate and $\Theta = \frac{P_{\mathsf{P}}\sigma^2_{\mathsf{PR}}}{\sigma^2_{X_i\mathsf{R}}}$. The parameter Θ is constant for a given network. It is dependent on the transmit power of the PU Tx as well as on the ratio of the average gains between following links: PU Tx to PU Rx and SU Tx to PU Rx.

3.3 Outage Probabilities of Secondary User Transmissions

Let $\mathcal{H}_1$ and $\mathcal{H}_0$, respectively, denote the hypotheses under which the PU Tx is active and inactive. Let $P_{E0_{XY}}$ and $P_{E1_{XY}}$ denote the outage probabilities of a transmission made by an SU

node X to another SU node Y under $\mathcal{H}_0$ and $\mathcal{H}_1$, respectively. Assuming all wireless links undergo Rayleigh fading, the outage probabilities of the X-Y link can be expressed as

$$P_{E0_{XY}} = Pr\{\gamma_{XY} < \gamma_{X\text{out}}\} = 1 - \exp\left(-\frac{\gamma_{X\text{out}}}{\bar{\gamma}_{XY}}\right), \tag{3.4}$$

$$P_{E1_{XY}} = Pr\left\{\frac{\gamma_{XY}}{1+\gamma_{PY}} < \gamma_{X\text{out}}\right\} = 1 - \frac{\exp\left(-\frac{\gamma_{X\text{out}}}{\bar{\gamma}_{XY}}\right)\bar{\gamma}_{XY}}{\gamma_{X\text{out}}\bar{\gamma}_{PY} + \bar{\gamma}_{XY}} \tag{3.5}$$

where γ_{XY} is the instantaneous SNR of the signal from an SU node X received at an SU node Y, $\gamma_{X\text{out}}$ is the outage *signal to interference plus noise ratio* (SINR), i.e., the SINR below which information from X is assumed to be lost, γ_{PY} is the instantaneous SNR of the PU signal at Y, $\bar{\gamma}_{XY}$ and $\bar{\gamma}_{PY}$ are the average SNRs of signals received at Y from X and P, respectively.

3.4 Cooperative Spectrum Sensing

It is well-known that cooperative spectrum sensing improves the overall detection performance [38–40, 42, 43]. However, it requires more resources and therefore, more complex to implement than standalone spectrum sensing. Also, the overall energy consumption in CSS increases due to involvement of multiple CSUs during the sensing stage. In order to reduce that, in this work a two-stage PU detection methodology is adopted which is similar to that in [61]. The first stage involves a standalone detection attempt by S. Only if this attempt by S yields a negative outcome, it seeks cooperation from the CSUs and a joint statistics with B is generated. A negative outcome could be the result of a miss detection of the PU or a correct detection about the spectral void.

3.4.1 Standalone Detection at S

In time-slot s_1, sensor nodes S and B independently evaluate the energy statistics. However, S makes an initial attempt to detect the PU Tx on its own. Let Ξ_S represent the event that the sensor S is able to detect a PU transmission. Let E_S represent the energy statistics at S. Let λ_S represent the detector threshold at S selected for this initial detection attempt. The probability of false alarm and the probability of detection of this standalone detection attempt by S can be

compactly represented as

$$P_{f,\mathsf{S}}(\lambda_{\mathsf{S}}) = Pr\{\Xi_{\mathsf{S}} \,|\, \mathcal{H}_0\} = Pr\{E_S > \lambda_{\mathsf{S}} \,|\, \mathcal{H}_0\} \tag{3.6}$$

and

$$P_{d,\mathsf{S}}(\lambda_{\mathsf{S}}) = Pr\{\Xi_{\mathsf{S}} \,|\, \mathcal{H}_1\} = Pr\{E_S > \lambda_{\mathsf{S}} \,|\, \mathcal{H}_1\} \tag{3.7}$$

More explicitly, $P_{f,\mathsf{S}}(\lambda_{\mathsf{S}})$ and $P_{d,\mathsf{S}}(\lambda_{\mathsf{S}})$ would be functions of the PU SNR at S and the time-bandwidth product. For those expressions derived under Rayleigh fading conditions, the reader is referred to [16].

3.4.2 Energy Statistics at B

The energy statistics gathered by B in s_1 is mapped onto one of the $D = 2^d$ discrete levels using a quantizer of d bits. The maximum output entropy quantization scheme [84] is used to transform a continuous domain test statistics to the discrete domain. The design of the quantizer is briefly discussed in this sub-section.

Let E_{B} denote the energy statistics at B. We define $E'_{\mathsf{B}} = \delta_{\mathsf{B}} E_{\mathsf{B}}$, where, $\delta_{\mathsf{B}} = \frac{\bar{\gamma}_{\mathsf{PB}}}{1+\bar{\gamma}_{\mathsf{PB}}}$ and $\bar{\gamma}_{\mathsf{PB}}$ is the average PU SNR at B. Let $f_{E'_{\mathsf{B}}}(x)$ represent the unconditional probability distribution function (PDF) of E'_{B}, and let $f_{E'_{\mathsf{B}}|\mathcal{H}_0}(x)$ and $f_{E'_{\mathsf{B}}|\mathcal{H}_1}(x)$ represent the conditional PDFs of E'_{B} under $\mathcal{H}_0$ and $\mathcal{H}_1$, respectively. The unconditional PDF can be represented in terms of conditional PDFs as

$$f_{E'_{\mathsf{B}}}(x) = Pr\{\mathcal{H}_0\}\, f_{E'_{\mathsf{B}}|\mathcal{H}_0}(x) + Pr\{\mathcal{H}_1\}\, f_{E'_{\mathsf{B}}|\mathcal{H}_1}(x) \tag{3.8}$$

where $Pr\{\mathcal{H}_0\}$ and $Pr\{\mathcal{H}_1\}$ denote the prior probability of $\mathcal{H}_0$ and $\mathcal{H}_1$, respectively. Since we consider the maximum output entropy quantizer, it corresponds to uninformative prior of the PU state, i.e., $Pr\{\mathcal{H}_0\} = Pr\{\mathcal{H}_1\} = 0.5$. Let $t_0, t_1, \ldots, t_D$ be the $D+1$ thresholds that are used by the maximum output entropy quantizer to map the continuous test statistics E'_{B} to a discrete domain. The lowest and the highest thresholds (i.e., t_0 and t_D) are set at zero and infinity, respectively. The other threshold values (i.e., t_1 through t_{D-1}) can be obtained by progressively solving the

following equation for $n = 1, 2, \ldots, D-1$.

$$\int_{t_{n-1}}^{t_n} f_{E'_{\mathsf{B}}}(x)dx = \frac{1}{D} \tag{3.9}$$

Let $E'_{\mathsf{B},q}$ be the random variable denoting the quantized energy statistics gathered at B. The energy level $e'_{\mathsf{B},q,n}$ corresponding to the nth quantization level is given as

$$e'_{\mathsf{B},q,n} = \frac{\int_{t_{n-1}}^{t_n} x f_{E'_{\mathsf{B}}}(x)dx}{\int_{t_{n-1}}^{t_n} f_{E'_{\mathsf{B}}}(x)dx} = D\int_{t_{n-1}}^{t_n} x f_{E'_{\mathsf{B}}}(x)dx \tag{3.10}$$

The probability mass function of $E'_{\mathsf{B},q}$ under either hypotheses $\mathcal{H}_i$ can be defined as

$$P_{E'_{\mathsf{B},q}|\mathcal{H}_i}(n) = \int_{t_{n-1}}^{t_n} f_{E'_{\mathsf{B}}|\mathcal{H}_i}(x)dx \quad \text{where} \quad i = 0, 1. \tag{3.11}$$

The quantized energy statistics $E'_{\mathsf{B},q}$ is transmitted through the reporting channel in s_3.

3.4.3 Joint Test Statistics

If standalone sensing in s_1, at the node S does not the indicate the presence of PU transmission, an attempt to generate a joint test statistics using the statistics gathered at S and B is made. Provided the relayed statistics $E'_{\mathsf{B},q}$ is successfully received at S in s_3 or s_4, the joint test statistics E'_C is given as

$$E'_C = E'_{\mathsf{B},q} + \delta_{\mathsf{S}} E_{\mathsf{S}} \tag{3.12}$$

where $\delta_{\mathsf{S}} = \frac{\bar{\gamma}_{\mathsf{PS}}}{1+\bar{\gamma}_{\mathsf{PS}}}$. Assuming, the analog counterpart of $E'_{\mathsf{B},q}$, (i.e., E'_{B}) were available at S, the true joint test statistics E_C [45] is given as

$$E_C = E'_{\mathsf{B}} + \delta_{\mathsf{S}} E_{\mathsf{S}}. \tag{3.13}$$

3.4.3.1 Distribution Function of E'_C

The cumulative distribution function (CDF) of E'_C under either hypothesis $\mathcal{H}_i, i = 0, 1$ can be expressed as

$$F_{C|\mathcal{H}_i}(x) = \sum_{n=1}^{D} F_{E'_{\mathsf{S}}|\mathcal{H}_i}(x - e'_{\mathsf{B},q,n}) P_{E'_{\mathsf{B},q}|\mathcal{H}_i}(n) \tag{3.14}$$

where $F_{E'_{\mathsf{S}}|\mathcal{H}_i}(x)$ is the CDF of $E'_{\mathsf{S}} = \delta_{\mathsf{S}} E_{\mathsf{S}}$ under $\mathcal{H}_i$.

3.4.4 Possible Issues in Implementation

The implementation complexity of the proposed CSS model is at par with other models reported in literature [60–62]. It uses low complexity energy detectors for sensing. Transmission of quantized statistics in the proposed scheme lowers the data-rate requirement of the reporting channels in comparison to *amplify and forward* based schemes. Moreover, the proposed scheme utilizes well tested features of contemporary wireless systems, such as CSMA/CA random access for minimizing collision among contending SUs and CRC for detecting outage of the reporting information.

In the proposed scheme, the long term availability of the LSSN and the power consumption may appear to be the issues. It is true that a single LSSN may not be operational for extended periods of time. However, like any other ad hoc network, an alternate network is formed as per requirement. Also, a mobile LSSN need not remain airborne all throughout its operation as may be perceived. It may perch itself in a suitable spot guided by REM in order to conserve battery power and be able to operate for longer durations.

3.5 Performance Analysis

3.5.1 False Alarm and Detection Probabilities for proposed CSS

Let Ξ_{S}^c denote the event that S has failed in detecting the PU in s_1 and λ_{C} denote the detection threshold set for the joint test statistics E'_C. Let $\mathcal{G}$ denote the event that the quantized statistics from B is successfully relayed to S. The probability of false alarm of the proposed scheme can

be expressed as

$$P_F = Pr\{\Xi_{\mathsf{S}} \mid \mathcal{H}_0\} + Pr\{\Xi_{\mathsf{S}}^c, \mathcal{G}, E'_C > \lambda_{\mathsf{C}} \mid \mathcal{H}_0\}$$
$$= P_{f,\mathsf{S}} + (1 - P_{f,\mathsf{S}})\beta_{\mathcal{H}_0} P_{CF} \tag{3.15}$$

where

$$\beta_{\mathcal{H}_0} = Pr\{\mathcal{G} \mid \mathcal{H}_0, \Xi_{\mathsf{S}}^c\} \tag{3.16}$$

and

$$P_{CF} = Pr\{E'_C > \lambda_{\mathsf{C}} \mid \mathcal{H}_0, \Xi_{\mathsf{S}}^c, \mathcal{G}\} \tag{3.17}$$

The term $\beta_{\mathcal{H}_0}$ denotes the probability that at least one among the direct path or the indirect link set up by the CSUs is successful in relaying the test statistics from B to S under $\mathcal{H}_0$. Let $\Psi = \{1, 2, \ldots, N\}$ denote the set of indices representing all CSUs. Let $\Phi_{m,j}$ denote the jth subset of Ψ containing m elements with its complement defined as $\Phi_{m,j}^c = \Psi \setminus \Phi_{m,j}$. Now, $\beta_{\mathcal{H}_0}$ can be expressed as

$$\beta_{\mathcal{H}_0} = 1 - P_{E0_{\mathsf{BS}}} \sum_{m=0}^{N} \sum_{j=1}^{\binom{N}{m}} \left[\prod_{l \in \Phi_{m,j}} (P_{E0_{\mathsf{C}_l\mathsf{S}}} - P_{E0_{\mathsf{SC}_l}})(1 - P_{E0_{\mathsf{BC}_l}}) \prod_{k \in \Phi_{m,j}^c} \left\{ 1 - (1 - P_{E0_{\mathsf{SC}_k}})(1 - P_{E0_{\mathsf{BC}_k}}) \right\} \right] \tag{3.18}$$

The derivation of the above expression is outlined in Appendix B.

The term P_{CF} can be expressed as

$$P_{CF}(x, \lambda'_{\mathsf{S}}) = \sum_{n \in T} \left(P'_{f,\mathsf{S}}(x - e'_{\mathsf{B},q,n}) - P'_{f,\mathsf{S}}(\lambda'_{\mathsf{S}}) \right) \left(P_{E'_{\mathsf{B},q} \mid \mathcal{H}_0}(n) / \{1 - P'_{f,\mathsf{S}}(\lambda'_{\mathsf{S}})\} \right) \tag{3.19}$$

where $T = \{l \mid e'_{\mathsf{B},q,l} > \lambda_{\mathsf{C}} - \lambda'_{\mathsf{S}}\}$ and $\lambda'_{\mathsf{S}} = \delta_{\mathsf{S}} \lambda_{\mathsf{S}}$ and $P'_{f,\mathsf{S}}(x) = P_{f,\mathsf{S}}(x/\delta_{\mathsf{S}})$. The derivation of the expression in (3.19) is outlined in Appendix C.

Following a similar approach the corresponding quantities associated with hypothesis $\mathcal{H}_1$ can also be obtained. Thus, the probability of detection under the proposed CSS scheme is given as

$$P_D = P_{d,\mathsf{S}} + (1 - P_{d,\mathsf{S}})\beta_{\mathcal{H}_1} P_{CD} \tag{3.20}$$

where $\beta_{\mathcal{H}_1}$ is given as

$$\beta_{\mathcal{H}_1} = 1 - P_{E1_{\mathrm{BS}}} \sum_{m=0}^{N} \sum_{j=1}^{\binom{N}{m}} \left[\prod_{l \in \Phi_{m,j}} (P_{E1_{\mathrm{C}_l\mathsf{S}}} - P_{E1_{\mathsf{SC}_l}})(1 - P_{E1_{\mathrm{BC}_l}}) \prod_{k \in \Phi^c_{m,j}} \left\{ 1 - (1 - P_{E1_{\mathsf{SC}_k}})(1 - P_{E1_{\mathrm{BC}_k}}) \right\} \right] \quad (3.21)$$

and

$$P_{CD}(x, \lambda'_{\mathsf{S}}) = \sum_{n \in T} \left(P'_{d,\mathsf{S}}(x - e'_{\mathsf{B},q,n}) - P'_{d,\mathsf{S}}(\lambda'_{\mathsf{S}}) \right) \left(P_{E'_{\mathsf{B},q}|\mathcal{H}_1}(n) / \{1 - P'_{d,\mathsf{S}}(\lambda'_{\mathsf{S}})\} \right) \quad (3.22)$$

with $P'_{d,\mathsf{S}}(x) = P_{d,\mathsf{S}}(x/\delta_{\mathsf{S}})$.

3.5.2 Standalone versus Joint Sensing

From (3.15) and (3.19), it can be noted that the overall probability of false alarm P_F is dependent on the detector threshold λ_{S} set at S for standalone sensing as well as the joint detection threshold λ_{C}. Let $P_{F,tar}$ denote the target false alarm set for the proposed CSS. There are multiple combinations of λ_{S} and λ_{C} which can satisfy the target false alarm constraint. In general, the power of the joint detector is greater than that of the standalone for the same level of the significance. Hence, it is generally expected that the overall false alarm constraint P_F is contributed entirely by the joint detector so as to yield the highest possible power of the resultant detector. However, we observe that the request for assistance in s_2 under $\mathcal{H}_0$ (i.e., when S correctly estimates the absence of PU in s_1) sets the trigger for adverse activation of multiple CSUs in s_3. This causes a hike in the overall energy consumption in the network. Also, if a contenting PU Tx manages to detect the PU on its own, it will not request for assistance in slot s_2. The CSUs, in this case, can spend the time-slot s_3 in sleep mode, thereby conserving their energy. In order to achieve this, in this work, $P_{f,\mathsf{S}}$ is set to a non-zero value. Algorithm 1 summarizes the approach for fixing the two thresholds λ_{S} and λ_{C}.

Remarks: The following points are to be noted regarding the setting of the thresholds using Algorithm 1:

- The approximation in Step 1 involves setting $\lambda_{\mathsf{S}} \rightarrow \infty$ in $P_{CF}(\lambda_C, \lambda_{\mathsf{S}})$. This allows to determine λ_C independently of λ_{S}.

Algorithm 1 Steps for setting the thresholds λ_S and λ_C

Output: $\lambda_{C,o}, \lambda_{S,o}$

1: Approximate $P_{CF}(\lambda_C, \lambda_S)$ as $\tilde{P}_{CF}(\lambda_C)$=1$-F_{C|\mathcal{H}_0}(\lambda_C)$, where $F_{C|\mathcal{H}_0}(\lambda_C)$ is given by (3.14).
2: Solve $P_{F,tar} - \tilde{P}_{CF}(\lambda_C) = 0$ for λ_C to obtain the solution $\lambda_{C,o}$.
3: Solve (3.15) for λ_S putting $P_F = P_{F,tar}$, $P_{f,S} = P_{f,S}(\lambda_S)$ and replacing P_{CF} with $\tilde{P}_{CF}(\lambda_{C,o})$ to obtain $\lambda_S = \lambda_{S,o}$.
4: **return** $\lambda_{C,o}, \lambda_{S,o}$

$$\bar{P}_{E0_{XY}} = 1 - \frac{1}{\bar{\gamma}_{XY,\max} - \bar{\gamma}_{XY,\min}} \gamma_{X\text{out}} \left[\Gamma\left(-1, \frac{\gamma_{X\text{out}}}{\bar{\gamma}_{XY,\max}}\right) - \Gamma\left(-1, \frac{\gamma_{X\text{out}}}{\bar{\gamma}_{XY,\min}}\right) \right], \tag{3.23}$$

$$\begin{aligned} \bar{P}_{E1_{XY}} = 1 - \frac{1}{\bar{\gamma}_{XY,\max} - \bar{\gamma}_{XY,\min}} \Bigg[& \gamma_{X\text{out}} \bar{\gamma}_{PY} \left\{ -\Gamma\left(0, \frac{\gamma_{X\text{out}}}{\bar{\gamma}_{XY,\max}}\right) + \Gamma\left(0, \frac{\gamma_{X\text{out}}}{\bar{\gamma}_{XY,\min}}\right) + \exp\left(\frac{1}{\bar{\gamma}_{PY}}\right) \left\{ \Gamma\left(0, \frac{\gamma_{X\text{out}}}{\bar{\gamma}_{XY,\max}} + \frac{1}{\bar{\gamma}_{PY}}\right) \right. \right. \\ & \left. \left. - \Gamma\left(0, \frac{\gamma_{X\text{out}}}{\bar{\gamma}_{XY,\min}} + \frac{1}{\bar{\gamma}_{PY}}\right) \right\} \right\} + \gamma_{X\text{out}} \left\{ \Gamma\left(-1, \frac{\gamma_{X\text{out}}}{\bar{\gamma}_{XY,\max}}\right) - \Gamma\left(-1, \frac{\gamma_{X\text{out}}}{\bar{\gamma}_{XY,\min}}\right) \right\} \Bigg], \end{aligned} \tag{3.24}$$

- The approximation of P_{CF} causes the actual false alarm $\tilde{P}_F$ to differ from the target false alarm $P_{F,tar}$. The deviation of $\tilde{P}_F$ from $P_{F,tar}$ is usually small for small $P_{F,tar}$ and the same has been verified in Section 3.7.

3.5.3 Ideal Scenario: Average SNR at SU nodes being known

In this case, the exact value of average SNR of each SU Tx is assumed to be known at another SU Rx, i.e., $\bar{\gamma}_{XY}$ being constant. Thus, using (3.4) and (3.5), the outage probability for each pair of SUs (say X and Y) can be calculated. The values of $\beta_{\mathcal{H}_0}$ and $\beta_{\mathcal{H}_1}$ can be subsequently determined using (3.18) and (3.21), respectively. The thresholds λ_S and λ_C can be determined using the procedure described in Section 3.5.2. The theoretical probability of detection can be determined using (3.20).

3.5.4 Realistic Scenario: Knowledge about the range of average SNR at SU nodes being available

In the practical scenario, the average SNR of each SU at another SU may not be available. This is because updating this value for each SU at another SU would require a large amount of control channel resources which may not be available for a secondary network. To deal with such a scenario, a nominal value of the average SNR $\bar{\gamma}_{XY,\text{nom}}$ for each SU Tx (say X) is

assumed at another SU Rx (say Y). The actual value of the average SNR is assumed to be uniformly distributed about the nominal value with a particular fractional spread $\delta_{\bar{\gamma}_{XY}}$, i.e., $\bar{\gamma}_{XY} \sim \mathcal{U}\left(\bar{\gamma}_{XY,\text{nom}}(1-\delta_{\bar{\gamma}_{XY}}),\ \bar{\gamma}_{XY,\text{nom}}(1+\delta_{\bar{\gamma}_{XY}})\right)$.

Let $\boldsymbol{\gamma}_{\mathsf{S}} = [\bar{\gamma}_{\mathsf{BS}}, \bar{\gamma}_{\mathsf{C}_1\mathsf{S}}, \ldots, \bar{\gamma}_{\mathsf{C}_N\mathsf{S}}, \bar{\gamma}_{\mathsf{BC}_1}, \ldots, \bar{\gamma}_{\mathsf{BC}_N}]^T$ be a random vector whose elements include the average SNR of B as well as that of N CSUs at S. Also included as elements of $\boldsymbol{\gamma}_{\mathsf{S}}$ are the average SNRs of B at each CSU. It is commonly assumed that the principle of reciprocity holds for the wireless links. Assuming, the same transmit power (as given by (3.3)) is adopted by all SUs during the reporting phase, it can be concluded that the SNR of S at C_i is identical to the SNR of C_i at S, i.e., $\bar{\gamma}_{\mathsf{SC}_k} = \bar{\gamma}_{\mathsf{C}_k\mathsf{S}}$. Note that the average SNR of S at each of the C_is is not included in $\boldsymbol{\gamma}_{\mathsf{S}}$.

Now, we can write

$$\mathbb{E}_{\boldsymbol{\gamma}_{\mathsf{S}}}[\beta_{\mathcal{H}_0}] = 1-\bar{P}_{E0_{\mathsf{BS}}}\sum_{m=0}^{N}\sum_{j=1}^{\binom{N}{m}}\left[\prod_{l\in\Phi_{m,j}}(\bar{P}_{E0_{\mathsf{C}_l\mathsf{S}}}-\bar{P}_{E0_{\mathsf{SC}_l}})(1-\bar{P}_{E0_{\mathsf{BC}_l}})\prod_{k\in\Phi^c_{m,j}}\left\{1-(1-\bar{P}_{E0_{\mathsf{SC}_k}})(1-\bar{P}_{E0_{\mathsf{BC}_k}})\right\}\right], \tag{3.25}$$

where $\mathbb{E}_W[\cdot]$ denotes the expectation operator over random variable W, $\bar{P}_{E0_{XY}} = \mathbb{E}_{\bar{\gamma}_{XY}}[P_{E0_{XY}}(\bar{\gamma}_{XY})]$, $X, Y \in \{\mathsf{B}, \mathsf{S}, \mathsf{C}_1, \mathsf{C}_2, \ldots, \mathsf{C}_N\}$, $X \neq Y$. Similarly, for hypothesis $\mathcal{H}_1$, the expression in (3.25) can be given as

$$\mathbb{E}_{\boldsymbol{\gamma}_{\mathsf{S}}}[\beta_{\mathcal{H}_1}] = 1-\bar{P}_{E1_{\mathsf{BS}}}\sum_{m=0}^{N}\sum_{j=1}^{\binom{N}{m}}\left[\prod_{l\in\Phi_{m,j}}(\bar{P}_{E1_{\mathsf{C}_l\mathsf{S}}}-\bar{P}_{E1_{\mathsf{SC}_l}})(1-\bar{P}_{E1_{\mathsf{BC}_l}})\prod_{k\in\Phi^c_{m,j}}\left\{1-(1-\bar{P}_{E1_{\mathsf{SC}_k}})(1-\bar{P}_{E1_{\mathsf{BC}_k}})\right\}\right], \tag{3.26}$$

where $\bar{P}_{E1_{XY}} = \mathbb{E}_{\bar{\gamma}_{XY}}[P_{E1_{XY}}(\bar{\gamma}_{XY})]$.

The probabilities $\bar{P}_{E0_{XY}}$ and $\bar{P}_{E1_{XY}}$ are given in (3.23) and (3.24), respectively, where the maximum/minimum limit of $\bar{\gamma}_{XY}$ is denoted by $\bar{\gamma}_{XY,\max}/\bar{\gamma}_{XY,\min}$. The probability of false alarm and the probability of detection are obtained by replacing $\beta_{\mathcal{H}_0}$ and $\beta_{\mathcal{H}_1}$ with $\mathbb{E}_{\boldsymbol{\gamma}_{\mathsf{S}}}[\beta_{\mathcal{H}_0}]$ and $\mathbb{E}_{\boldsymbol{\gamma}_{\mathsf{S}}}[\beta_{\mathcal{H}_1}]$ in (3.15) and (3.20) from (3.25) and (3.26), respectively. The resulting probabilities are denoted

as P_{Fa} and P_{Da} and can be expressed as

$$P_{Fa} = P_{f,\mathrm{S}} + (1 - P_{f,\mathrm{S}})\mathbb{E}_{\gamma_{\mathrm{S}}}[\beta_{\mathcal{H}_0}]P_{CF} \tag{3.27}$$

$$P_{Da} = P_{d,\mathrm{S}} + (1 - P_{d,\mathrm{S}})\mathbb{E}_{\gamma_{\mathrm{S}}}[\beta_{\mathcal{H}_1}]P_{CD} \tag{3.28}$$

3.6 Review of Selective-Reporting Based Cooperative Spectrum Sensing

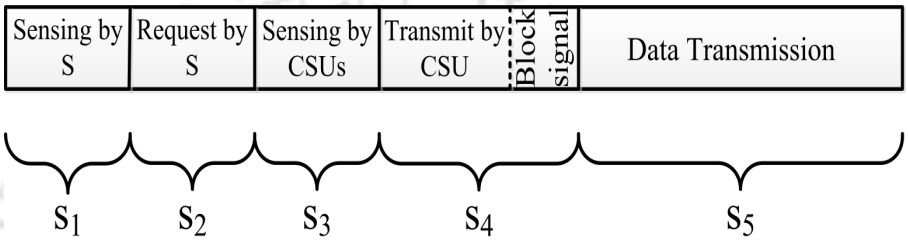

Figure 3.3: *Secondary network time-slot structure for the BSR scheme.*

The performance of the CSS scheme proposed in this paper is compared with that of the best-selection reporting (BSR) scheme presented in [61]. The BSR scheme is shown to outperform the traditional schemes in [61]. Both the proposed and the BSR schemes use slotted structures for sensing, reporting and data transmission. The network time slot for the BSR scheme is shown in Figure 3.3. It can be seen that the number of sub-slots used during the reporting phase in either of the schemes is four (if the *request for assistance* slot is also counted in the BSR scheme as done for the proposed scheme). The CSU possessing the best reporting channel is used in both these schemes to report back to the SU node S. However, there exist three fundamental differences between the two schemes:

(i) Unlike the LSSN in the proposed scheme, there is no leading node in the BSR scheme. Moreover, in the latter scheme all the CSUs are actively involved in sensing the PU Tx. Whereas, in the former, they are only used for the purpose of relaying the sensing information received from the LSSN.

(ii) In BSR, the number of slots where a SU transmits during the reporting phase is two (s_2 and s_4). Whereas, that is three (s_2, s_3 and s_4), in the case of the proposed scheme.

(iii) Unlike BSR which uses single bit quantization in reporting, the proposed scheme can use multi-bit quantization while reporting the decision statistics.

Due to the difference in the number of active transmission slots the power constraint associated with BSR is $P_{s_t,BSR}$ instead of P_{s_t}. It can be expressed as

$$P_{s_t,BSR} = \frac{2\Theta[1-(1-P_{\text{Pout}})^{(1/2)}]}{(1-P_{\text{Pout}})^{(1/2)}\gamma_{\text{Pout}}} \tag{3.29}$$

As per the system model proposed in [61], the BSR network time-slot does not support any blocking slot to prevent simultaneous data transmission by multiple SU transmitters. For a fair comparison with the proposed scheme, we include a similar slot for the BSR scheme. Also, the effect of outage of the *request for assistance* signal in the analysis is not included in [61]. In our implementation of BSR, we have included that effect. Thus the probabilities of false alarm and detection for the BSR scheme are given as

$$P_{F,BSR} = 1-(1-P_{f,\text{S}})\sum_{m=0}^{N}\sum_{j=1}^{\binom{N}{m}}\left[\prod_{l\in\Phi_{m,j}}(\bar{P}_{E0_{\text{C}_l\text{S}}}-\bar{P}_{E0_{\text{SC}_l}})P_{f,\text{C}_l}\prod_{k\in\Phi^c_{m,j}}\left\{1-(1-\bar{P}_{E0_{\text{SC}_k}})P_{f,\text{C}_k}\right\}\right] \tag{3.30}$$

$$P_{D,BSR} = 1-(1-P_{d,\text{S}})\sum_{m=0}^{N}\sum_{j=1}^{\binom{N}{m}}\left[\prod_{l\in\Phi_{m,j}}(\bar{P}_{E1_{\text{C}_l\text{S}}}-\bar{P}_{E1_{\text{SC}_l}})P_{d,\text{C}_l}\prod_{k\in\Phi^c_{m,j}}\left\{1-(1-\bar{P}_{E1_{\text{SC}_k}})P_{d,\text{C}_k}\right\}\right] \tag{3.31}$$

where $P_{f,X}$ and $P_{d,X}$ represent the probabilities of false alarm and detection at SU node X, respectively. The derivations of these expressions are briefly outlined in Appendix D.

The overall false alarm constraint for the BSR scheme is set assuming a common threshold λ_{BSR} across all sensors as done in [61]. The numerical value of λ_{BSR} (let it be $\lambda_{BSR,o}$) is obtained by putting $P_{f,X} = P_{f,BSR}(\lambda_{BSR})$, setting $P_{f,BSR} = P_{F,tar}$ and solving (3.30) for λ_{BSR}.

3.7 Results and Discussion

Numerical and simulation experiments are performed to evaluate the performance of the proposed CSS system for different levels of quantization used while reporting, under different operating conditions. The term PU-SNR is used to denote the SNR of any signal transmitted by the primary user at another node. Likewise, the term SU-SNR is used to denote the SNR of any

signal transmitted by an SU. For discussions in this section, some of the salient parameters are assumed to be set as follows: tolerable primary outage probability $P_{\text{Pout}} = 0.05$, PU information rate $r_{\text{P}} = 3$ bits/s/Hz, information rate of the transmitted signal by S in slot s_2 $r_{\text{S}} = 1 \times 10^{-3}$ bits/s/Hz, $\Theta = -1$ dB, and the noise variance at an SU $\sigma_n^2 = 1$, number of sensing samples =1000. The information rate associated with the reporting signal is proportional to d, i.e., the number of bits used by the quantizer at B. The constant of proportionality is set as 1×10^{-3}. Let σ_{XY}^2 denote the nominal average of the channel gain between X and Y. The nominal average SNR $\bar{\gamma}_{XY,\text{nom}}$ is related to σ_{XY}^2 as $\bar{\gamma}_{XY,\text{nom}} = P_{s_t} \frac{\sigma_{XY}^2}{\sigma_n^2}$. Monte-Carlo simulations are performed to validate the analytical results. In Figure 3.4, the simulated and analytical values of the probability of detection under different system conditions are plotted as a function of N and show close agreement with each other. To avoid cluttering, only analytical results are presented in subsequent figures. Experiments are carried out for varying quantization levels $d = 1, \ldots, 5$ and different PU-SNR

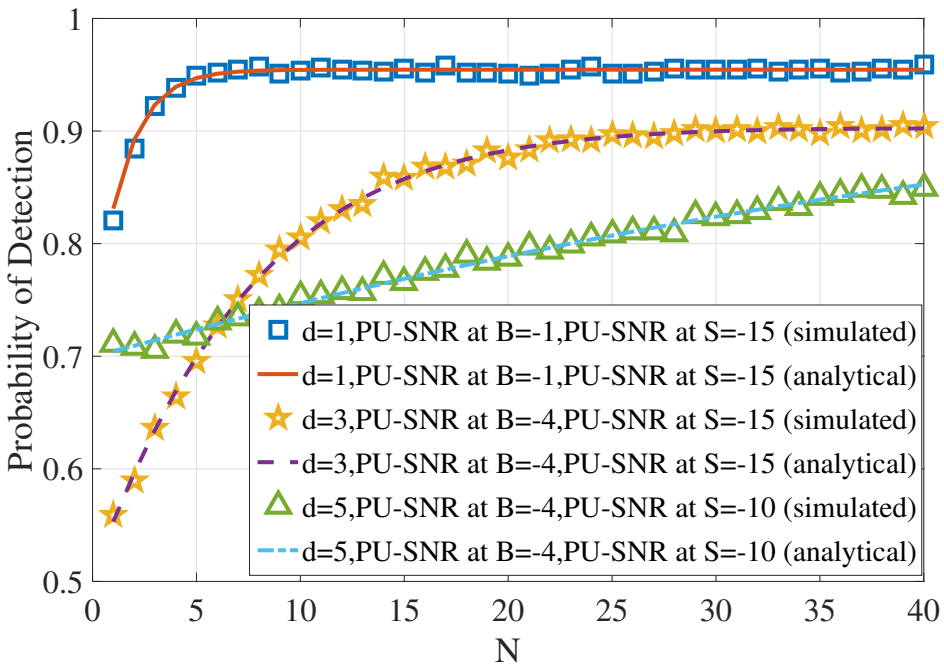

Figure 3.4: *Plot of analytical and simulated values of probability of detection as a function of number of cooperators. All SNRs are in dB.* $P_{Fa} = 0.1$, $\sigma_{\text{BC}_l}^2 = 0.3$, $\delta_{\bar{\gamma}_{\text{BC}_l}^2} = 0.1$, $\sigma_{\text{C}_l\text{S}}^2 = 0.5$, $\delta_{\bar{\gamma}_{\text{C}_l\text{S}}^2} = 0.1$.

at SU nodes (B, C_l and S). In Figure 3.5, the variation of the probability of detection with N is plotted for $d = 1, 2$ only to avoid clutter. From those experiments, following observations can

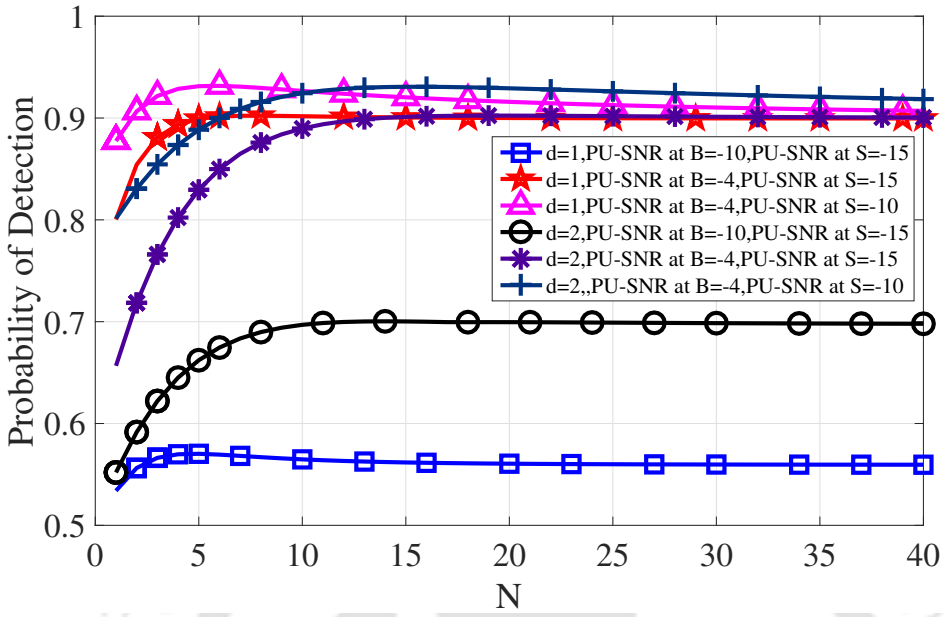

Figure 3.5: *Variation of probability of detection as a function of number of cooperators for* $d = 1, 2$. *All SNRs are in dB.* $P_{Fa} = 0.1$, $\sigma^2_{\mathrm{BC}_l} = 0.3$, $\delta_{\bar{\gamma}^2_{\mathrm{BC}_l}} = 0.1$, $\sigma^2_{\mathrm{C}_l\mathrm{S}} = 0.5$, $\delta_{\bar{\gamma}^2_{\mathrm{C}_l\mathrm{S}}} = 0.1$.

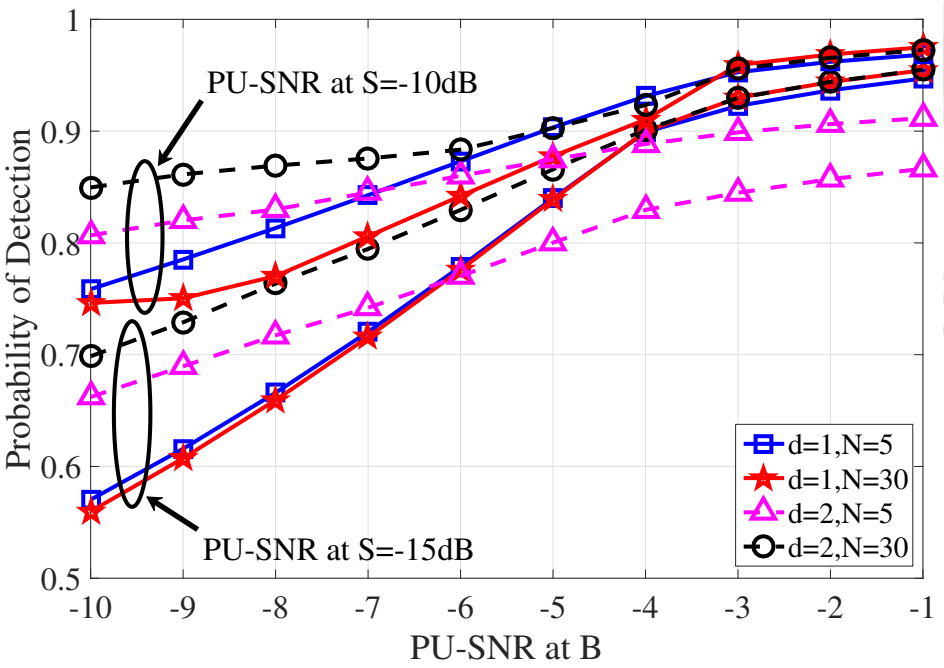

Figure 3.6: *Variation of probability of detection as a function of* $\bar{\gamma}_{\mathrm{PB}}$. *All SNRs are in dB.* $P_{Fa} = 0.1$, $\sigma^2_{\mathrm{BC}_l} = 0.3$, $\delta_{\bar{\gamma}^2_{\mathrm{BC}_l}} = 0.1$, $\sigma^2_{\mathrm{C}_l\mathrm{S}} = 0.5$, $\delta_{\bar{\gamma}^2_{\mathrm{C}_l\mathrm{S}}} = 0.1$.

be drawn.

- The increase in the PU-SNR at either B or S node increases the probability of detection

as expected.

- In terms of detection performance, in order to benefit from the use of higher number of quantization levels, the number of CSUs has to be large. In other words, if the number of CSUs is less, it is better to stick to a scheme with lower number of quantization levels.
- When the PU-SNR at B is low, better performance is achieved for a higher level of quantization even with a lesser number of CSUs.
- If the number of CSUs is less and the PU-SNR at B is high, 1-bit quantizer outperforms a higher bit ones.

The above points can also be verified from Figure 3.6 where the probability of detection is plotted against the PU-SNR at B. Note that the physical node S may be different at different times as there is a contest for winning each network time-slot by contending secondary transmitters. Thus it is possible that the PU-SNR at S sometimes is better than at other times. When this is so, it is possible to reap the benefit of cooperative gains. In Figure 3.5, when we compare the plots that correspond to different values of PU-SNR at S (-10 dB and -15 dB) but same value of PU-SNR at B (-4 dB). It is evident that the performance of the system improves if S itself has a good PU-SNR. If, however, the PU-SNR at S is close to zero and comparatively less than the PU-SNR at B, the statistics generated at this node hardly makes a difference. This can also be verified from (3.12). As the PU-SNR at S tends to zero, δ_{S} tends to zero. Hence, the joint test statistics tends to the quantized test statistics generated at B, i.e., $E'_C \rightarrow E'_{\mathsf{B},q}$.

In Figure 3.7, the effect of approximating $P_{CF}(\lambda_C, \lambda_{\mathsf{S}})$ by $\tilde{P}_{CF}(\lambda_C)$ is shown. Note that $\tilde{P}_{CF}(\lambda_{C,o}) = P_{CF}(\lambda_{C,o}, \infty)$. It is easy to verify that $P_{CF}(\lambda_{C,o}, \infty) \geq P_{CF}(\lambda_{C,o}, \lambda_{\mathsf{S}})$ for any value of λ_{S}. Hence, the target probability of false alarm sets the upper bound on the actual probability of false alarm. From Figure 3.7, it can be verified that the actual false alarm is indeed less than the target false alarm. In Figure 3.8, the probability of detection P_D is plotted against the target probability of false alarm. For low target probability of false alarm, it can be observed that higher quantization provides a significant increase in the detection probability for both moderate and low PU-SNR values at B and S. Figure 3.9 shows a comparison between the BSR [61] and

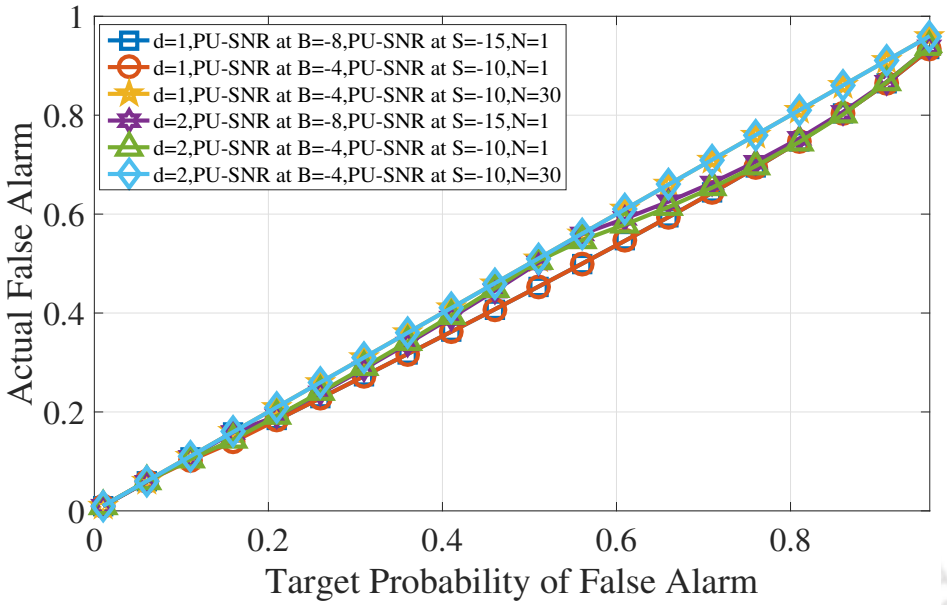

Figure 3.7: *Impact of the approximation,* $P_{CF}(\lambda_C, \lambda_S)$ *as* $\tilde{P}_{CF}(\lambda_C)$ *. All SNRs are in dB.* $\sigma^2_{\mathrm{BC}_l} = 0.3$, $\delta_{\tilde{\gamma}^2_{\mathrm{BC}_l}} = 0.1$, $\sigma^2_{\mathrm{C}_l\mathrm{S}} = 0.5$, $\delta_{\tilde{\gamma}^2_{\mathrm{C}_l\mathrm{S}}} = 0.1$.

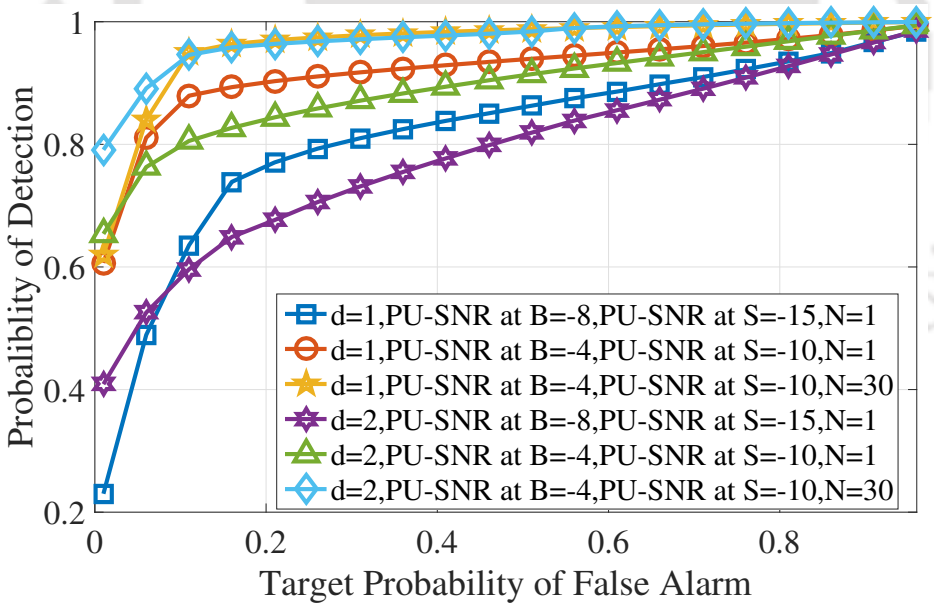

Figure 3.8: *Receiver operating characteristics. All SNRs are in dB.* $\sigma^2_{\mathrm{BC}_l} = 0.3$, $\delta_{\tilde{\gamma}^2_{\mathrm{BC}_l}} = 0.1$, $\sigma^2_{\mathrm{C}_l\mathrm{S}} = 0.5$, $\delta_{\tilde{\gamma}^2_{\mathrm{C}_l\mathrm{S}}} = 0.1$.

the proposed schemes. It can be observed that the proposed scheme can perform better than the BSR scheme if the CSUs or S have poor PU-SNR with the number of cooperators being less. The performance improvement achieved with the proposed CSS scheme for a lesser number of

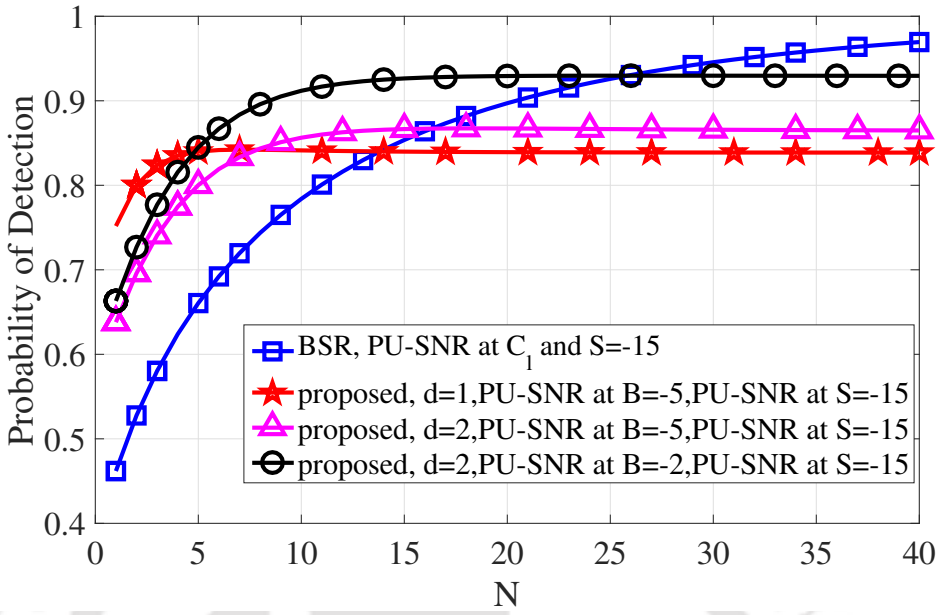

Figure 3.9: *Comparison of the proposed scheme with the BSR [61] scheme.* $P_{Fa} = 0.1$, $\sigma^2_{\mathrm{BC}_l} = 0.3$, $\delta_{\bar{\gamma}^2_{\mathrm{BC}_l}} = 0.1$, $\sigma^2_{\mathrm{C}_l\mathrm{S}} = 0.5$, $\delta_{\bar{\gamma}^2_{\mathrm{C}_l\mathrm{S}}} = 0.1$.

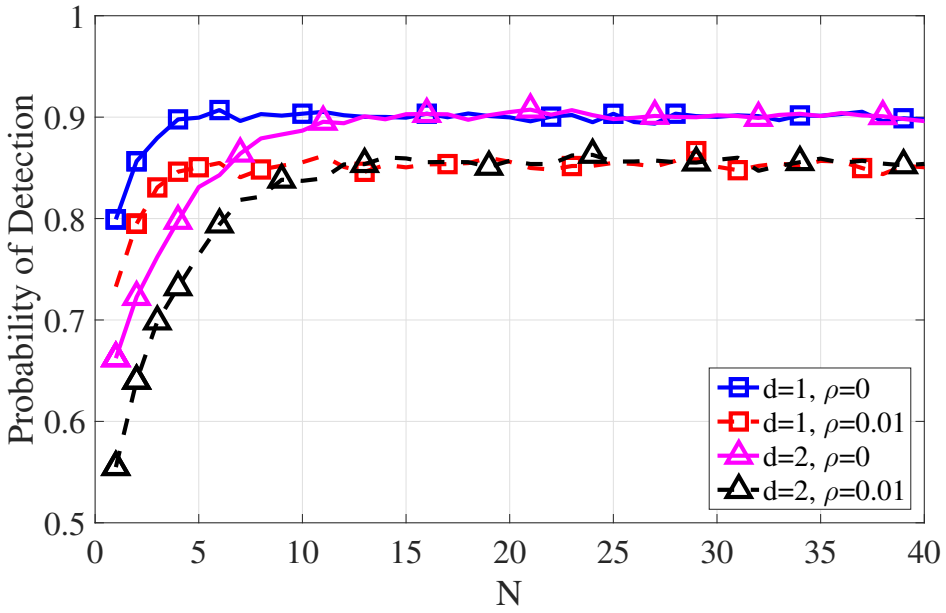

Figure 3.10: *Results of simulation showing effect of noise uncertainty. Here,* ρ *is the deviation from the nominal noise variance* $\sigma^2_n = 1$. $P_{Fa} = 0.1$, $\sigma^2_{\mathrm{BC}_l} = 0.3$, $\delta_{\bar{\gamma}^2_{\mathrm{BC}_l}} = 0.1$, $\sigma^2_{\mathrm{C}_l\mathrm{S}} = 0.5$, $\delta_{\bar{\gamma}^2_{\mathrm{C}_l\mathrm{S}}} = 0.1$, *nominal PU-SNRs at* B *and* S *are* -4 *dB and* -15 *dB, respectively.*

cooperators is attributed to the following factors:

(i) Availability of a mobile node (LSSN) which can locate itself in an area of good PU signal reception.

(ii) Flexibility of employing multi-level soft decision fusion in place of hard decision fusion.

(iii) Lack of the diversity in sensing being effectively compensated by the diversity in relaying.

For higher number of cooperators, it is seen that the BSR scheme outperforms the proposed scheme. Thus, if the number of cooperators is very large it is reasonable for CSUs to carry out sensing as done in the BSR scheme rather than relaying the statistics of another good sensor (LSSN) for improved CSS. However, this performance gain in the BSR scheme will be achieved at the cost of hiked energy consumption due to sensing by a large number of CSUs.

Although the energy detector is simple to implement, it is known to suffer from the phenomenon of noise uncertainty [85] at low SNR. Noise uncertainty is an artefact of improper estimation of noise power/PU-SNR due to short observation time [85]. In this work, the noise/PU-SNR estimate at B and S's location are assumed to be acquired from REM. Unlike spectrum sensors for cognitive radios, there is no time-constraint associated with the detectors used for estimating noise variance while charting REM. Hence, the problem of uncertain noise power can be eliminated to a large extent by depending on REM. Let ρ denote the deviation of the actual noise variance from the nominal value σ_n, i.e., $\mathbb{E}[w^2] \sim \mathcal{U}\left((1-\rho)\sigma_n^2, (1+\rho)\sigma_n^2\right)$ [85], where w denotes the noise. Figure 3.10 shows the effect of noise uncertainty on the detection performance. With the increase in noise uncertainty, the detector threshold has to be increased in order to maintain the false alarm constraint. Consequently, the detection performance degrades with the increase in ρ.

The energy detector used in the network model can be replaced by other detectors (possibly more robust to noise uncertainty) at the cost of added complexity. Note that the closed form expressions derived in this work for the overall probability of false alarm and probability of detection in (3.15) and (3.20) are generic (i.e., expressed in terms of probabilities of false alarm and detection of the detection scheme) and are valid for any other detectors.

3.8 Summary

This chapter deals with a decentralized CSS scheme capable of operating in the absence of dedicated reporting channel. The proposed CSS scheme comprises of a leading secondary

sensing node (LSSN) in addition to a number of cooperating secondary sensors (CSUs). The LSSN is preferably a mobile sensing node. Thus, making use of radio environment map, it can place itself where the PU TX signal reception is good. The CSS network also supports soft decision fusion of the variable bit quantized test statistics directly transmitted by the LSSN to the transmitting SU or relayed through one of the CSUs. The proposed network model also includes features to resolve conflicts among contending SU transmitters. Closed form expressions for the probabilities of detection and false alarm have been derived and validated using simulations. The proposed CSS scheme is noted to outperform the recently reported best selection relaying [61] scheme, and the same is attributed to the use of the quantized statistics and a mobile secondary sensor.

The spectrum sensing schemes discussed in Chapter 2 as well as this chapter happen to operate in single-band sensing mode. These techniques can easily be extended to multi-band sensing scenarios by deploying independent sensor for each frequency band and repeating the setups for each of these bands. Although multi-band spectrum sensing is well treated in the literature, most of the existing techniques are not suited for fast changing signals. In the following chapter, we present a novel spectrum sensing technique based on sparse presentation to deal with fast changing wide-band signals.

4

Spectrum Sensing for Frequency Hopping Spread Spectrum Signals

Contents

Frequency hopping spread spectrum (FHSS) is an important wideband access technique. It is especially popular in military and secure communication due to its robustness to interception and frequency selective fading. There are very limited works that look into the matter of spectrum sensing in the presence of frequency hopping PUs for cognitive radio applications. This chapter addresses the problem of tracking one or more FHSS PUs in real-time. Throughout this chapter, we consider the wideband of interest (WBOI) as the range of frequencies over which a set of FHSS PUs operate. The WBOI is assumed to be equally divided into multiple non-overlapping bands of frequencies, each of which corresponds to a single channel of the FHSS scheme. The objective is to develop efficient detection techniques that can indicate the presence of one or more FHSS PUs in the WBOI. It is essentially a multi-band spectrum sensing problem. The detection of the FHSS PU(s) under very low SNR conditions within the shortest possible time is a challenging task. In this work, the principle behind sparse representation classification (SRC) [86] has been adopted for detecting FHSS primary users. The SRC approach has already been successfully explored for classification in many other fields such as image classification [86] and speaker verification [87].

The rest of this chapter is organized as follows. Section 4.1 presents the system model. Section 4.2 briefly describes an FFT averaging ratio based spectrum sensing algorithm [73] which has been used to provide a performance comparison to the proposed approach. Section 4.3 provides a review of SRC. In Section 4.4, the adaptation of SRC for the problem of detecting FHSS PU(s) is discussed. Section 4.5 describes the setup used for the simulation and compares the performances with that of the FFT based spectrum sensing method. Finally, the summary of the work is presented in Section 4.6.

4.1 Operating Scenario and Signal Model

First we describe the broad setting under which the spectrum sensing task is carried out by an SU. Since the scenario considered in this chapter involves very dynamic FHSS PUs, a non-cooperative sensing model is adopted. Cooperative spectrum sensing is not appropriate for this situation because any additional time required by the SU devices to communicate and

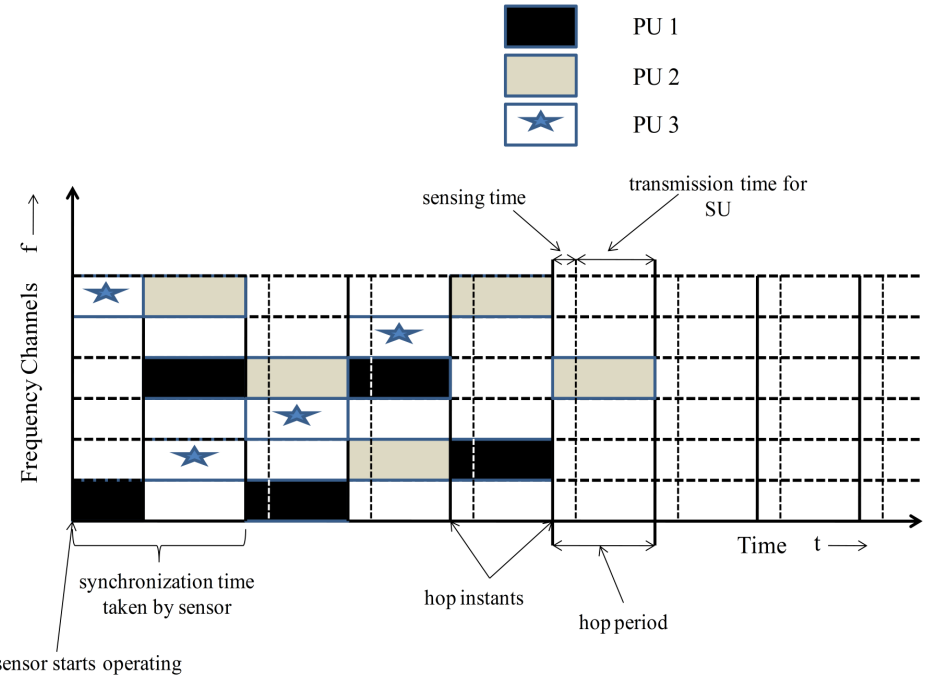

Figure 4.1: *Figure showing the sensing scenario with three FHSS PUs randomly accessing the available frequency channels. The rectangular boxes represent the occupancy by the corresponding PUs along time and frequency axes.*

cooperate may further elongate the sensing process, leaving little or no time for them to utilize the available spectrum before the PUs switch their state of operation (in this case the operating channel).

The following additional assumptions are made regarding the spectrum sensing scenario.

A1) There are N_c number of non-overlapping frequency channels in the WBOI.

A2) A maximum of N_p number of frequency hopping PUs operate in the WBOI and $N_p \leq N_c$.

A3) The baseband bit stream transmitted by PUs are modulated using a digital modulation scheme such as amplitude shift keying (ASK), phase shift keying (PSK) or frequency shift keying (FSK).

A4) The active PUs employ orthogonal hopping sequences and their hopping instants are synchronized so that there is no interference among themselves.

A5) The hop periods of the PUs are equal and constant. The SU has the complete knowledge about the hop period of the PUs.

A6) The number of active PU transmitters change with time in a random manner.

A7) The information regarding the number of FHSS PUs active at any instant of time and the frequency channels they occupy are not available to the SU.

A8) The channel information is not available to the SU.

Figure 4.1 displays a typical sensing scenario with a maximum of three FHSS PUs and six frequency channels. Spectrum sensing begins with a synchronization phase meant to align the sensing process with the PUs' hop instants. Thereafter, the periodic sensing and transmission phase by the SU commences. The SU transmits within a hop period after the spectrum sensing stage in one of the channels perceived to be vacant. The initial synchronization is achieved when the sensor identifies the hopping instants. This can be achieved by continuously sensing the spectrum at the beginning phase and looking out for the first instant where a new PU signal first appears in any one of the previously vacant bands.

The signals transmitted by the PUs suffer multipath fading and are corrupted by additive white Gaussian noise (AWGN) at the receiver end. The signal received at the SU detector can be expressed as

$$x(n) = \sum_{i \in \Lambda_{m,j}} h_i(n) * s_i(n) + w(n) \quad \text{for} \quad m = 1, 2, \ldots, N_p \text{ and } j = 1, 2, \ldots, 2^m \tag{4.1}$$

where, $\Lambda_{m,j}$ denotes the jth subset of the index set $\{1, 2, \ldots, N_p\}$ containing exactly m elements. The index set is the set of indices representing all possible PUs, $s_i(n)$ is the transmitted signal by the PU with index i, $h_i(n)$ is the multipath channel between the PU denoted by ith index and the SU, $*$ denotes the convolution operator and $w(n)$ is AWGN.

4.2 FFT Averaging Ratio (FAR) based Sensing

For contrast purpose, we have used FAR detector which a FFT based spectrum sensing method proposed in [73]. In [74], the application of this algorithm is demonstrated for a frequency hopping primary user on a real-time platform.

Let $x(n)$ denote the incoming wideband signal at the FFT based sensor input. The input signal is segmented into T_F frames $x_t(n),\ t = 0, 1, ..., T_F - 1$ and N_F point FFT is computed for each frame after necessary zero-padding. The FFT for the tth frame is given as

$$X_t(l) = \sum_{n=0}^{N_F-1} x_t(n)g(n)e^{-j\frac{2\pi ln}{N_F}}, \quad \text{for} \ \ l = 0, 1, ..., N_F - 1 \tag{4.2}$$

where $g(n)$ is the window function.

In contrast to the real signal considered in [73], a complex baseband signal $x(n)$ is considered in this work. Hence, all N_F coefficients are retained for subsequent computations. The power spectral density (PSD) of $x_t(n)$ is calculated as

$$Z_t(l) = |X_t(l)|^2 \tag{4.3}$$

The average PSD of T_F consecutive frames is given as

$$Z_{avg}(l) = \frac{1}{T_F} \sum_{t=0}^{T_F-1} Z_t(l) \tag{4.4}$$

The average across all frequency tones is given as

$$Z_m = \frac{1}{N_F} \sum_{l=0}^{N_F-1} Z_{avg}(l) \tag{4.5}$$

The normalized test statistics for deciding presence of signal on the lth frequency bin is given as

$$r(l) = \frac{Z_{avg}(l)}{Z_m} \tag{4.6}$$

The PU is declared to be occupying the pth channel if:

(i) $l = \arg\max_j r(j),\ \text{for} \ \ j = 0, 1, ..., N_F - 1$

(ii) $r(l) > t_h$ where t_h is a preset threshold

(iii) the lth bin corresponds to the pth channel

Note t_h is decided based on the percentage of noise-only signals that are required to be rejected.

4.3 Review of Sparse Representation Classification

In this section, we briefly review the basics of sparse representation and sparse representation classification.

4.3.1 Sparse Representation of Signals

Sparse representation of signals has received a great deal of attention over the last few years [12–14, 88]. In this paradigm, the signal is approximated as a sparse linear combination of a few elementary signals from a larger set of signals as

$$\mathbf{y} \approx \mathbf{D}\mathbf{x} \tag{4.7}$$

where, $\mathbf{y}$ is $N \times 1$ signal vector, $\mathbf{D}$ is $N \times K$ matrix and $\mathbf{x}$ is $K \times 1$ vector having only few non-zero entries.

The matrix $\mathbf{D}$ is commonly referred to as the *dictionary* while its columns as the *atoms* [66]. Given a dictionary, the sparse representation of a signal is obtained by greedy algorithms such as matching pursuit (MP) [89], orthogonal matching pursuit (OMP) [90] or l_1-norm minimization algorithm like basis pursuit (BP) [91].

The dictionary is usually data-dependent and is created by collecting the examples of the signal in form of a matrix. This type of dictionary is referred to as the *exemplar dictionary*. Alternatively, the dictionaries are also learned directly from the data using suitable algorithms and are reported to have better attributes than the exemplar dictionary [92]. The dictionary learning problem can be mathematically represented as

$$\min_{\mathbf{D},\mathbf{X}} \{\|\mathbf{Y} - \mathbf{D}\,\mathbf{X}\|_2^2\} \quad \text{subject to} \quad \|\boldsymbol{x}_i\|_0 \leq T_0 \tag{4.8}$$

where, $\mathbf{Y}$ is the set of training vectors, $\mathbf{D}$ is the dictionary, $\mathbf{X}$ is the set of sparse vectors corresponding to $\mathbf{Y}$ and T_0 is the constraint on sparsity.

The K-SVD [92] is the most commonly used algorithm for solving the dictionary learning problem defined in Eq. 4.8. It basically involves an iterative procedure which consists of two principle stages:

(i) determination of sparse coefficients of the data with respect to a current version of the dictionary

(ii) given the sparse representation of the data updating each of the atoms (columns) of the dictionary

4.3.2 Sparse Representation Classification

The sparse representation classification (SRC) has been used for classification purpose in a number of pattern recognition tasks [14, 86, 87, 93]. It is an approach for signal classification in which the sparse representation of a target signal is achieved over an exemplar dictionary. Let $\mathbf{a}_{ij}$ represent the jth training example from the ith class, then, a test signal $\mathbf{y}_i$ from the ith class can be represented as

$$\begin{aligned} \mathbf{y}_i &\approx \alpha_{i1}\mathbf{a}_{i1} + \alpha_{i2}\mathbf{a}_{i2} + ... + \alpha_{iN}\mathbf{a}_{iN} \\ &= \mathbf{A}_i\boldsymbol{\alpha}_i \end{aligned} \tag{4.9}$$

where, N is the number of training examples.

Now, if an exemplar dictionary is formed by the concatenation of training examples from all Q classes as

$$\mathbf{A} = [\mathbf{A}_1\ \mathbf{A}_2\ \ldots\ \mathbf{A}_Q]$$

Given a test signal $\mathbf{y}$ belonging to an unknown ith class, its sparse representation over the dictionary $\mathbf{A}$ is determined as

$$\mathbf{y} \approx \mathbf{A}\boldsymbol{\alpha} \tag{4.10}$$

where, $\boldsymbol{\alpha} = [0...0\ \alpha_{i1}...\alpha_{iN}\ 0...0]^T$, is a sparse vector whose all but coefficients associated with the ith class are expected to be zero. Thus, finding the sparse coefficients with respect to $\mathbf{A}$, identifies the unknown class of the test signal $\mathbf{y}$.

4.4 SRC based Tracking of Frequency Hopping Primary User

In this section, the adaptation of the SRC approach for the problem of classifying communication signals belonging to different channels is described. The signals belonging to a particular channel are associated with a single class. Thus, if there are N_c channels, there will be corresponding N_c classes of signals. As discussed in previous section, any given signal during test phase will be a sparse linear combination of its training specimens provided that sufficient number of specimens are collected. In the system considered here, the sensing slots stretches across multiple symbols. As a result of this, more training specimens from a channel class would be required so as to accurately represent the test signals of chosen sensing period. The use of a very large size exemplar dictionary for classification may not be feasible for spectrum sensing purpose due to increased complexity in finding the sparse representation. Further in case of the exemplar dictionary it is not straight forward how to optimally choose the specimens from the development data for creating the dictionary. This choice is *critical* when the size of the designed dictionary is required to be kept to be minimal to reduce the latency in sensing.

To address this issue, we have decided to learn a compact dictionary for each channel and then concatenate them to create the required exemplar dictionary as

$$\mathbf{D} = [\mathbf{D}_1 \; \mathbf{D}_2 \; \ldots \; \mathbf{D}_Q]$$

where $\mathbf{D}_i$ denotes the compact learned dictionary created for ith channel using a large number of examples with help of K-SVD algorithm. The resulting dictionary $\mathbf{D}$ is referred to as the *learned-exemplar dictionary* (LED) in this work.

In this work we consider that the baseband signalling scheme of all FHSS PUs is identical, i.e., the baseband digital modulation scheme, baud rate and pulse shaping filter adopted by all PUs are same and follow some common standard. Training data consists of distortion-less signals, i.e., in absence of AWGN and multipath fading. More details about how these training signals are generated are discussed in Section 4.5. At the SU receiver, the received wideband RF signal encompassing the entire WBOI is I-Q demodulated and translated to the baseband using a high frequency sinusoid with frequency between the start and end limits of the WBOI.

Training signals comprise of associated I and Q waveforms corresponding to each channel such that on modulating with the same sinusoid used in demodulation of the received signal, their spectrum would fall in the corresponding RF frequency channel.

Each sub-dictionary $\boldsymbol{D}_i$ is learned using training signals from the ith channel and K-SVD [92] algorithm. Each sub-dictionary has K_c atoms. Additional details of dictionary learning are provided in Section 4.5. The *learned exemplar dictionary* is denoted by $\boldsymbol{D}$ and is formed by horizontal concatenation of sub-dictionaries $\boldsymbol{D}_i$s corresponding to each of the N_c channels. The dictionary $\boldsymbol{D}$ has a total of $K_c N_c$ atoms and is defined as

$$\boldsymbol{D} = [\boldsymbol{D}_1 \boldsymbol{D}_2 \ldots \boldsymbol{D}_{N_c}] \tag{4.11}$$

It is to be noted that dictionary learning is an offline process so the complexity associated with K-SVD algorithm has no affect during sensing. An additional fact to be noted here is that during the learning phase only the characteristics of the primary user signals are captured rather than the channel characteristics. The learned characteristics (in the form of atoms of the dictionary) are then employed during the detection phase. As a result the detector is blind to the channel characteristics.

4.4.1 Detection of PU Transmissions

In order to avoid the use of faster analog-to-digital converters (ADCs) at the detector front-end we adopt a sub-sampling approach while sampling the received target signal.

The sub-sampling factor F_c is given as

$$F_c = \frac{f_s}{f_{\text{ADC}}} \tag{4.12}$$

where, f_s is the rate at which the training signals are sampled, and f_{ADC} is the common sampling rate of all the ADCs.

Instead of employing a single pair of uniform samplers at the I-Q sub-branches, we have employed $Ceil(F_c)$ pairs of uniform sampling ADCs to obtain the sampled versions of the I-Q sub-branches at different offsets. $Ceil(.)$ denotes the ceiling function. Each ADC pair installed

in a branch samples at $(\frac{1}{F_c})$th rate at which the training signals are sampled and all ADCs are time synchronized. In the discrete domain, the signal received at each pair of ADC branch may be expressed as the projection of the higher sampled vector on a sub-sampling matrix. For instance, if a real signal of 1 sec duration originally sampled at 10 Hz is sub-sampled by factor of 2, the corresponding sub-sampling matrices would be

$$\begin{bmatrix} 1 & 0 & 0 & 0 & 0 & 0 & 0 & 0 & 0 & 0 \\ 0 & 0 & 1 & 0 & 0 & 0 & 0 & 0 & 0 & 0 \\ 0 & 0 & 0 & 0 & 1 & 0 & 0 & 0 & 0 & 0 \\ 0 & 0 & 0 & 0 & 0 & 0 & 1 & 0 & 0 & 0 \\ 0 & 0 & 0 & 0 & 0 & 0 & 0 & 0 & 1 & 0 \end{bmatrix}$$

and

$$\begin{bmatrix} 0 & 1 & 0 & 0 & 0 & 0 & 0 & 0 & 0 & 0 \\ 0 & 0 & 0 & 1 & 0 & 0 & 0 & 0 & 0 & 0 \\ 0 & 0 & 0 & 0 & 0 & 1 & 0 & 0 & 0 & 0 \\ 0 & 0 & 0 & 0 & 0 & 0 & 0 & 1 & 0 & 0 \\ 0 & 0 & 0 & 0 & 0 & 0 & 0 & 0 & 0 & 1 \end{bmatrix}$$

Let $\boldsymbol{\Phi}_l$ denote the sub-sampling matrix corresponding to the lth pair of ADC sub-branch. If $\boldsymbol{x}$ represents the received signal vector sampled at rate f_s and $\tilde{\boldsymbol{x}}$ represents the l_2 normalized version of $\boldsymbol{x}$ given as

$$\tilde{\boldsymbol{x}} = \frac{\boldsymbol{x}}{\|\boldsymbol{x}\|_2} \tag{4.13}$$

then the signal vector appearing at the lth ADC output is given as

$$\boldsymbol{x}_l = \boldsymbol{\Phi}_l \tilde{\boldsymbol{x}} \tag{4.14}$$

The dictionary $\tilde{\boldsymbol{D}}_l$ for the lth branch is derived as follows

$$\tilde{\boldsymbol{D}}_l = NormCol\,(\boldsymbol{\Phi}_l \boldsymbol{D}) \tag{4.15}$$

where, $NormCol(\boldsymbol{H})$ denotes the function normalizing the columns of the matrix $\boldsymbol{H}$. The lth branch signal is sparse coded over dictionary $\tilde{\boldsymbol{D}}_l$ using OMP [90] to obtain the sparse vector $\boldsymbol{y}_l$ such that

$$\boldsymbol{x}_l = \tilde{\boldsymbol{D}}_l \boldsymbol{y}_l \tag{4.16}$$

The PU transmission is declared to be present in the kth channel if,

$$\underset{l}{Avg}\left(\|\mathbf{y}'_l \odot \boldsymbol{\delta}_k\|_1\right) > t_h \tag{4.17}$$

where

$$\mathbf{y}'_l = \frac{1}{F_c} Diag\left(\boldsymbol{r}_l\right) \boldsymbol{y}_l \tag{4.18}$$

$\boldsymbol{r}_l$ is a $K_c N_c \times 1$ size vector containing the original Euclidean lengths of the columns of $(\boldsymbol{\Phi}_l \boldsymbol{D})$ before transformation into normalized version $\tilde{\boldsymbol{D}}_l$ using (4.15), $Diag\,(.)$ is an operator that shapes a given vector into a diagonal matrix, and $\odot$ denotes the element-wise vector multiplication operator, $\boldsymbol{\delta}_k$ denotes a $K_c N_c \times 1$ indicator vector selecting the indices corresponding to the kth channel such that

$$\delta_k(n) = \begin{cases} 1, & \text{for } n = (k-1)K_c + 1, ..., kK_c \\ 0, & \text{otherwise} \end{cases} \tag{4.19}$$

and t_h is a predefined threshold to detect the presence of the signal in the observed data.

4.4.2 Implementation Complexity of the Proposed Detector

The proposed sparse representation based spectrum sensor implements the sensing operation in two stages:

(i) Computation of sparse coefficients of the received signal at each of the u-branches using OMP algorithm.

(ii) Combination of decisions from all branches as described by (4.17) to determine channel occupancy status.

The time complexity of computing the sparse coefficients at each of the parallel branches using OMP is approximately $2Sm_sK_cN_c + 3S^2m_s$. Here, m_s denotes number of samples obtained at the output of an ADC pair combined during a sensing period and S denotes the chosen sparsity constraint value. This includes:

i) $(2m_s - 1)K_cN_c$ floating point operations (flops) involved in the matrix-vector multiplication operation required for determining highest correlated dictionary atom at each iteration and,

ii) $4m_si$ flops required for computing least squares solution and $2m_si$ flops required for residual update at the ith iteration.

The second stage is common to any detector which may work in a fixed frequency-slotted spectrum sensing scenario considered for this work. This stage involves $(K_c - 1)N_cu$ flops associated with taking binary decisions for N_c channels using K_c atoms per channel and u sensors.

The time complexity of the proposed algorithm is linear with dictionary size while quadratic with sparsity constraint value. It is therefore, necessary to keep the sparsity constraint value to a minimum, while maintaining the detection performance.

4.5 Simulation, Results and Discussion

Table 4.1: Percentage of detection (P_d) at varying SNR and different number of active PUs for FAR and learned-exemplar dictionary (LED) based methods with sensing time equal to 5 symbol periods. The number of atoms chosen for LED is 30×16 . For simulation, the received signal is sampled at 128 MHz. For the dictionary based method a sub-sampling factor, F_c of 4 is applied reducing the effective sampling rate to 32 MHz.

SNR (dB)	FAR [73] Number of active PU Transmitters					LED (480 atoms) Number of active PU Transmitters				
	5	4	3	2	1	5	4	3	2	1
0	57.05	63.88	75.99	87.18	98.34	88.92	93.38	95.08	96.58	99.09
-5	56.28	65.05	73.14	84.92	97.90	86.86	89.85	91.24	95.43	97.42
-10	52.60	60.81	70.11	79.33	90.40	79.83	82.30	84.87	87.63	92.94
-15	43.40	49.97	57.56	66.85	75.44	60.50	65.87	67.70	70.19	73.64

Table 4.2: Percentage of detection (P_d) at varying SNR and different number of active PUs for FAR and LED based methods with sensing time equal to 2 symbol periods. Other parameters are set same as in Table 4.1.

SNR (dB)	FAR [73] Number of active PU Transmitters					LED (480 atoms) Number of active PU Transmitters				
	5	4	3	2	1	5	4	3	2	1
0	28.48	39.78	57.99	77.80	97.89	84.17	89.75	91.72	95.58	97.52
-5	26.97	39.41	54.90	71.58	90.58	83.02	83.59	87.05	88.85	90.46
-10	24.08	34.07	47.90	63.39	79.97	69.89	73.90	74.79	75.56	75.77
-15	18.74	25.24	34.54	43.64	52.28	47.59	52.02	53.60	53.71	53.97

For simulation, we have modulated the baseband binary bit stream using Gaussian frequency shift keying (GFSK) modulation scheme. The signal closely resembles *Bluetooth* signal transmitting at basic rate [72]. Baud rate is set at 1 Mega symbols per second or equivalently the symbol period T_s is set to 1μs. The time-bandwidth product of the Gaussian filter is 0.5. The modulation index μ is kept as 0.32. The bandwidth of each channel is 1 MHz. We have considered 16 channels for simulation. Thus, the total bandwidth of interest is 16 MHz.

The LED is created using training signals from each of 16 channels. As mentioned in Section 4.4, noiseless and unfaded signals fragments generated using GFSK modulation and specifications stated previously are used for the training. Equally sliced portions at random instants from a long baseband transmission are extracted as training specimens. Signals are sampled at rate f_s and the time length of training signals is set equal to the desired sensing time T_{sns} of the detector. The signals so generated are modulated into 16 different carrier frequencies spaced 1 MHz apart to simulate their presence in different channels. This operation is done in the baseband instead of the actual RF frequency band. For instance, in order to translate a signal to an RF channel in the 2.4 GHz band, it would actually require additional modulation using a suitable carrier of high frequency f_h to do so. In our simulation, the carrier frequency that would have been required to translate to that RF frequency is equal to the start band frequency (2.4 GHz for instance) added to half the the total bandwidth of interest (8 MHz). This is done in order to bring down the sampling requirements. The converse process in order to deal with the real RF signal would require the detector signal to bring down the received signal to baseband

using I-Q demodulation and the associated carrier of frequency f_h. All signals in this work are simulated in the baseband.

The resultant training signals are complex. The real and imaginary components are stacked in the form of column vectors such that all the real components lie on the top half of the vectors followed by the imaginary components. The training set for a particular channel consists of such vectors from associated training signals stacked in the form of a matrix. This training set is used to obtain the sub-dictionary $\boldsymbol{D}_i$ for the ith channel using the K-SVD algorithm. The number of atoms in $\boldsymbol{D}_i$ is K which is kept constant for all channel sub-dictionaries. The LED $\boldsymbol{D}$ is then obtained using (4.11).

ITU Indoor Office-A [94] channel model is adopted for the simulations. The signal received at the detector front-end is an aggregate of transmissions from variable number of PUs relayed through multipath channels and corrupted by AWGN as represented by (4.1). Varying numbers of active PUs ranging from 0 to 5 are considered to simulate the spectrum sensing scenario.

The proposed approach has been contrasted with FAR spectrum detector [73]. Unlike most conventional spectrum sensing algorithms based on cyclostationary or eigen analysis based features, the FFT based detectors are relatively less complex due to minimal number of computations required and can easily be applied to wideband sensing scenario like the one under consideration. FFT based sensors are basically energy detectors and require less sensing time than cyclostationary or eigen value based detectors to arrive at a decision under moderate SNR conditions. Since fast sensing is necessary for the scenario involving FHSS primary user, we chose to compare the proposed method with FAR. In contrast to the proposed method, FAR utilizes Fourier bases to decompose the received signal into a non-sparse representation. The salient feature of FAR algorithm is its ability to maintain a constant false alarm rate (CFAR) under varying and unknown SNR scenarios. Similar CFAR property is also noted in the proposed method. The detection threshold need not be altered to account for the changing SNR conditions while retaining the same noise rejection capabilities. The decision thresholds of both the methods also remains fairly invariant to the number of active transmitters that are present in the band of interest.

Figures 4.2 and 4.3 plot the sensitivity of the optimal detection threshold to varying SNR conditions and number of PU transmitters for the proposed dictionary based and FAR methods respectively.

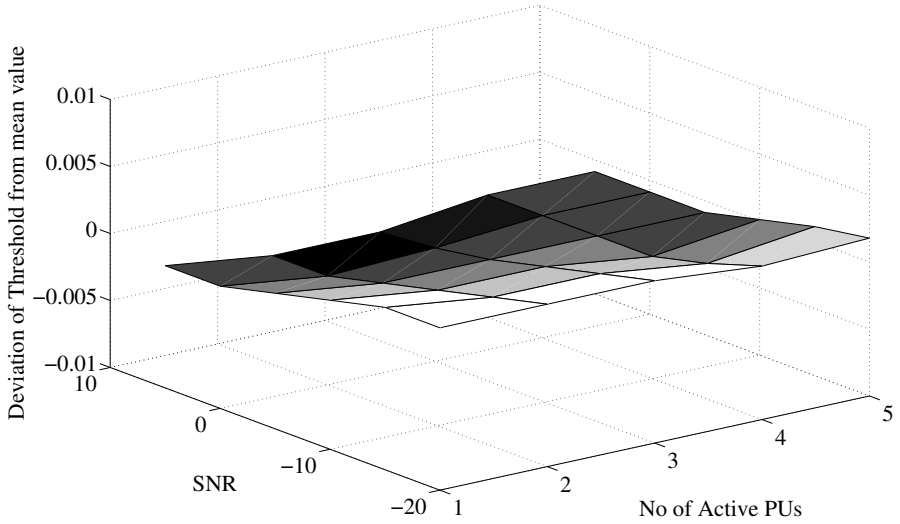

Figure 4.2: *Figure showing the deviation of the optimal decision threshold from the mean value for the proposed method. The noise rejection ratio is maintained at* 10% *under varying SNR conditions and different number of active PUs. The SNR and number of PUs range from -20 dB to 5 dB and 1 to 5, respectively. The standard deviation of the optimal threshold values considering all possible combination of SNR conditions and number of active PUs turns out to be* 1.7×10^{-6}.

For the LED based method, similar to the training signals, the received signals are separated into real and imaginary components and stacked as column vectors of real values. The received signals are l_2 normalized as in 4.13 and effectively down-sampled at each of the lth ADC branches mentioned in Section 4.4.1 using the sampling matrices $\mathbf{\Phi}_l$. This is equivalent to using slower ADCs at the I and Q branches of each of the sampling branches and obtain a signal sampled at a lower rate than the training signal. It is worth noting that the training signals are generated offline and as such the constrain on ADC speed does not relate to these signals.

For the FAR detector, the sampling rate adopted is same as that of the training signals for the LED based method. This means higher speed ADCs are installed at the detector front-end for this method. Unlike LED based method, the received vector is not transformed into a real vector but retained as it is.

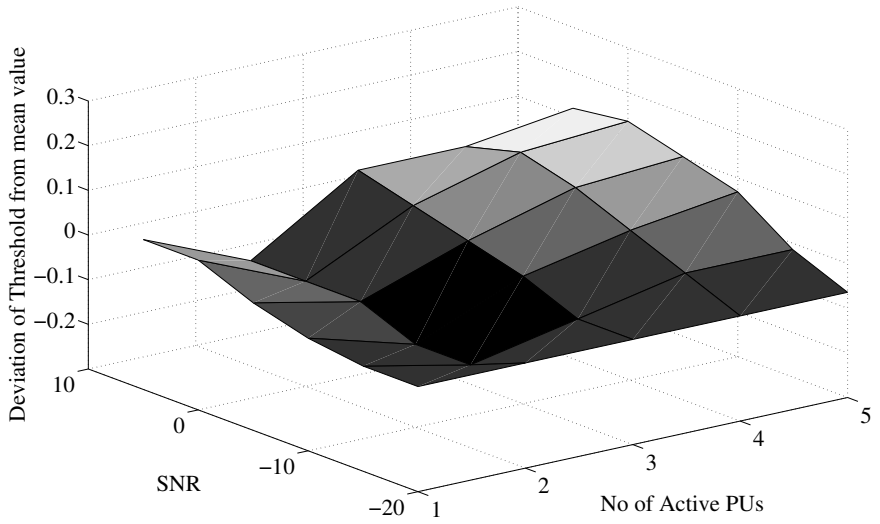

Figure 4.3: *Figure showing the deviation of the optimal decision threshold from the mean value for the FAR method. Noise rejection ratio, SNR conditions and number of active PUs are same as for the dictionary based method. The standard deviation of the optimal threshold values considering all possible combination of SNR conditions and number of active PUs turns out to be* 5.6×10^{-3}.

Table 4.1 and Table 4.2 give the average detection performances for the FAR and the LED based methods for sensing periods T_{sns} equal to 5 and 2 symbol periods, respectively. The FAR method uses 1024 point FFT and 4 time-frames for averaging. For the LED based method, the values for sparsity constraint are set 10 and 16 for testing and training, respectively. The false alarm rate is fixed at 10%. For these set of simulations, the active channels are placed far apart so that there is minimal effect of inter-channel interference on the performances.

On comparing Table 4.1 and Table 4.2, we can make the following observations:

- In general, the detection performances for the LED based method are superior to that of the FAR method under the observed SNRs. Except for single PU case, the proposed LED approach is outperformed by the FAR method in particularly at lower SNR values.

- The performance of both the FAR and the LED based methods decrease when the sensing period is reduced. The degradations observed in the FAR method are more drastic than those noted for the LED based method. On comparing the performances for the 5 PU case, we note that the LED method with 2 symbol period sensing outperforms that of the

FAR method with 5 symbol period sensing.

The detection performances of the LED based method is noted to be significantly better than that of the FAR method for most of the cases. In our understanding the possible reason for the same lie in:

- the use of a data-dependent dictionary rather than the fixed Fourier bases
- finding the sparse representation of targets rather than orthogonal projections

Since the dictionary used in the LED based approach is derived from the type of signals to be detected using K-SVD, the atoms tend to have higher correlation with the target to be detected. Unlike generic Fourier basis vectors used in the FAR method, the atoms of the LED based approach provide a degree of matching gain for a time limited segment of the target. Due to finite length of observation of the target the Fourier basis leaks the energy into the adjacent channels leading to degradation in performance.

Secondly, the sparse representation adopted in LED based method helps suppress unwanted noise as long as sparsity constraint is appropriately chosen. During sparse coding only the highest coefficients are retained which happen to correspond to the PU signal(s) when it(they) are actually present. Since the atoms have significantly higher correlation with PU signals than they have with noise, sparse coding using such atoms would yield a limited set of higher valued coefficients at even low SNR but only when signal is present. This holds for some minimum SNR beyond which the noise rejection capabilities are lost depending on the difference between the value of sparsity constraint chosen and actual number of transmitters present in the band of interest. The mismatch between chosen sparsity and number of PU present explains why the performances in the a single PU case drops compared to the FAR method at very low SNR. The average performance though is noted to be significantly better than that of the FAR method even at lower SNR considering variable number of active PUs present in the band.

The degradation of detection performances for both the methods due to reduced sensing time is expected. A shorter signal leaves lesser scope for averaging out the white noise thereby decreasing the performance. However, the larger drop in performance of the FAR method can

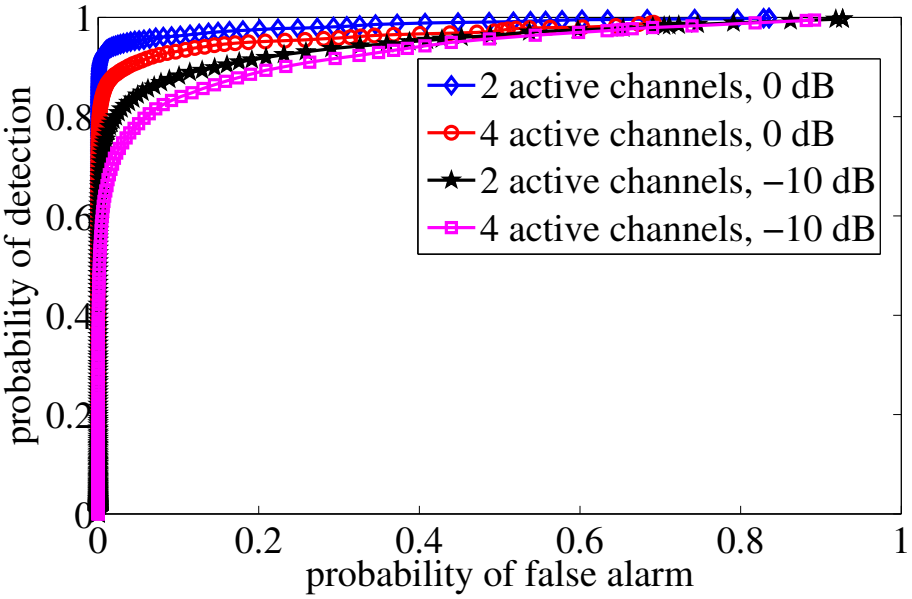

Figure 4.4: *Plot of probability of detection vs probability of false alarm for the LED based method for different number of active channels and SNR conditions.*

again be attributed to the phenomenon of frequency leakage. Shorter sensing period leads to greater leakage of energy of the signal of interest into adjacent channels. The matching gain provided by dictionary atoms reduces such kind of leakage for the LED based method.

The region of convergence plots for the LED and the FAR based methods are plotted in Figure 4.4 and Figure 4.5, respectively. The superior performance of the LED based method over FAR is also evident from these plots.

4.5.1 Effects of Inter-channel Interference on Detection Performance

Tables 4.1 and 4.2 list the detection performances under cases when the active channels are sufficiently far apart so as not cause significant inter-channel interference. The performances under the condition when two PUs are very closely placed in the band are however, expected to be different. Table 4.3 shows the detection performances when two active PU transmitters lie in different locations in the band relative to each other.

It is observed that the FAR method has an advantage when the active channels happen to be just adjacent to each other. This is attributed to the fact that the frequency leakage from nearby channels contribute to the increased energy of the adjacent channel leading to an improved

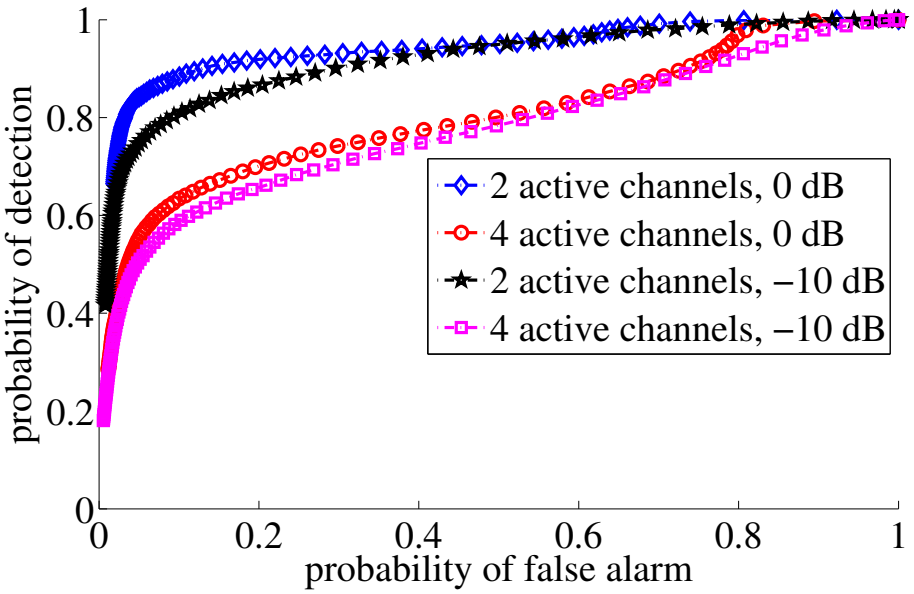

Figure 4.5: *Plot of probability of detection vs probability of false alarm for the FAR based method for different number of active channels and SNR conditions.*

Table 4.3: Percentage of detection (P_d) at varying SNR when two active PUs are present (i) at farthest possible channels (Ch 1, Ch 16), (ii) with a vacant channel in between (Ch 8, Ch 10), (iii) in adjacent channels (Ch 8, Ch 9). Sensing time is 5 symbol period. Other parameters are set same as in Table 4.1.

SNR (dB)	FAR [73] Busy Channels			LED (480 atoms) Busy Channels		
	1, 16	8, 10	8, 9	1, 16	8, 10	8, 9
0	87.18	87.15	99.64	96.58	97.40	97.62
-5	84.92	83.60	98.97	95.43	93.53	95.78
-10	79.33	77.88	95.75	87.63	86.68	87.48
-15	66.85	64.49	83.98	70.19	71.54	68.94

performance. Though this may seem as an obvious advantage of the FAR method, in reality, the frequency leakage causes the detection performance to drop in other cases when the active channels are not adjacent to each other. Since, it is very unlikely to have active PUs located at adjacent channels most of the time, this effect may not provide an overall advantage to the FAR method. The performance of LED based method is however, noted to be consistent throughout all the observed cases for a particular SNR.

4.6 Summary

In this chapter, spectrum sensing using sparse coding on LED for detection of multiple unknown number of FHSS primary users has been proposed. The LED based technique is compared with an FFT based method which utilizes sampled signals obtained at higher rate than the proposed method. The detection performances for the LED based method are still found to be superior when the sensing time is kept very short. For achieving decent detection performances, slower ADCs can be installed at the detector front-end for the proposed method.

5

Conclusion and Future Works

CR technology offers the promise of tackling the problem of spectrum scarcity by using strategies for secondary spectrum access. Secondary spectrum access of the licensed spectrum can increase the utilization of the radio spectrum. A lot of research effort has been put into the development of efficient secondary spectrum access techniques. Independent studies have been conducted into several aspects related to spectrum access such as overlay and underlay access, signal detection, cooperative sensing, performance analysis of systems under different fading conditions, security related issues so on and so forth. Consolidation of these research works is imperative for developing practical and versatile CR systems. Secondary spectrum access strategies are needed to be well-defined for practical systems operating under different scenarios. Certain practical constrains, such as implementation of reporting mechanisms in the absence of dedicated reporting channels are not adequately dealt with in the existing literature. Moreover, spectrum sensing strategies for detecting certain specific kind of radio transmitters such as frequency hopping PUs are not often discussed. This thesis work has dealt with new sensing strategies for dealing with following realistic issues:

(i) Implementation of spectrum sensing in CR networks without dedicated reporting channels in

   (a) centralized CSS architecture and,

   (b) decentralized CSS architecture.

(ii) Detection of highly dynamic frequency hopping spread spectrum primary user signals.

First, the problem of spectrum sensing in a centralized CSS network, in the absence of dedicated reporting channels was considered. Most prior works did not consider the operation of a traditional centralized CSS network in the absence of dedicated reporting channels. However, this work is based on the assumption that the reporting channels are shared with the PU licensed channel. The work considers the utilization of the information of the difference in the outage rates of the reported decisions due to the presence and the absence of the PU while deriving the optimal n-out-of-K voting rule. An improvement in the performance is observed, compared

to the case when this information of the difference in the outage rates is not considered. This model considers all CSUs to be within close range of each other. Hence, they are assumed to experience similar average PU-SNR levels.

A group of smart stationary devices (internet of things) operating opportunistically inside a room in close proximity of one another in the TV white space may be presented as a practical example of the scenario where a secondary network may adopt such a centralized CSS strategy. Elements in such a network are close enough to experience similar SNR levels from a single TV station operating in a particular channel thus matching the system assumptions.

Secondly, a decentralized CSS network operating in the absence of dedicated reporting channels is presented. This CSS model supports a two stage detection process - standalone and joint test. The actual spectrum sensing is done by two SU nodes only, whereas the other CSUs aid in relaying the reported test statistics on demand, when standalone test fails and joint test becomes necessary. The test statistics to be reported is quantized to reduce the data rate requirement during reporting. In addition to performing spectrum sensing, the proposed network model also aids in the selection of a unique transmitting SU Tx among multiple contending SUs as well as removal of any conflicts among them. The second solution may be applicable in the case of more spatially expansive adhoc secondary networks. This model may be adopted to support multiple secondary portable devices operating in the TV white space. Such a network can operate in the presence of a single PU Tx.

Thirdly, sparse coding based spectrum sensing solution is presented for the detection of FHSS PUs in the WBOI. Because of the very dynamic nature of the PUs involved in this case, only non-cooperative sensing strategy is considered. Through simulations, the performance of the proposed sensing scheme is shown to be superior compared to the state-of-the-art FAR based sensing scheme. This strategy may be applied to utilize the spectrum bands allocated to FHSS PUs, as for example those reserved for defence applications.

The primary focus of this thesis work has been on the spectrum sensing aspect of cognitive radio. There are other issues which need to be considered to build a complete working model of a cognitive radio network. These includes, issues related to network initialization and network

security. Moreover, the models presented in Chapter 2 and Chapter 3 deals with only a single PU Tx operating in a single band. Such a model cannot be adopted to operate, for instance, in a cellular network. The noise model considered in this thesis is Gaussian. Some of the areas which can be looked into in the future are highlighted below:

- Design of strategies for minimizing requirement of control channel resources during initial network setup.
- Inclusion of security measures for preventing misuse of random access protocols in the proposed decentralized CSS architecture.
- Design and analysis of strategies without dedicated reporting channels for multi-band CSS scenarios in presence of multiple spatially distributed non-synchronous primary users.
- Study of the performance of different spectrum sensing algorithms under non-Gaussian noise.

A

Asymptotic Total Error

As the detection threshold $\lambda \to \infty$, $P_{f_i}(\lambda) \to 0$ and $P_{d_i}(\lambda) \to 0$. Therefore, from (2.8) it can be verified that $S(n_K, \lambda) = 0$ for all cases except when $n_K = 0$. The optimal value of n_K without considering the difference in outage rates is given as [42, Eqn. 8]

$$n_{K_{\text{opt}}}(\lambda) = \min\left\{K, \left\lceil \frac{K}{1+\alpha(\lambda)} \right\rceil\right\}. \tag{A.1}$$

It can be noted that when n_K is chosen as (A.1), for any given N, $n_K = 0$ only for $K = 0$. Thus, using (2.7) and (2.8), (2.12) can be derived. For the proposed rule, it can be verified that the optimal value $n_{K_{\text{opt}}}$ given by (2.10), increases as K increases. Thus there exists a largest value of $K = K_l$ beyond which $n_{K_{\text{opt}}}$ cannot be zero. To recover K_l, we solve the following inequality

$$\lim_{\lambda\to\infty} \frac{K\left[1+\beta(\lambda)\right] + [N-K]\,\theta(\lambda)}{1+\alpha(\lambda)} \leq 0. \tag{A.2}$$

Using the fact that $\alpha(\lambda) \geq 0$, we have

$$K_l = \left\lfloor \frac{-N\log(P_{E1_i}/P_{E0_i})}{\log[\{(1-P_{E1_i})P_{E0_i}\}/\{(1-P_{E0_i})P_{E1_i}\}]} \right\rfloor. \tag{A.3}$$

Now, $\lim_{\lambda\to\infty} S(n_{K_{\text{opt}}}, \lambda)$

$$= \begin{cases} \binom{N}{K}\left[P_{E0_i}^{N-K}(1-P_{E0_i})^K - P_{E1_i}^{N-K}(1-P_{E1_i})^K\right], & 0 \leq K \leq K_l \\ 0, \quad \text{otherwise.} \end{cases} \tag{A.4}$$

On combining (2.7) and (A.4), the expression in (2.11) follows.

B

Derivation of $\beta_{\mathcal{H}_i}$

Let, $\Phi_{m,j}$ denote the jth subset of Ψ containing m elements, $\Phi^c_{m,j} = \Psi \setminus \Phi_{m,j}$ and $l_1, l_2, \ldots, l_m$ denote the m elements of $\Phi_{m,j}$. Physically, $\Phi_{m,j}$ here represents the set of CSUs which have successfully decoded both the request signal from S in s_2 and the reported test statistics from B in s_3.

Now,

$$\beta_{\mathcal{H}_i} = 1 - Pr\{\text{Outage of direct signal carrying test statistics from B to S}|\mathcal{H}_i\} \times Pr\{\text{Outage of relayed test statistics from B to S by CSU network}|\mathcal{H}_i\}. \quad \text{(B.1)}$$

Where,

$$\begin{aligned} &Pr\{\text{Outage of relayed test statistics from B to S by CSU network}|\mathcal{H}_i\} \\ &= \sum_{m=0}^{N} \sum_{j=1}^{\binom{N}{m}} Pr\{\Phi_{m,j}, \gamma_{\mathrm{C}_{l_1}\mathrm{S}} < \gamma_{\mathrm{Bout}}, \gamma_{\mathrm{C}_{l_2}\mathrm{S}} < \gamma_{\mathrm{Bout}}, \ldots, \gamma_{\mathrm{C}_{l_m}\mathrm{S}} < \gamma_{\mathrm{Bout}}|\mathcal{H}_i\} \\ &= \sum_{m=0}^{N} \sum_{j=1}^{\binom{N}{m}} Pr\{\Phi_{m,j}|\mathcal{H}_i\} Pr\{\gamma_{\mathrm{C}_{l_1}\mathrm{S}} < \gamma_{\mathrm{Bout}}, \gamma_{\mathrm{C}_{l_2}\mathrm{S}} < \gamma_{\mathrm{Bout}}, \ldots, \gamma_{\mathrm{C}_{l_m}\mathrm{S}} < \gamma_{\mathrm{Bout}}|\mathcal{H}_i, \Phi_{m,j}\} \\ &= \sum_{m=0}^{N} \sum_{j=1}^{\binom{N}{m}} Pr\{\Phi_{m,j}|\mathcal{H}_i\} \prod_{l \in \Phi_{m,j}} Pr\{\gamma_{\mathrm{C}_l\mathrm{S}} < \gamma_{\mathrm{Bout}}|\mathcal{H}_i, \Phi_{m,j}\} \end{aligned} \quad \text{(B.2)}$$

and,

$$\begin{aligned} &Pr\{\gamma_{\mathrm{C}_{l_k}\mathrm{S}} < \gamma_{\mathrm{Bout}}|\mathcal{H}_i, \Phi_{m,j}\} \\ &= Pr\{\gamma_{\mathrm{C}_{l_k}\mathrm{S}} < \gamma_{\mathrm{Bout}}|\mathcal{H}_i, \gamma_{\mathrm{SC}_{l_1}} > \gamma_{\mathrm{Sout}}, \gamma_{\mathrm{SC}_{l_2}} > \gamma_{\mathrm{Sout}}, \ldots, \gamma_{\mathrm{SC}_{l_m}} > \gamma_{\mathrm{Sout}}, \gamma_{\mathrm{BC}_{l_1}} > \gamma_{\mathrm{Bout}}, \ldots, \gamma_{\mathrm{BC}_{l_m}} > \gamma_{\mathrm{Bout}}\} \end{aligned} \quad \text{(B.3)}$$

Applying the principle of reciprocity for the CSU-S wireless links (i.e., $\gamma_{\mathrm{SC}_{l_k}} = \gamma_{\mathrm{C}_{l_k}\mathrm{S}}$) and the fact that all wireless channels are independent we have,

$$\begin{aligned} Pr\{\gamma_{\mathrm{C}_{l_k}\mathrm{S}} < \gamma_{\mathrm{Bout}} | \mathcal{H}_i, \Phi_{m,j}\} &= Pr\{\gamma_{\mathrm{C}_{l_k}\mathrm{S}} < \gamma_{\mathrm{Bout}} | \mathcal{H}_i, \gamma_{\mathrm{SC}_{l_k}} > \gamma_{\mathrm{Sout}}\} \\ &= Pr\{\gamma_{\mathrm{C}_{l_k}\mathrm{S}} < \gamma_{\mathrm{Bout}} | \mathcal{H}_i, \gamma_{\mathrm{C}_{l_k}\mathrm{S}} > \gamma_{\mathrm{Sout}}\} \\ &= \frac{Pr\{\gamma_{\mathrm{Sout}} < \gamma_{\mathrm{C}_{l_k}\mathrm{S}} < \gamma_{\mathrm{Bout}} | \mathcal{H}_i\}}{Pr\{\gamma_{\mathrm{C}_{l_k}\mathrm{S}} > \gamma_{\mathrm{Sout}} | \mathcal{H}_i\}} \\ &= \frac{P_{Ei_{\mathrm{C}_{l_k}\mathrm{S}}} - P_{Ei_{\mathrm{SC}_{l_k}}}}{1 - P_{Ei_{\mathrm{SC}_{l_k}}}} \end{aligned} \tag{B.4}$$

Again,

$$Pr\{\Phi_{m,j} | \mathcal{H}_i\} = \prod_{l \in \Phi_{m,j}} (1 - P_{Ei_{\mathrm{SC}_l}})(1 - P_{Ei_{\mathrm{BC}_l}}) \prod_{k \in \Phi^c_{m,j}} \left\{1 - (1 - P_{Ei_{\mathrm{SC}_k}})(1 - P_{Ei_{\mathrm{BC}_k}})\right\} \tag{B.5}$$

Also we have,

$$Pr\{\text{Outage of direct signal carrying test statistics from B to S} | \mathcal{H}_i\} = P_{Ei_{\mathrm{BS}}} \tag{B.6}$$

Substituting (B.4) and (B.5) in (B.2) and using (B.2) and (B.6) in (B.1), we get the expressions (3.18) and (3.21).

C

Derivation of P_{CD} and P_{CF}

Let us consider the joint event $\{E'_{\mathrm{B},q} + E'_{\mathrm{S}} > x, E'_{\mathrm{S}} < \lambda'_{\mathrm{s}} | \mathcal{H}_1, \mathcal{G}\}$.

Now, let $E'_{\mathrm{B},q} = e'_{\mathrm{B},q,l}$, then we have the relations

$$e'_{\mathrm{B},q,l} + E'_{\mathrm{S}} > x \tag{C.1}$$

$$E'_{\mathrm{S}} < \lambda'_{\mathrm{s}} \tag{C.2}$$

From (C.1) and (C.2), we have

$$e'_{\mathrm{B},q,l} > x - \lambda'_{\mathrm{s}}. \tag{C.3}$$

Let $T = \{l \,|\, e'_{\mathrm{B},q,l} > \lambda_{\mathrm{C}} - \lambda'_{\mathrm{s}}\}$ be a set, then,

$$\begin{aligned}
&Pr\{E'_{\mathrm{B},q} + E'_{\mathrm{S}} > x, E'_{\mathrm{S}} < \lambda'_{\mathrm{s}} | \mathcal{H}_1, \mathcal{G}\} \\
&= \sum_{n \in T} Pr\{e'_{\mathrm{B},q,n} + E'_{\mathrm{S}} > x, E'_{\mathrm{S}} < \lambda'_{\mathrm{s}}, E'_{\mathrm{B},q} = e'_{\mathrm{B},q,n} | \mathcal{H}_1, \mathcal{G}\} \\
&= \sum_{n \in T} \left[Pr\{x - e'_{\mathrm{B},q,n} < E'_{\mathrm{S}} < \lambda'_{\mathrm{s}} | \mathcal{H}_1, \mathcal{G}\, E'_{\mathrm{B},q} = e'_{\mathrm{B},q,n}\} P_{E'_{\mathrm{B},q}|\mathcal{H}_1}(n) \right] \\
&= \sum_{n \in T} \left(P'_{d,\mathrm{S}}(x - e'_{\mathrm{B},q,n}) - P'_{d,\mathrm{S}}(\lambda'_{\mathrm{s}}) \right) P_{E'_{\mathrm{B},q}|\mathcal{H}_1}(n)
\end{aligned} \tag{C.4}$$

where $P'_{d,\mathrm{S}}(x) = P_{d,\mathrm{S}}(x/\delta_{\mathrm{s}})$.

Thus we have,

$$\begin{aligned}
P_{CD} &= Pr\{E'_{\mathrm{B},q} + E'_{\mathrm{S}} > x | \mathcal{H}_1, E'_{\mathrm{S}} < \lambda'_{\mathrm{s}}, \mathcal{G}\} \\
&= \frac{Pr\{E'_{\mathrm{B},q} + E'_{\mathrm{S}} > x, E'_{\mathrm{S}} < \lambda'_{\mathrm{s}} | \mathcal{H}_1, \mathcal{G}\}}{Pr\{E'_{\mathrm{S}} < \lambda'_{\mathrm{s}} | \mathcal{H}_1\}} \\
&= \frac{\sum_{n \in T} \left(P'_{d,\mathrm{S}}(x - e'_{\mathrm{B},q,n}) - P'_{d,\mathrm{S}}(\lambda'_{\mathrm{s}}) \right) P_{E'_{\mathrm{B},q}|\mathcal{H}_1}(n)}{1 - P'_{d,\mathrm{S}}(\lambda'_{\mathrm{s}})}
\end{aligned} \tag{C.5}$$

The derivation of P_{CF} is identical after replacing $\mathcal{H}_1$ with $\mathcal{H}_0$ and $P'_{d,\mathrm{S}}$ and $P_{d,\mathrm{S}}$ with $P'_{f,\mathrm{S}}$ and $P_{f,\mathrm{S}}$, respectively.

D

Probability of False Alarm and Detection for BSR

Let Ξ and Ξ^c, respectively represent the events that S detects and fails to detect the PU in the standalone detection sub-slot. Then the probability of detection can be expressed as

$$\begin{aligned}
P_{D,BSR} &= Pr\{\Xi|\mathcal{H}_1\} + Pr\{\Xi^c, \text{success in detection by the CSU network}|\mathcal{H}_1\} \\
&= Pr\{\Xi|\mathcal{H}_1\} + Pr\{\Xi^c|\mathcal{H}_1\} Pr\{\text{success in detection by the CSU network}|\mathcal{H}_1, \Xi^c\} \\
&= Pr\{\Xi|\mathcal{H}_1\} + Pr\{\Xi^c|\mathcal{H}_1\} \left[1 - Pr\{\text{failure in detection by the CSU network}|\mathcal{H}_1, \Xi^c\}\right] \\
&= 1 - Pr\{\Xi^c|\mathcal{H}_1\} Pr\{\text{failure in detection by the CSU network}|\mathcal{H}_1, \Xi^c\} \qquad \text{(D.1)}
\end{aligned}$$

Let, $\Phi_{m,j}$ denote the jth subset of Ψ containing m elements, $\Phi^c_{m,j} = \Psi \setminus \Phi_{m,j}$ and $l_1, l_2, \ldots, l_m$ denote the m elements of $\Phi_{m,j}$. The remaining course of the proof is similar to that of the derivation of $\beta_{\mathcal{H}_i}$ done in Appendix B. However, the physical interpretation of the set $\Phi_{m,j}$ is different. Physically, $\Phi_{m,j}$ here represents the set of CSUs which have successfully decoded both the request signal from S and also detected the PU. Let γ_{Cout} denote the outage signal to noise and interference ratio of any reported signal from CSU to S. Now,

$$\begin{aligned}
&Pr\{\text{failure in detection by the CSU network}|\mathcal{H}_1, \Xi^c\} \\
&= \sum_{m=0}^{N} \sum_{j=1}^{\binom{N}{m}} Pr\{\Phi_{m,j}, \gamma_{\text{C}_{l_1}\text{S}} < \gamma_{\text{Cout}}, \gamma_{\text{C}_{l_2}\text{S}} < \gamma_{\text{Cout}}, \ldots, \gamma_{\text{C}_{l_m}\text{S}} < \gamma_{\text{Cout}}|\mathcal{H}_1, \Xi^c\} \\
&= \sum_{m=0}^{N} \sum_{j=1}^{\binom{N}{m}} Pr\{\Phi_{m,j}|\mathcal{H}_1, \Xi^c\} Pr\{\gamma_{\text{C}_{l_1}\text{S}} < \gamma_{\text{Cout}}, \gamma_{\text{C}_{l_2}\text{S}} < \gamma_{\text{Cout}}, \ldots, \gamma_{\text{C}_{l_m}\text{S}} < \gamma_{\text{Cout}}|\mathcal{H}_1, \Xi^c, \Phi_{m,j}\} \\
&= \sum_{m=0}^{N} \sum_{j=1}^{\binom{N}{m}} \left[Pr\{\Phi_{m,j}|\mathcal{H}_1, \Xi^c\} \times \prod_{l \in \Phi_{m,j}} Pr\{\gamma_{\text{C}_l\text{S}} < \gamma_{\text{Cout}}|\mathcal{H}_1, \Xi^c, \Phi_{m,j}\} \right] \qquad \text{(D.2)}
\end{aligned}$$

Now, let E_{C_l} represent the energy statistics at C_l, $\lambda_{BSR,o}$ represents the detector threshold set at each CSU.

$$\begin{aligned}
&Pr\{\gamma_{\text{C}_{l_k}\text{S}} < \gamma_{\text{Cout}}|\mathcal{H}_1, \Xi^c, \Phi_{m,j}\} \\
&= Pr\{\gamma_{\text{C}_{l_k}\text{S}} < \gamma_{\text{Cout}}|\mathcal{H}_1, \Xi^c, \gamma_{\text{SC}_{l_1}} > \gamma_{\text{Sout}}, \gamma_{\text{SC}_{l_2}} > \gamma_{\text{Sout}}, \ldots, \gamma_{\text{SC}_{l_m}} > \gamma_{\text{Sout}}, E_{\text{C}_{l_1}} > \lambda_{BSR,o}, \ldots, E_{\text{C}_{l_m}} > \lambda_{BSR,o}\} \qquad \text{(D.3)}
\end{aligned}$$

Applying a similar argument of reciprocity, independent operation of individual spectrum sensors and unrelated wireless links as in Appendix B, we have

$$Pr\{\gamma_{\mathrm{C}_{l_k}\mathrm{S}} < \gamma_{\mathrm{Cout}} | \mathcal{H}_1, \Xi^c, \Phi_{m,j}\} = \frac{P_{E1_{\mathrm{C}_{l_k}\mathrm{S}}} - P_{E1_{\mathrm{SC}_{l_k}}}}{1 - P_{E1_{\mathrm{SC}_{l_k}}}}. \tag{D.4}$$

Also,

$$Pr\{\Phi_{m,j} | \mathcal{H}_1, \Xi^c\} = \prod_{l \in \Phi_{m,j}} (1 - P_{Ei_{\mathrm{SC}_l}}) P_{d\mathrm{C}_l} \times \prod_{k \in \Phi^c_{m,j}} \left\{1 - (1 - P_{Ei_{\mathrm{SC}_k}}) P_{d\mathrm{C}_k}\right\} \tag{D.5}$$

and

$$Pr\{\Xi^c | \mathcal{H}_1\} = 1 - P_{d,\mathrm{S}} \tag{D.6}$$

Thus, using (D.4) and (D.5) in (D.2), substituting (D.2) and (D.6) in (D.1) and taking the expectation of the resulting expression with respect to $\boldsymbol{\gamma}_{\mathbf{S}}$, we get the required expression for $P_{D,BSR}$.

Similarly, the expression for $P_{F,BSR}$ can be derived by replacing $\mathcal{H}_1$ by $\mathcal{H}_0$ and $P_{d,\mathrm{S}}$ by $P_{f,\mathrm{S}}$ in the above derivations.

Bibliography

[1] A. Gluhak, S. Krco, M. Nati, D. Pfisterer, N. Mitton, and T. Razafindralambo, "A survey on facilities for experimental internet of things research," *IEEE Communications Magazine*, vol. 49, no. 11, pp. 58–67, Nov. 2011.

[2] FCC, "Spectrum Policy Task Force, Report of the Spectrum Efficiency Working Group," FCC, Tech. Rep. ET Docket 02-135, Nov. 2002.

[3] J. Mitola III and G. Q. Maguire Jr., "Cognitive radio: Making software radios more personal," *IEEE Personal Communications*, vol. 6, no. 4, pp. 13 –18, Aug. 1999.

[4] S. Haykin, "Cognitive radio: Brain-empowered wireless communications," *IEEE Journal on Selected Areas in Communications*, vol. 23, no. 2, pp. 201–220, Feb. 2005.

[5] R. Tandra, A. Sahai, and S. M. Mishra, "What is a spectrum hole and what does it take to recognize one?" *Proceedings of the IEEE*, vol. 97, no. 5, pp. 824 –848, May 2009.

[6] S. Srinivasa and S. Jafar, "Cognitive radios for dynamic spectrum access - the throughput potential of cognitive radio: A theoretical perspective," *IEEE Communications Magazine*, vol. 45, no. 5, pp. 73–79, May 2007.

[7] M. Costa, "Writing on dirty paper (corresp.)," *IEEE Transactions on Information Theory*, vol. 29, no. 3, pp. 439–441, May 1983.

[8] T. M. C. Chu, H. Phan, and H. J. Zepernick, "Hybrid interweave-underlay spectrum access for cognitive cooperative radio networks," *IEEE Transactions on Communications*, vol. 62, no. 7, pp. 2183–2197, Jul. 2014.

[9] T. Yucek and H. Arslan, "A survey of spectrum sensing algorithms for cognitive radio applications," *IEEE Communications Surveys and Tutorials*, vol. 11, no. 1, pp. 116 –130, quarter 2009.

[10] E. Axell, G. Leus, E. G. Larsson, and H. V. Poor, "Spectrum sensing for cognitive radio : State-of-the-art and recent advances," *IEEE Signal Processing Magazine*, vol. 29, no. 3, pp. 101–116, 2012.

[11] S. M. Kay, *Fundamentals of Statistical Signal Processing*. Prentice Hall PTR, 1993, vol. 2, pp. 254–257.

[12] X. Gao, N. Wang, D. Tao, and X. Li, "Face sketch-photo synthesis and retrieval using sparse representation," *IEEE Transactions on Circuits and Systems for Video Technology*, vol. 22, no. 8, pp. 1213–1226, 2012.

[13] J. Yang, J. Wright, T. Huang, and Y. Ma, "Image super-resolution via sparse representation," *IEEE Transactions on Image Processing*, vol. 19, no. 11, pp. 2861–2873, 2010.

[14] J. Wright, Y. Ma, J. Mairal, G. Sapiro, T. Huang, and S. Yan, "Sparse representation for computer vision and pattern recognition," *Proceedings of the IEEE*, vol. 98, no. 6, pp. 1031–1044, 2010.

[15] H. Urkowitz, "Energy detection of unknown deterministic signals," *Proceedings of the IEEE*, vol. 55, no. 4, pp. 523 – 531, Apr. 1967.

[16] F. F. Digham, M. S. Alouini, and M. K. Simon, "On the energy detection of unknown signals over fading channels," *IEEE Transactions on Communications*, vol. 55, no. 1, pp. 21–24, Jan. 2007.

[17] H. Al-Hmood and H. S. Al-Raweshidy, "Analysis of energy detection with diversity receivers over non-identically distributed κ-μ shadowed fading channels," *Electronics Letters*, vol. 53, no. 2, pp. 83–85, 2017.

[18] Y. Chen, "Improved energy detector for random signals in Gaussian noise," *IEEE Transactions on Wireless Communications*, vol. 9, no. 2, pp. 558 –563, Feb. 2010.

[19] V. Kostylev, "Energy detection of a signal with random amplitude," in *Proc. IEEE International Conference on Communications*, vol. 3, 2002, pp. 1606–1610.

[20] N. Beaulieu and Y. Chen, "Improved energy detectors for cognitive radios with randomly arriving or departing primary users," *IEEE Signal Processing Letters*, vol. 17, no. 10, pp. 867 –870, Oct. 2010.

[21] S. Herath, N. Rajatheva, and C. Tellambura, "Energy detection of unknown signals in fading and diversity reception," *IEEE Transactions on Communications*, vol. 59, no. 9, pp. 2443–2453, 2011.

[22] A. Muller, J. Coon, and R. Piechocki, "Diversity analysis for energy detection-based spectrum sensing," *IET Communications*, vol. 6, no. 7, pp. 759–764, May 2012.

[23] J. Y. Wu, C. H. Wang, and T. Y. Wang, "Performance analysis of energy detection based spectrum sensing with unknown primary signal arrival time," *IEEE Transactions on Communications*, vol. 59, no. 7, pp. 1779–1784, Jul. 2011.

[24] R. Tandra and A. Sahai, "Fundamental limits on detection in low SNR under noise uncertainty," in *Proc. International Conference on Wireless Networks, Communications and Mobile Computing*, vol. 1, 2005, pp. 464–469 vol.1.

[25] ——, "SNR walls for feature detectors," in *Proc. IEEE International Symposium on Dynamic Spectrum Access Networks*, 2007, pp. 559–570.

[26] W. Gardner, "Spectral correlation of modulated signals: Part I–analog modulation," *IEEE Transactions on Communications*, vol. 35, no. 6, pp. 584–594, 1987.

[27] W. Gardner, W. Brown, and C.-K. Chen, "Spectral correlation of modulated signals: Part II–digital modulation," *IEEE Transactions on Communications*, vol. 35, no. 6, pp. 595–601, 1987.

[28] P. D. Sutton, K. E. Nolan, and L. E. Doyle, "Cyclostationary signatures in practical cognitive radio applications," *IEEE Journal on Selected Areas in Communications*, vol. 26, no. 1, pp. 13–24, Jan. 2008.

[29] K. L. Du and W. H. Mow, "Affordable cyclostationarity-based spectrum sensing for cognitive radio with smart antennas," *IEEE Transactions on Vehicular Technology*, vol. 59, no. 4, pp. 1877–1886, May 2010.

[30] M. Derakhshani, T. Le-Ngoc, and M. Nasiri-Kenari, "Efficient cooperative cyclostationary spectrum sensing in cognitive radios at low SNR regimes," *IEEE Transactions on Wireless Communications*, vol. 10, no. 11, pp. 3754–3764, Nov. 2011.

[31] G. Huang and J. K. Tugnait, "On cyclostationarity based spectrum sensing under uncertain Gaussian noise," *IEEE Transactions on Signal Processing*, vol. 61, no. 8, pp. 2042–2054, Apr. 2013.

[32] P. Sepidband and K. Entesari, "A CMOS spectrum sensor based on quasi-cyclostationary feature detection for cognitive radios," *IEEE Transactions on Microwave Theory and Techniques*, vol. 63, no. 12, pp. 4098–4109, Dec. 2015.

[33] S. Kozowski, "Implementation and verification of cyclostationary feature detector for DVB-T signals," *IET Signal Processing*, vol. 10, no. 2, pp. 162–167, 2016.

[34] S. Chaudhari, M. Kosunen, S. Mkinen, J. Oksanen, M. Laatta, J. Ojaniemi, V. Koivunen, J. Ryynnen, and M. Valkama, "Performance evaluation of cyclostationary-based cooperative sensing using field measurements," *IEEE Transactions on Vehicular Technology*, vol. 65, no. 4, pp. 1982–1997, Apr. 2016.

[35] Y. Zeng and Y.-C. Liang, "Eigenvalue-based spectrum sensing algorithms for cognitive radio," *IEEE Transactions on Communications*, vol. 57, no. 6, pp. 1784–1793, 2009.

[36] S. K. Sharma, S. Chatzinotas, and B. Ottersten, "Eigenvalue-based sensing and SNR estimation for cognitive radio in presence of noise correlation," *IEEE Transactions on Vehicular Technology*, vol. 62, no. 8, pp. 3671–3684, Oct. 2013.

[37] A. Kortun, T. Ratnarajah, M. Sellathurai, C. Zhong, and C. B. Papadias, "On the performance of eigenvalue-based cooperative spectrum sensing for cognitive radio," *IEEE Journal of Selected Topics in Signal Processing*, vol. 5, no. 1, pp. 49–55, Feb. 2011.

[38] A. Ghasemi and E. S. Sousa, "Collaborative spectrum sensing for opportunistic access in fading environments," in *Proc. IEEE International Symposium on New Frontiers in Dynamic Spectrum Access Networks*, Nov. 2005, pp. 131–136.

[39] G. Ganesan and Y. Li, "Cooperative spectrum sensing in cognitive radio, Part I: Two user networks," *IEEE Transactions on Wireless Communications*, vol. 6, no. 6, pp. 2204–2213, 2007.

[40] ——, "Cooperative spectrum sensing in cognitive radio, Part II: Multiuser networks," *IEEE Transactions on Wireless Communications*, vol. 6, no. 6, pp. 2214–2222, 2007.

[41] E. Visotsky, S. Kuffner, and R. Peterson, "On collaborative detection of TV transmissions in support of dynamic spectrum sharing," in *Proc. IEEE International Symposium on New Frontiers in Dynamic Spectrum Access Networks*, Nov. 2005, pp. 338–345.

[42] W. Zhang, R. K. Mallik, and K. B. Letaief, "Optimization of cooperative spectrum sensing with energy detection in cognitive radio networks," *IEEE Transactions on Wireless Communications*, vol. 8, no. 12, pp. 5761–5766, Dec. 2009.

[43] S. Althunibat, M. D. Renzo, and F. Granelli, "Optimizing the k-out-of-n rule for cooperative spectrum sensing in cognitive radio networks," in *Proc. IEEE Global Communications Conference (GLOBECOM)*, Dec. 2013, pp. 1607–1611.

[44] E. C. Y. Peh, Y. C. Liang, Y. L. Guan, and Y. Zeng, "Cooperative spectrum sensing in cognitive radio networks with weighted decision fusion schemes," *IEEE Transactions on Wireless Communications*, vol. 9, no. 12, pp. 3838–3847, Dec. 2010.

[45] J. Ma, G. Zhao, and Y. Li, "Soft combination and detection for cooperative spectrum sensing in cognitive radio networks," *IEEE Transactions on Wireless Communications*, vol. 7, no. 11, pp. 4502–4507, Nov. 2008.

[46] S. Chaudhari, J. Lunden, V. Koivunen, and H. V. Poor, "Cooperative sensing with imperfect reporting channels: Hard decisions or soft decisions?" *IEEE Transactions on Signal Processing*, vol. 60, no. 1, pp. 18–28, Jan. 2012.

[47] R. Fan and H. Jiang, "Optimal multi-channel cooperative sensing in cognitive radio networks," *IEEE Transactions on Wireless Communications*, vol. 9, no. 3, pp. 1128–1138, Mar. 2010.

[48] S. Atapattu, C. Tellambura, and H. Jiang, "Energy detection based cooperative spectrum sensing in cognitive radio networks," *IEEE Transactions on Wireless Communications*, vol. 10, no. 4, pp. 1232–1241, Apr. 2011.

[49] H. Sadeghi and P. Azmi, "Performance analysis of linear cooperative cyclostationary spectrum sensing over Nakagami-*m* fading channels," *IEEE Transactions on Vehicular Technology*, vol. 63, no. 9, pp. 4748–4756, Nov. 2014.

[50] S. Maleki, G. Leus, S. Chatzinotas, and B. Ottersten, "To AND or to OR: On energy-efficient distributed spectrum sensing with combined censoring and sleeping," *IEEE Transactions on Wireless Communications*, vol. 14, no. 8, pp. 4508–4521, Aug. 2015.

[51] W. Ejaz, G. Hattab, T. Attia, M. Ibnkahla, F. Abdelkefi, and M. Siala, "Joint quantization and confidence-based generalized combining scheme for cooperative spectrum sensing," *IEEE Systems Journal*, vol. PP, no. 99, pp. 1–12, 2016.

[52] H. Guo, N. Reisi, W. Jiang, and W. Luo, "Soft combination for cooperative spectrum sensing in fading channels," *IEEE Access*, vol. 5, pp. 975–986, 2017.

[53] H. Sadeghi, P. Azmi, and H. Arezumand, "Cyclostationarity-based cooperative spectrum sensing over imperfect reporting channels," *AEU - International Journal of Electronics and Communications*, vol. 66, no. 10, pp. 833 – 840, 2012.

[54] M. B. Ghorbel, H. Nam, and M. S. Alouini, "Soft cooperative spectrum sensing performance under imperfect and non identical reporting channels," *IEEE Communication Letters*, vol. 19, no. 2, pp. 227–230, Feb. 2015.

[55] W. Han, J. Li, Z. Li, J. Si, and Y. Zhang, "Efficient soft decision fusion rule in cooperative spectrum sensing," *IEEE Transactions on Signal Processing*, vol. 61, no. 8, pp. 1931–1943, Apr. 2013.

[56] Y. Abdi and T. Ristaniemi, "Joint local quantization and linear cooperation in spectrum sensing for cognitive radio networks," *IEEE Transactions on Signal Processing*, vol. 62, no. 17, pp. 4349–4362, Sep. 2014.

[57] I. Hwang and J. W. Lee, "Cooperative spectrum sensing with quantization combining over imperfect feedback channels," *IEEE Transactions on Signal Processing*, vol. 65, no. 3, pp. 721–732, Feb. 2017.

[58] C. Sun, W. Zhang, and K. B. Letaief, "Cluster-based cooperative spectrum sensing in cognitive radio systems," in *Proc. IEEE International Conference on Communications*, Jun. 2007, pp. 2511–2515.

[59] Y. Wang, C. Feng, Z. Zeng, and C. Guo, "A robust and energy efficient cooperative spectrum sensing scheme in cognitive radio networks," in *Proc. 11th International Conference on Advanced Communication Technology*, vol. 01, Feb. 2009, pp. 640–645.

[60] Y. Zou, Y. D. Yao, and B. Zheng, "A selective-relay based cooperative spectrum sensing scheme without dedicated reporting channels in cognitive radio networks," *IEEE Transactions on Wireless Communications*, vol. 10, no. 4, pp. 1188–1198, Apr. 2011.

[61] Z. Dai, J. Liu, and K. Long, "Selective-reporting-based cooperative spectrum sensing strategies for cognitive radio networks," *IEEE Transactions on Vehicular Technology*, vol. 64, no. 7, pp. 3043–3055, Jul. 2015.

[62] R. Kishore, C. K. Ramesha, and T. Sawant, "Superior selective reporting mechanism for cooperative spectrum sensing in cognitive radio networks," in *Proc. International Conference on Wireless Communications, Signal Processing and Networking (WiSPNET)*, Mar. 2016, pp. 426–431.

[63] B. Farhang-Boroujeny, "Filter bank spectrum sensing for cognitive radios," *IEEE Transactions on Signal Processing*, vol. 56, no. 5, pp. 1801–1811, May 2008.

[64] Z. Quan, S. Cui, A. H. Sayed, and H. V. Poor, "Optimal multiband joint detection for spectrum sensing in cognitive radio networks," *IEEE Transactions on Signal Processing*, vol. 57, no. 3, pp. 1128–1140, Mar. 2009.

[65] Z. Tian and G. Giannakis, "A wavelet approach to wideband spectrum sensing for cognitive radios," in *Proc. 1st International Conference on Cognitive Radio Oriented Wireless Networks and Communications*, Jun. 2006, pp. 1–5.

[66] E. Candes and M. Wakin, "An introduction to compressive sampling," *IEEE Signal Processing Magazine*, vol. 25, no. 2, pp. 21–30, Mar. 2008.

[67] Z. Tian, "Compressed wideband sensing in cooperative cognitive radio networks," in *Proc. IEEE Conference on Global Telecommunications*, 2008, pp. 1–5.

[68] M. Mishali and Y. C. Eldar, "Blind multiband signal reconstruction: Compressed sensing for analog signals," *IEEE Transactions on Signal Processing*, vol. 57, no. 3, pp. 993–1009, Mar. 2009.

[69] F. Zeng, C. Li, and Z. Tian, "Distributed compressive spectrum sensing in cooperative multihop cognitive networks," *IEEE Journal of Selected Topics in Signal Processing*, vol. 5, no. 1, pp. 37–48, Feb. 2011.

[70] H. Sun, W. Y. Chiu, J. Jiang, A. Nallanathan, and H. V. Poor, "Wideband spectrum sensing with sub-Nyquist sampling in cognitive radios," *IEEE Transactions on Signal Processing*, vol. 60, no. 11, pp. 6068–6073, Nov. 2012.

[71] C. P. Yen, Y. Tsai, and X. Wang, "Wideband spectrum sensing based on sub-Nyquist sampling," *IEEE Transactions on Signal Processing*, vol. 61, no. 12, pp. 3028–3040, Jun. 2013.

[72] *Specification of the Bluetooth System, Volume 1*, Bluetooth SIG, Inc., February 2001.

[73] Z. Chen, N. Guo, and R. C. Qiu, "Demonstration of real-time spectrum sensing for cognitive radio," *IEEE Communications Letters*, vol. 14, no. 10, pp. 915–917, Oct. 2010.

[74] R. Prasanna and B. Amrutur, "Cognitive radio implementation for a frequency hopping primary signal," in *Proc. National Conference on Communications (NCC)*, 2013, pp. 1–5.

[75] C. Phillips, M. Ton, D. Sicker, and D. Grunwald, "Practical radio environment mapping with geostatistics," in *Proc. IEEE International Symposium on Dynamic Spectrum Access Networks*, Oct. 2012, pp. 422–433.

[76] E. C. Y. Peh, Y. C. Liang, Y. L. Guan, and Y. Zeng, "Optimization of cooperative sensing in cognitive radio networks: A sensing-throughput tradeoff view," *IEEE Transactions on Vehicular Technology*, vol. 58, no. 9, pp. 5294–5299, Nov. 2009.

[77] J. C. Shen and E. Alsusa, "An efficient multiple lags selection method for cyclostationary feature based spectrum-sensing," *IEEE Signal Processing Letters*, vol. 20, no. 2, pp. 133–136, 2013.

[78] Y. Zhao, J. Gaeddert, L. Morales, K. Bae, J. S. Um, and J. H. Reed, "Development of radio environment map enabled case- and knowledge-based learning algorithms for IEEE 802.22 WRAN cognitive engines," in *Proc. International Conference on Cognitive Radio Oriented Wireless Networks and Communications*, Aug. 2007, pp. 44–49.

[79] Y. Zhao, L. Morales, J. Gaeddert, K. K. Bae, J. S. Um, and J. H. Reed, "Applying radio environment maps to cognitive wireless regional area networks," in *Proc. IEEE International Symposium on New Frontiers in Dynamic Spectrum Access Networks*, Apr. 2007, pp. 115–118.

[80] T. Cai, J. van de Beek, B. Sayrac, S. Grimoud, J. Nasreddine, J. Riihijärvi, and P. Mähönen, "Design of layered radio environment maps for RAN optimization in heterogeneous LTE systems," in *Proc. IEEE International Symposium on Personal, Indoor and Mobile Radio Communications*, Sep. 2011, pp. 172–176.

[81] Y. D. Yao and A. U. H. Sheikh, "Outage probability analysis for microcell mobile radio systems with cochannel interferers in Rician/Rayleigh fading environment," *Electronics Letters*, vol. 26, no. 13, pp. 864–866, Jun. 1990.

[82] V. Atanasovski, J. van de Beek, A. Dejonghe, D. Denkovski, L. Gavrilovska, S. Grimoud, P. Mhnen, M. Pavloski, V. Rakovic, J. Riihijarvi, and B. Sayrac, "Constructing radio environment maps with heterogeneous spectrum sensors," in *Proc. IEEE International Symposium on Dynamic Spectrum Access Networks*, May 2011, pp. 660–661.

[83] J. Riihijärvi, J. Nasreddine, and P. Mähönen, "Demonstrating radio environment map construction from massive data sets," in *Proc. IEEE International Symposium on Dynamic Spectrum Access Networks*, Oct. 2012, pp. 266–267.

[84] D. Messerschmitt, "Quantizing for maximum output entropy (corresp.)," *IEEE Transactions on Information Theory*, vol. 17, no. 5, pp. 612–612, Sep. 1971.

[85] R. Tandra, "Fundamental limits on detection in low SNR," Master's thesis, University of California, Berkeley, 2003.

[86] J. Wright, A. Yang, A. Ganesh, S. Sastry, and Y. Ma, "Robust face recognition via sparse representation," *IEEE Transactions on Pattern Analysis and Machine Intelligence*, vol. 31, no. 2, pp. 210–227, 2009.

[87] Haris BC and R. Sinha, "Sparse representation over learned and discriminatively learned dictionaries for speaker verification," in *Proc. IEEE International Conference on Acoustics, Speech and Signal Processing (ICASSP)*, 2012, pp. 4785–4788.

[88] ——, "Robust speaker verification with joint sparse coding over learned dictionaries," *IEEE Transactions on Information Forensics and Security*, vol. 10, no. 10, pp. 2143–2157, Oct. 2015.

[89] S. Mallat and Z. Zhang, "Matching pursuits with time-frequency dictionaries," *IEEE Transactions on Signal Processing*, vol. 41, no. 12, pp. 3397–3415, 1993.

[90] T. Cai and L. Wang, "Orthogonal matching pursuit for sparse signal recovery with noise," *IEEE Transactions on Information Theory*, vol. 57, no. 7, pp. 4680–4688, 2011.

[91] E. Candes, J. Romberg, and T. Tao, "Robust uncertainty principles: Exact signal reconstruction from highly incomplete frequency information," *IEEE Transactions on Information Theory*, vol. 52, no. 2, pp. 489–509, 2006.

[92] M. Aharon, M. Elad, and A. Bruckstein, " K-SVD: An algorithm for designing overcomplete dictionaries for sparse representation," *IEEE Transactions on Signal Processing*, vol. 54, no. 11, pp. 4311–4322, 2006.

[93] A. Julazadeh, M. Marsousi, and J. Alirezaie, "Classification based on sparse representation and Euclidian distance," in *Proc. IEEE Visual Communications and Image Processing (VCIP)*, 2012, pp. 1–5.

[94] *Guidelines for evaluation of radio transmission technologies for IMT-2000*, ITU-R Recommendation M.1225, 1997.

List of Publications

Conference Publications

1. **Kukil Khanikar**, Rohit Sinha and Ratnajit Bhattacharjee, "**Sparse Representation Based Tracking of Frequency Hopping Primary User for Cognitive Radio**," *in Proc. International Conference on Signal Processing and Communications*, July 2014.

2. **Kukil Khanikar**, Rohit Sinha and Ratnajit Bhattacharjee, "**Sparse Representation Based Tracking of Frequency Hopping Primary User for Cognitive Radio**," *in Proc. National Conference on Communications*, February 2015.

Journal Publications

1. **Kukil Khanikar**, Rohit Sinha and Ratnajit Bhattacharjee, "**Incorporating Primary User Interference for Enhanced Spectrum Sensing**," *IEEE Signal Processing Letters*, vol. 24, no. 7, pp. 1039 - 1043, July 2017.

2. **Kukil Khanikar**, Rohit Sinha and Ratnajit Bhattacharjee, "**Cooperative Spectrum Sensing using Quantized Energy Statistics in the Absence of Dedicated Reporting Channel**," in IEEE Transactions on Vehicular Technology (doi: 10.1109/TVT.2018.2791020).